Universidade de Lisboa

Faculdade de Farmácia

Probing the Pyrimidine Scaffold for Malaria Liver Stage Inhibition: Synthesis and Biological Evaluation in *P. berghei*-infected hepatocytes

Rúben Alexandre Dâmaso Coutinho

Dissertação orientada pela Doutora Rita Capela e coorientada pelo Professor Doutor Rui Moreira.

Mestrado em Química Farmacêutica e Terapêutica

2020

Universidade de Lisboa

Faculdade de Farmácia

Probing the Pyrimidine Scaffold for Malaria Liver Stage Inhibition: Synthesis and Biological Evaluation in *P. berghei*-infected hepatocytes

Rúben Alexandre Dâmaso Coutinho

Dissertação orientada pela Doutora Rita Capela e coorientada pelo Professor Doutor Rui Moreira.

Mestrado em Química Farmacêutica e Terapêutica

2020

Acknowledgements

First, I would like to thank my supervisor Doctor Rita Capela for all the scientific support and knowledge, wonderful guidance, critics and opinions through this project. I am also very grateful for all the support given to me during my laboratorial work.

I would like to express my gratitude to my co-supervisor Professor Doctor Rui Moreira for this opportunity to work in the MedChem group, reception on his laboratory, extensive knowledge transmitted to me and guidance.

I would also like to thank to the Doctor Miguel Prudêncio and his lab technician Doctor Denise Francisco and researcher Doctor Diana Fontinha for their availability on the execution and treatment of the antimalarial biological assays results and allowing me to be present during the process.

I also want to thank to Doctor Marta Afonso for the execution and treatment of the anticancer biological assays results.

A special thanks to Doctor João Pedro Pais for all the support and assistance through the several hardships faced over the last months of this thesis.

I would like to thank to all my colleagues from the laboratory for the incredible environment, amusing moments and aid in the laboratory work, in special to André Campaniço and Jorge Grilo for their patience and helpfulness through my stay in the laboratory.

I would also like to express my gratitude to all my friends from the laboratory and college who accompanied me through this time, gifting me with unforgettable moments. Without them, this experience would not be the same.

Finally, I would like to thank to all my friends, my girlfriend Vera, and my family, with special attention to my mother. Their support, affection and encouragement were very precious to me. It is thanks to them this accomplishment was possible.

Abstract

Malaria is one of the world major infectious diseases. In 2018 it affected 228 million people worldwide. Human malaria is caused by five species of *Plasmodium*, of which *P. falciparum* is the deadliest parasite. *Plasmodium* parasites are transmitted through the bites of infected *Anopheles* mosquitoes. Before the parasites start consuming hemoglobin on the symptomatic blood stage, they need to go through the obligatory and asymptomatic liver stage.

Most antimalarial drugs target the erythrocytic parasites. Generally, these drugs have no effect in the hepatic forms of the parasite due to the distinct biology between both stages. Thus, it is highly desirable to target the hepatic stage in order to achieve prophylaxis, eradicate the dormant forms (hypnozoites) caused by *P. vivax* and *P. ovale*, and block the transmission of the parasites to the mosquito vectors. Additionally, to oppose the emergence of resistant strains, combined therapies and hybrid drugs can be used. Several compound classes have anti-liver stage activity. However, it has been difficult to develop an efficacious prophylactic drug due to the lack of known liver stage targets. Primaquine is an 8-aminoquinoline antimalarial with potent activity against liver stage parasites and is one of the few drugs with hypnozontocidal activity. As primaquine, other 8-aminoquinolines also have prophylactic activity, despite few being active against the dormant forms such as tafenoquine. However, this compound class is unsuitable for glucose 6-phosphate dehydrogenase deficient individuals. Antifolates, alkaloids, antibiotics and pyrimidines are some examples of classes with compounds active against the liver stage. A series of tetraoxane-pyrimidine nitrile hybrids as dual-stage antimalarials was found by Oliveira and co-workers. The pyrimidine nitrile moiety (a Michael acceptor) exhibited to be active against blood stages by inhibiting the falcipain-2. Although this enzyme is only expressed on the blood stage, this same moiety also exhibited activity against the liver stage. Thus, suggesting the presence of potential target(s) containing an active cysteine on the pre-erythrocytic stages.

In this work two compounds with a Michael acceptor group, compounds **64** and **65**, were synthetized and their biological activity was evaluated against the BS and LS. Both compounds exhibited mild inhibitory activity to the LS. IC_{50} of LS was not determined for compound **64** due to possible toxicity, whereas compound **65** exhibited an IC_{50} = 9.49 µM. However only one of the compounds showed to inhibit BS parasites (compound **64**). Furthermore, anticancer activity was tested for both compounds and these exhibited low anticancer efficacy. On the monolayer assay compounds **64** and **65** exhibited IC_{50} = 35.56 µM and 28.96 µM, respectively. On the CSC-like spheres assay these compounds exhibited IC_{50} = 0.77 µM and 0.70 µM, respectively.

Keywords: malaria, liver stage, hybrid drugs, pyrimidine derivatives.

Resumo

A malária é uma das principais doenças infeciosas a nível mundial. Em 2018 esta doença infetou 228 milhões de pessoas, das quais 405 mil morreram em todo o mundo. Anualmente são gastos vários biliões de dólares americanos na tentativa de controlar e erradicar a malária. Contudo, apesar do número de casos e mortes causados por esta doença terem vindo a diminuir ao longo dos anos, a Organização Mundial de Saúde considera que demore mais de uma década até que a malária seja totalmente erradicada.

A malaria é causada por parasitas protozoários do género *Plasmodium*. Em humanos esta doença pode ser causada por cinco diferentes espécies: *P. falciparum*, *P. vivax*, *P. ovale*, *P. malariae* e *P. knowlesi*. Destas espécies de *Plasmodium*, o *P. falciparum* é a espécie predominante na maioria das regiões afetadas por esta doença, sendo responsável por 99.7% dos casos em África, para além de ser a espécie responsável pela maioria das mortes a nível global.

Os parasitas *Plasmodium* necessitam de dois hospedeiros distintos: um vetor mosquito e um hospedeiro vertebrado. Em humanos, os parasitas são geralmente transmitidos através da picada do mosquito fêmea *Anopheles* infetado e têm duas fases distintas quando no corpo humano, a fase hepática e a fase sanguínea. Quando o mosquito se alimenta de sangue, liberta os esporozoítos existentes nas glândulas salivares para o sangue do hospedeiro vertebrado. Após entrarem na corrente sanguínea, os parasitas migram para os hepatócitos dando início à fase hepática, assintomática para o hospedeiro. Adicionalmente, é na fase hepática que ocorre o desenvolvimento das formas latentes (hipnozoítos) das espécies *P. vivax* e *P. ovale*. Os hipnozoítos podem ficar inativos nas células hepáticas até vários anos.

Após a fase hepática, os parasitas regressam à corrente sanguínea para invadirem os eritrócitos, dando começo à fase sanguínea. Dentro dos eritrócitos, os parasitas evitam as defesas imunitárias do hospedeiro e degradam a hemoglobina dos mesmos, permitindo o seu crescimento e replicação. O consumo excessivo de hemoglobina por parte do parasita é a causa dos sintomas no hospedeiro.

O tratamento para a malária deve ser iniciado nas primeiras 24 horas após o aparecimento de sintomas. No entanto, os primeiros sintomas causados pelos parasitas *Plasmodium* são muito semelhantes a outras doenças febris, dificultando o seu diagnóstico. Quando não tratada nestas 24 horas, a malária pode desenvolver-se em malária severa, podendo causar malaria cerebral, ou mesmo a morte.

Tradicionalmente, as terapias contra a malária têm a fase sanguínea como alvo. No entanto, a fase hepática é obrigatória e essencial para a maturação e replicação dos parasitas, sendo um alvo importante no controlo e erradicação da malária. De forma geral, os fármacos que atuam na fase sanguínea não têm atividade contra os parasitas

hepáticos devido às diferenças biológicas entre as duas fases dos parasitas. Assim, é altamente desejável desenvolver fármacos ativos para a fase hepática, ou para ambas as fases, de modo a exercer profilaxia, erradicar as formas latentes, evitar o aparecimento de estirpes resistentes e bloquear a transmissão dos parasitas para o vetor mosquito. Adicionalmente, outros modos de combater o desenvolvimento de resistência aos vários fármacos são: utilização de terapias combinadas, ou fármacos híbridos.

Atualmente, é recomendado pela Organização Mundial de Saúde recorrer a terapias combinadas baseadas em artemisininas para o tratamento da malária, de modo a reduzir o risco de aparecimento de resistência. As artemisininas são compostos apenas ativos contra as formas eritrocíticas, e já existem casos de resistência a estas moléculas. O desenvolvimento de resistência aos vários fármacos é a principal razão para que a terapêutica contra a malária não seja tão eficaz quanto desejado. A cloroquina, fármaco antimalárico que permitiu a erradicação da malária de muitos países, hoje em dia é ineficaz contra os parasitas *Plasmodium* devido ao aparecimento de estirpes resistentes a este composto.

Várias classes de compostos têm atividade contra a fase hepática. No entanto, tem sido difícil desenvolver um fármaco com efeito profilático eficiente devido à falta de conhecimento sobre a biologia dos parasitas hepáticos e respetivos alvos terapêuticos. A primaquina é uma 8-aminoquinolina com potente atividade para os parasitas pré-eritrocíticos, para além de ser um dos poucos fármacos com atividade hipnozoiticida. Além da primaquina, outras 8-aminoquinolinas também exibem atividade profilática, apesar de poucas serem ativas contra as formas latentes como é o caso da tafenoquina. No entanto, o uso desta classe de compostos não é indicado para pessoas com deficiência a nível da enzima glucose 6-fosfato desidrogenase, devido aos seus efeitos secundários.

Dentro dos grupos dos antifolatos, alcalóides, antibióticos, anti-histamínicos, inibidores do complexo bc_1, pirimidinas, entre outros, podem ser encontradas moléculas com atividade para a fase hepática. Entre os vários compostos abordados destacaram-se dois devido aos seus baixos valores de IC_{50} na fase hepática: o decoquinato (177 pM) e a nigericina (< 1 pM). O primeiro composto é um inibidor do complexo bc_1 da cadeia eletrónica mitocondrial do parasita, enquanto que o segundo composto é um antibiótico ionóforo cujo alvo são transportadores de iões K^+.

As pirimidinas nitrilo geralmente são compostos ativos para a fase sanguínea. No entanto, Oliveira e colaboradores descobriram uma série de híbridos tetraoxano-pirimidina nitrilo com atividade para ambas as fases do parasita. A unidade pirimidina nitrilo (grupo aceitador de Michael) destas moléculas é um inibidor da falcipaína-2, enzima expressa apenas nos parasitas eritrocíticos. No entanto, a mesma unidade revelou também ter atividade inibitória para os parasitas hepáticos. Isto sugere a existência de um ou mais alvos terapêuticos com um resíduo de cisteína ativo na fase hepática. Apesar de estar descrita a possível atividade antimalárica de tetraoxanos na

fase hepática, nestes híbridos essa hipótese não é considerada, pela existência de atividade hepática num composto apenas com a unidade pirimidina nitrilo.

Neste projeto foram sintetizados dois compostos com um grupo aceitador de Michael, e com potencial atividade inibitória para as fases sanguínea e hepática. Duas pirimidinas substituídas na posição 2 com uma unidade acrilato, cujas atividades inibitórias contra a malária (fases sanguínea e hepática) e células cancerígenas do tipo estaminais foram avaliadas. No entanto, não foi possível expor o alvo terapêutico destas moléculas na fase hepática.

Ao longo do trabalho laboratorial certas reações foram otimizadas. Por exemplo, na obtenção dos compostos finais efetuou-se um acoplamento de Suzuki-Miyaura na posição 2 de duas pirimidinas distintas. Quando esta reação foi efetuada numa pirimidina não substituída na posição 5, o rendimento obtido foi de 6% (composto **64**). Por outro lado, verificou-se que a mesma reação numa 5-bromopirimidina levou à obtenção do composto di-substituído, **65**, com um rendimento de 13%.

Ambos os compostos mostraram ter atividade moderada contra os parasitas hepáticos, o composto **65** exibiu um valor de IC_{50} = 9.49 μM. O valor de IC_{50} do composto **64** não foi determinado devido à possibilidade de toxicidade nas concentrações mais elevadas. Quanto à avaliação da inibição de parasitas sanguíneos, apenas um dos compostos mostrou atividade (composto **64**), sendo esta reduzida relativamente a outros compostos com grupos aceitadores de Michael. Para além disso, os compostos finais foram também testados numa linha de células cancerígenas do tipo estaminais do cólon humano (HT-29), e ambos apresentaram baixa atividade inibitória. Nos ensaios em monocamada os compostos **64** e **65** apresentaram valores de IC_{50} = 35.56 μM e 28.96 μM, respetivamente. Nos ensaios em células cancerígenas estaminais do tipo esferóides os valores de IC_{50} determinados foram de 0.77 μM e 0.70 μM, respetivamente.

O facto dos compostos **64** e **65** conterem um grupo na posição 2 que atua como aceitador de Michael, e apresentarem atividade para a fase hepática (composto **64** também apresentou atividade para a fase sanguínea), reforça a hipótese de existir um alvo que contenha uma cisteína ativa para esta mesma fase. Assim, este trabalho serve de diretriz para a síntese de híbridos e sondas químicas estruturalmente relacionadas com os compostos **64** e **65**, possibilitando a compreensão do mecanismo de ação destes na fase hepática.

Palavras-chave: malária, fase hepática, fármacos híbridos, derivados pirimidina.

Table of Content

List of Figures

List of Schemes

List of Tables

Symbols and abbreviations

δ – Chemical Shift

^{1}H NMR – Proton Nuclear Magnetic Resonance

1D – 1-Dimensional

^{13}C NMR – Carbon Nuclear Magnetic Resonance

^{13}C-APT NMR – Carbon Nuclear Magnetic Resonance (Attached Proton Test)

2D – 2-Dimensional

5-Fu – Fluorouracil

5-HPQ – 5-Hydroxy-Primaquine

5-PQQI – 5-Quinoneimine

ACN – Acetonitrile

AcOH – Acetic Acid

ACT – Artemisinin Combination Therapy

ADME – Absorption, Distribution, Metabolization And Excretion

ADQ – Amodiaquine

AFR – African Region

AMR – American Region

ART – Artemisinin

bFGF – Basic Fibroblast Growth Factor

Boc – tert-Butyloxycarbonyl Protective Group

bs – Broad Singlet

BS – Blood Stage

calc. – Calculated

$CDCl_3$ – Deuterated Chloroform

COSY – Correlation Spectroscopy

CNS – Central Nervous System

CPR – Cytochrome P450 Reductase

CQ – Chloroquine

CSC – Cancer Stem Like Cells

CYP2D6 – Cytochrome P450 2D6

d – Doublet

dd – Double Doublet

DABCO – (1,4-Diazabicyclo[2.2.2]Octane)

DDT – Dichloro-Diphenyl Trichloro-Ethane

DHA – Dihydroartemisinin

DHFR – Dihydrofolate Reductase

DHODH – Dihydroorotate Dehydrogenase

DIPEA – *N*,*N*-Diisopropylethylamine

DMEM/F12 – Dulbecco's Modified Eagle Medium/Nutrient Mixture F-12

DMF – Dimethylformamide

DMSO – Dimethyl Sulfoxide

DV – Digestive Vacuole

EC_{50} – Half Maximal Effective Concentration

ED_{100} – Effective Dose For 100% of the Population

EGF – Epidermal Growth Factor

EMR – Eastern Mediterranean Region

eq. – Equivalent

ER – Endoplasmic Reticulum

ESI – Electrospay Ionization

EtOH – Ethanol

exp. – Experimental

FCS – Fetal Calf Serum

FLAB – Firefly Luciferase Assay Buffer

FP – Falcipain

FPIX – Ferriprotoporphyrin IX

G6PD – Glucose 6-Phosphate Dehydrogenase

HEPES – 4-(2-Hydroxyethyl)-1-Piperazine Ethanesulfonic Acid

HMBC – Heteronuclear Multiple Bond Correlation

HMQC – Heteronuclear Multiple-Quantum Correlation

HPLC – High-Performance Liquid Chromatography

IC_{50} – Half Maximal Inhibitory Concentration

***i*PrOH –** Isopropanol

IR – Infrared Radiation

LS – Liver Stage

m – Multiplet

MB – Methylene Blue

MCM – Malaria Complete Medium

MeOH – Methanol

MoA – Mechanism of Action

MP – Melting Point

MS – Mass Spectrometry

$NaBH_3CN$ – Sodium Cyanoborohydride

NBS – *N*-Bromosuccinimide

N.D. – Not Determined

NMR – Nuclear Magnetic Resonance

ov – Over Night

PBS – Phosphate-Buffered Saline

PCR – Polymerase Chain Reaction

$Pd(PPh_3)_4$ – Tetrakis(Triphenylphosphine) Palladium(0)

PfCRT– *Plasmodium falcipain* Chloroquine Resistance Transporter

ppm – Parts Per Million

PQ – Primaquine

PYR – Pyrimethamine

pyra – pyrazolidine

pyri – pyrimidine

q – Quartet

RBC – Red Blood Cells

ROS – Oxygen Radical Species

rt – Room Temperature

s – Singlet

Sal – Salinomycin

SEAR – South-East Asia Region

t – Triplet

***t*-BuOH –** tert-Butanol

TLC – Thin-Layer Chromatography

TQ – Tafenoquine

US – United States

US$ – United States Dollar

WHO – World Health Organization

WPR – Western Pacific Region

WWII – World War II

Chapter I

I. Introduction

I.1 Malaria

Although malaria is preventable and curable, it is one of the world major infectious diseases. It is caused by parasitic microorganisms of genus *Plasmodium* that require two hosts, a mosquito vector, in general, and a vertebrate host. On humans, the transmission generally occurs through the bite of infected female *Anopheles* mosquito when it feeds from human blood.[1,2] The *Plasmodium* species responsible for malaria on humans are *P. vivax*, *P. falciparum*, *P. malariae*, *P. ovale* and *P. knowlesi*. From those, *P. falciparum* is the responsible for most malaria cases and deaths.[3,4] This same species is responsible for about 99.7% of malaria cases in Africa region (AFR), about 50% in the South-East Asia region (SEAR), 71% in the Eastern Mediterranean region (EMR) and 65% in the Western Pacific region (WPR). Whereas the parasite *P. vivax* is responsible for most of the cases in the American region (AMR) (75%).[5]

Since the end of the World War II (WWII) malaria was eliminated from about 80 countries[6], of which several are now developed countries. This was possible due to the use of an efficient antimalarial drug, chloroquine (CQ) **1**[3,7] (**figure I.1)**, and the insecticide dichloro-diphenyl trichloro-ethane (DDT).[8] Unfortunately, beside mosquito vectors rapidly developed resistance to DDT, resistant *Plasmodium* strains to CQ started to emerge, leading to malaria prevalence to resurge in tropical countries in the 1970's.[8,9] On the last two decades the donor fundings to fight malaria increased substantially, leading to improved control efforts and increased enthusiasm for malaria eradication. This, consequently, led to a reduction of malaria prevalence.[10] Nowadays most of malaria cases are focused on the areas around the equator[11], as showed in **figure I.2**.

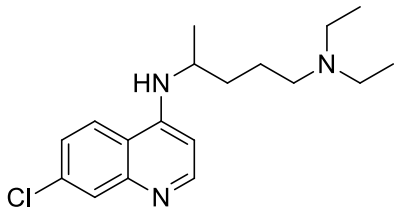

1

Figure I.1 – Structure of chloroquine (CQ) **1**.

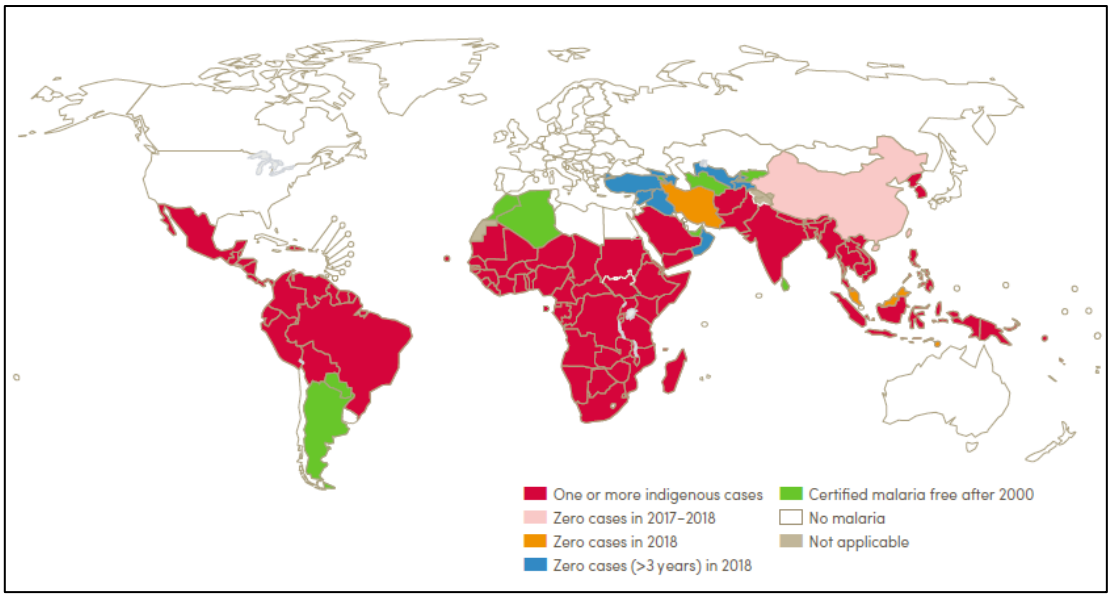

Figure I.2 – Countries with indigenous cases in 2000 and their status by 2018. (adapted from[5])

As reported by the World Health Organization (WHO), in 2018 there were about 228 million malaria cases and 405 thousand deaths. AFR was the most affected region in 2018, with 93% of total worldwide cases (213 million) and 94% of total malaria deaths. Nevertheless, the SEAR (3.4% of total malaria cases), EMR (2.1%), WPR (<1%) and the AMR (<1%) are also at risk. Furthermore, only 5 countries accounted for 50% of all malaria cases worldwide: Nigeria (25%), Democratic Republic of the Congo (12%), Uganda (5%), Mozambique (4%), and Niger (4%).[5]

According to the areas most affected by malaria in 2018, roughly half of the world's population is at risk of malaria.[5] Within this population, certain groups are more vulnerable to get affected, or even killed by malaria, such as children under 5 years old, pregnant women and HIV patients. Infants under 5 years old are the group with more deaths caused by malaria, which accounted for about 67% in 2018.[5]

Sub-Saharan Africa is the world's most burdened area by malaria due to: its hot and humid weather year round, which favours transmission; the presence of one of the most efficient malaria vector, *Anopheles gambiae* complex; the predominance of *P. falciparum*, which is the deadliest parasite species in humans; and lack of resources and socio-economic instability, hindering an efficient malaria control.[11]

In 2018 the total funding for malaria control and eradication reached US$ 2.7 billion, with 30% of this funding being provided by the governments of endemic countries. The region where more fundings were expended was AFR, with nearly 75% of the total funding. Next to the AMR (7%), SEAR (6%), EMR and WPR (5% each).[5]

I.1.1 *Plasmodium* Life Cycle

Plasmodium life cycle (**figure I.3**) begins with a bite of an infected female *Anopheles* mosquito in a vertebrate host, when taking a blood meal. In this process, the mosquito injects saliva containing the parasite's sporozoites that will migrate to the bloodstream in order to reach the liver, beginning the asymptomatic liver stage (LS) that lasts about 6 days.[12,13] Here, the sporozoites roam through several hepatocytes, the constituent cells of the main parenchymal tissue of the liver, until they invade a last hepatocyte. At this point, the sporozoites will mature into schizonts. After maturation, each schizont bursts into thousands of merozoites.[12,13] In the species *P. vivax* and *P. ovale*, some hepatic sporozoites develop into hypnozoites, a latent parasitic form that stays dormant in the hepatocytes for between 2 weeks and several years before awakening to cause relapses.[3]

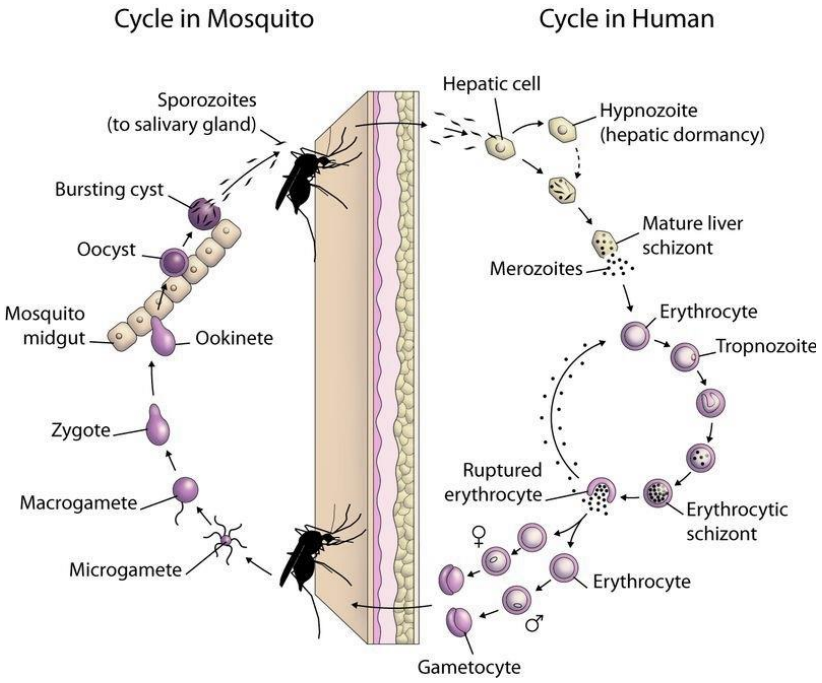

Figure I.3 – *Plasmodium* life cycle. (adapted from[14])

The merozoites are released into the blood vessels in order to infect erythrocytes and start a series of asexual reproduction cycles, starting the blood stage (BS). In the erythrocytes, the merozoites develop into trophozoites (ring stage), which will give rise to new schizonts. The schizonts will origin several new merozoites, which will be released into the blood stream, destroying the erythrocyte host in the process. Each new merozoite invades a fresh erythrocyte and this cycle repeats multiple times.[12] This asexual replication cycle is associated with the symptoms of malaria, more specifically, when the number of merozoites reaches around 100 million.[3,15] It is in the red blood cells (RBC) that the parasites evade the host immune system and feed on the hemoglobin to gather the nutrients it requires to grow and develop, spending most of its life cycle on this cell type.[15,16]

Over the blood schizogony some merozoites, about 1%, differentiate into female and male gametocytes[17], to be taken up by a female *Anopheles* mosquito during a following blood meal. Once in the mosquito midgut, the gametocytes mature and subsequently develop into the respective gametes. Here, each male gamete fertilizes a female one, giving origin to the zygote. Following this process, the zygote differentiates into the ookinete, a motile zygote, which will cross the mosquito midgut wall, to evolve into an oocyst and produce thousands of sporozoites. Once the sporozoites maturate, they migrate to the mosquito salivary glands, to be able to infect a new vertebrate host on a posterior blood meal.[13,17]

I.1.2 Treatment and Diagnosis

While the vertebrate host suffers sequelae from bearing the parasite, the same does not occur to the mosquito vector. The pathogenic effects are caused by the destruction of erythrocytes due to the hemoglobin consumption by the parasite blood stages[18], which are exclusive to the vertebrate host.

Usually, malaria symptoms appear 10 to 15 days after being transmitted. Malaria first symptoms are common to many other febrile illnesses, which are: headache, chills, fever and vomiting. Due to this fact, the symptoms may be mild and difficult to diagnose as malaria. When not treated within the first symptomatic 24 hours, the infection can progress to severe malaria and periodically lead to death.[19]

Severe malaria is often caused by *P. falciparum* and its most common symptoms in children are severe anaemia, respiratory distress and hypoglycemia, while in adults the symptoms are jaundice and multi-organ failure. Moreover, cerebral malaria and acidosis can occur to all age groups suffering from severe malaria.[3,19]

In addition to the goal of treating this disease, it is desirable to diagnose malaria as soon as possible after the infection in order to decrease transmission. The standard laboratory diagnosis for malaria is through microscopic examination of blood films, which is economic, rapid and efficient. Two sorts of blood films can be used: thin blood films, which preserve the parasite's appearance, and allow to confirm the parasite species; and thick blood films, which are more sensitive and are used to screen the presence of malaria parasite, even in low levels of infection. There are many other diagnosis methods for malaria, such as polymerase chain reaction (PCR), microarray, etc.[20]

I.1.3 Falcipain as a target

One of the most relevant BS targets are the Falcipains (FP). These enzymes are papain-family cysteine proteases of the *P. falciparum*, predominantly expressed in the

BS of the parasite life cycle. There are four FPs, Falcipain-1 (FP-1); Falcipain-2 (FP-2); Falcipain-2' (FP-2'), which is nearly identical to FP-2; and Falcipain-3 (FP-3).[21,22]

FP-1 exists in low quantity and does not exhibit any role in hemoglobin degradation, by which will not be referred to henceforward. On the other hand, FP-2, FP-2' and FP-3 are mainly expressed in the digestive vacuole (DV)[21–23], where they hydrolyze the host erythrocyte hemoglobin in order to supply amino acids to the parasite proteic synthesis, and gather energy to sustain the parasite metabolic needs.[21,23] Moreover, FP-2 is the first to be synthetized in the erythrocytic cycle, being expressed in early trophozoites, whilst FP-2' and FP-3 are mostly expressed in late trophozoites and early schizonts.[21] However, FP-2 and FP-3 are the most essential enzymes in the erythrocytic forms.[22]

FP-2 is highly responsible for the hemoglobin hydrolysis, both directly and through activation of the plasmepsins. Moreover, FP-2 has the essential role to cleave ankyrin and protein 4.1. The cleavage of these proteins leads to the release of the mature merozoites through the RBC membrane disruption. FP-2 is considered the main target for antimalarial drug design.[21–23]

The inhibition of these proteases leads to interruption of hemoglobin hydrolysis, a crucial process for the parasite survival. This interruption stops the parasite development and eventually leads to its death.

Cysteine protease inhibitors are known to contain an electrophilic moiety (Michael acceptor groups), such as vinyl sulfones, halomethyl ketones and arylnitriles.[21,23,24] These electrophilic functionalities suffer a nucleophilic attack from the sulfur atom present in the active site cysteine, forming a covalent thioimidate adduct, thus inhibiting the enzyme.[25,26] However, moieties with strong electrophilicity have an increased susceptibility to carry out side reactions, due to their pronounced reactivity.[21]

I.1.4 Compounds with antimalarial activity

Despite the many efforts made to treat malaria, therapy efficacy remains compromised primarily due to the development of drug-resistant strains of malaria parasites. As there is drug-resistance for most available antimalarial drugs, it is required to design new antimalarials in order to overtake this problem.[27] The use of antimalarial combined therapy has been practiced to delay the development of drug resistant parasites and increase the efficacy of antimalarial treatments.[28] A possible definition for antimalarial combined therapy is: simultaneous use of more than one antimalarial drug with different targets in the parasite and independent modes of action.[29]

Traditionally, the development of antimalarial drugs has been focused on the BS. Due to the different metabolism and biology between the LS and BS parasites, generally, drugs conceived to inhibit the BS have no effect in the hepatic stage.[30]

Moreover, despite the disclosure of genes and proteins expressed in the LS keeps increasing, the knowledge about the complex biology of *Plasmodium* spp. pre-erythrocytic stages is limited due to the difficulty in studying this stage of the parasites. Thus, very few drugs are available to the LS, such as primaquine **2** (PQ) (**figure I.4**), which is also one of the few drugs with hypnozontocidal activity.[13,31]

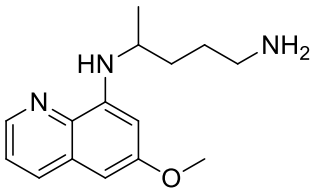

2

Figure I.4 – Structure of primaquine (PQ) **2**.

It is highly desirable to target the hepatic stage, as this is an obligatory step in the parasite maturation and replication; the number of hepatic parasites is considerably low comparing to the blood parasites number, decreasing the possibility of drug resistance development; the transmission would also be disrupt; and the LS is the appropriate target to hinder the formation and eradication of the dormant forms, the hypnozoites.[13] Furthermore, the complete inhibition of hepatic stage parasites maturation would lead to an efficacious prophylaxis.[32]

I.1.4.1 Quinolinemethanols

Quinolines are aromatic compounds containing two fused rings with a nitrogen atom, instead of a carbon. Quinine **3** (**figure I.5**), a natural quinoline, was the first documented drug used to treat malaria.[33]

Quinine is an alkaloid found in the bark of cinchona tree. It is known to be used as an antimalarial drug at least since the 17th century, however quinine was only isolated two centuries later.[12,34] This compound acts only in the asexual parasites of the BS, allowing the transmission cycle to continue. Nonetheless this alkaloid is an efficient antimalarial, interfering on the hemozoin polymerization process.[34] Nowadays it is recommended to use quinine in combined therapies, as second-line treatment.[35]

During the Vietnam War, US soldiers kept dying from malaria due to CQ-resistant parasites. To counteract this, the US government funded the largest drug discovery programme at the time. After the war, two antimalarial drugs with activity in CQ-resistant strains, mefloquine **4** (commercialized as Lariam) and halofantrine **5** (commercialized as Halfan) (**figure I.5**), were discovered.[36] Both drugs have prophylactic activity and are also blood schizonticides, which mechanism of action (MoA) are thought to be similar to quinine.[37,38] Besides, neither quinine nor halofantrine may be effective against mefloquine-resistant strains.[39]

Due to severe adverse effects, both these drugs became a concern to the pharmaceutical community. Mefloquine is a chiral molecule, its (+) enantiomer is responsible for the antimalarial activity, while the (–) enantiomer binds to adenosine receptors in the central nervous system (CNS) causing neurological side effects, such as acute anxiety, depression and hallucinations. Due to these effects, mefloquine has been discontinued.[38,40] Halofantrine is a phenanthrene related to quinine. Its significant cardiotoxicity can cause cardiac arrhythmias, making halofantrine no longer recommended to treat, or prevent malaria.[41]

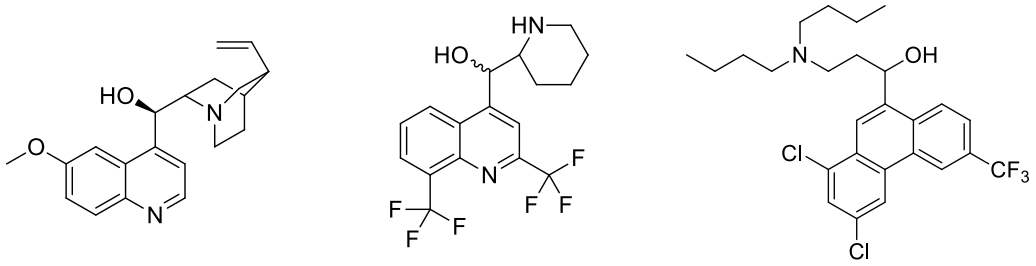

3 **4** **5**

Figure I.5 – Structures of quinine **3**, mefloquine **4** and halofantrine **5**.

I.1.4.2 4-Aminoquinolines

Several quinolines with an amino moiety at the fourth position are described to have antimalarial activity, such as CQ **1** (**figure I.1**) and amodiaquine (ADQ) **6** (**figure I.6**).[42] CQ was the first drug produced at a large scale in order to treat and prevent malaria, after WWII. It is a blood schizonticide, acting only in the stages where hemoglobin digestion occurs.[39]

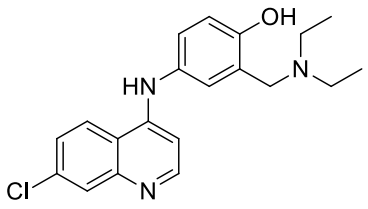

6

Figure I.6 – Structure of amodiaquine (ADQ) **6**.

During the BS, the parasites hydrolyze the hemoglobin from the host erythrocyte, to obtain amino acids for their intraerythrocytic growth and multiplication. Digestion of hemoglobin occurs in the parasite DV and produces free Fe(III)heme, a toxic by-product.[43] This by-product, also called α-hematin, or ferriprotoporphyrin IX (FPIX), is the non-proteic component of hemoglobin, which inhibits enzymes and destabilizes membranes, leading to parasite death. To counteract the FPIX build-up, the parasite crystalizes at least 95% of it into hemozoin (malaria pigment), which is insoluble and inert.[43] Hemozoin crystals consist in dimeric Fe(III)heme (named β-hematin) linked through hydrogen bonds (**figure I.7**). In its dimeric form, the ferric iron

of each α-hematin moiety is chelated onto a carboxyl side chain of the adjacent moiety.[39]

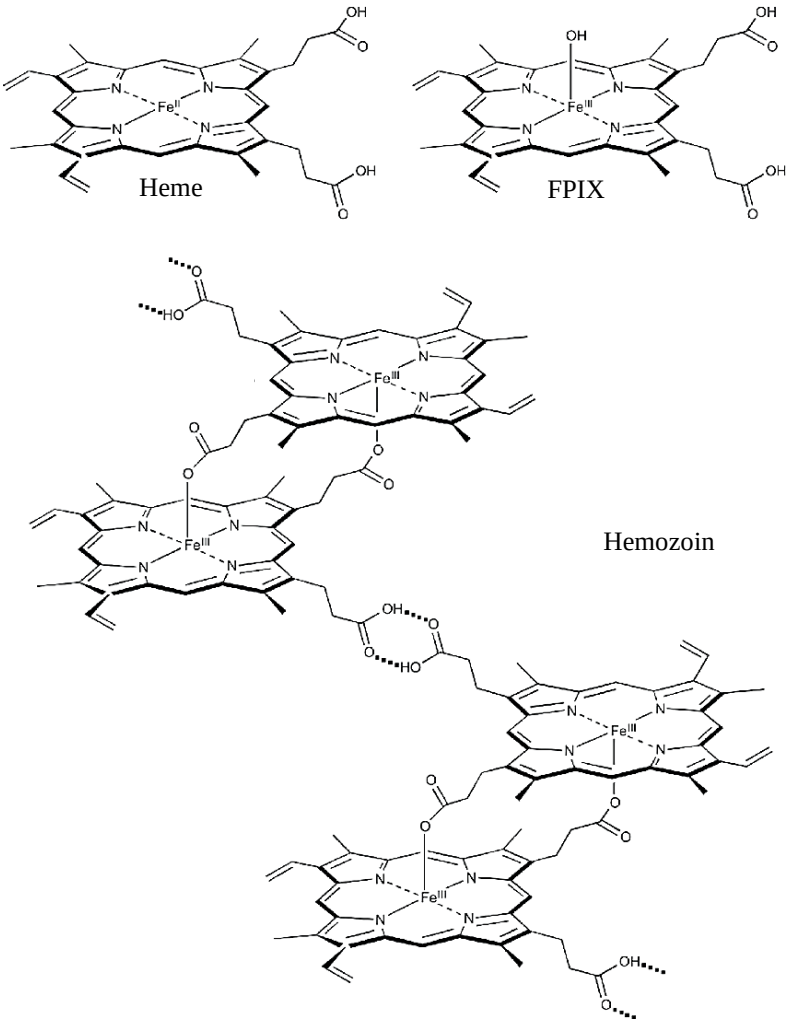

Figure I.7 – Chemical structures of heme, FTIX and hemozoin. (adapted from[44])

CQ is a diprotic weak base ($pK_{a1} = 8.1$, $pK_{a2} = 10.2$ at 37ºC) that can exist in its unprotonated, monoprotonated and diprotonated forms. At physiological pH about 10% of CQ is unprotonated. In this state, CQ is able to diffuse freely across membranes to acidic environments such as the DV, which is kept at pH ~ 5 in order to maintain the desired activity of the enzymes within. Once inside the DV, CQ protonates and loses its ability to diffuse out freely, thus being trapped inside this acidic organelle. Due to the H^+ ions trapping by CQ, the pH inside DV suffers an elevation, leading to more H^+ ions to be pumped inside the vesicle to re-establish de acidic pH. Thus, the more H^+ ions are pumped into the DV, more CQ will diffuse into this organelle due to the difference between the two pH gradients. This leads to an irreversible build-up of CQ inside the DV in a concentration > 100-fold excess, compared to the environment outside this vesicle.[33,45]

After entering the DV, CQ forms a complex with FPIX that causes a dose-dependent inhibition of hemozoin polymeration and thereby an increase of free

Fe(III)heme. The free Fe(III)heme, which is mainly in the uncharged protonation state when in low pH, diffuses out of the DV to the cytoplasm, where is deprotonated to form an anionic species. Out of the DV, free Fe(III)heme associates with various organelle membranes, leading to membrane destabilization and consequently to parasite death.[43]

For being so advantageous, CQ was widely used to treat malaria. This molecule was very effective against malaria, cheap and safe even for children and pregnant women.[46] Due to its extensive use, parasite strains resistant to CQ started to emerge. Nowadays CQ nearly has no effect in many malarious regions.[47] The resistance to this drug is caused by a mutation in the *Plasmodium falciparum* chloroquine resistance transporter (PfCRT), present in the DV membrane. This mutation allows the PfCRT to actively transport diprotonated CQ out of the DV to the cytoplasm, preventing the drug to achieve therapeutic concentrations inside this acidic vesicle.[48,49] In *Plasmodium* strains without this mutation the CQ efflux also occurs, although it happens much slower, enabling the drug to accumulate inside the DV.[50]

ADQ is an antimalarial drug with similar structure and activity to CQ, although it is effective against some strains resistant to CQ.[51] Like CQ, ADQ is a blood schizonticide that interferes with hemoglobin digestion. Besides that, ADQ inhibits gametocyte maturation/gamete exflagellation through a distinct mechanism, granting ADQ dual-activity.[17] Nowadays it is recommended to take ADQ in a combined therapy with artesunate to treat uncomplicated malaria, so that the risk of drug resistance emergence is reduced regarding to monotherapy.[52] Artesunate is an endoperoxide, a drug class that will be covered later.

The first 4-aminoquinoline to exhibit significant activity against LS parasites was the fluoroaminoquinoline **7** (**figure I.8**) with outstanding inhibitory activity *in vitro* (IC_{50} = 0.31 µM). *In vivo*, compound **7** at 80 mg/kg reduced the parasite liver load by 92%. Additionally, this compound has activity against asexual BS parasites.[53]

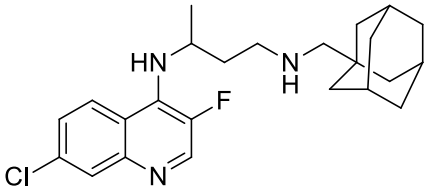

7

Figure I.8 – Structure of fluoroaminoquinoline **7**.

I.1.4.3 8-Aminoquinolines

Methylene blue (MB) **8** (**figure I.9**) was the first synthetic drug used to treat malaria, in 1891. It is a synthetic water-soluble dye that is selectively absorbed by malaria parasites.[33] This drug stopped being used as an antimalarial drug since new and

better antimalarials started being developed. Nonetheless, when *P. falciparum* glutathione reductase was acknowledged as a drug target, the interest in MB as an antimalarial resurged, because of its inhibitory activity to this enzyme.[54]

After several substitutions on MB, which improved antimalarial activity significantly, pamaquine **9** (**figure I.9**) was synthetized in 1925. Although pamaquine does not have prophylactic activity, it prevented malaria relapse, thus showing activity against the hypnozoites. However this drug causes severe side effects in the CNS, therefore it is no longer recurrently used.[55,56] Further investigations on molecules of similar structure lead to the discovery of PQ **2**.[33]

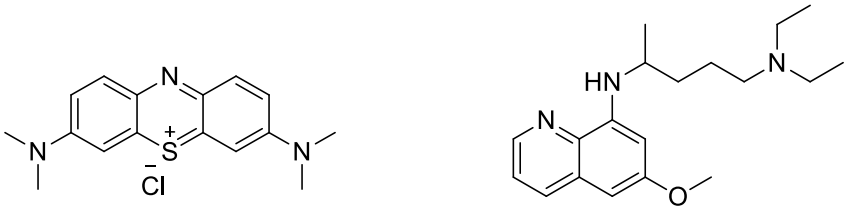

8 **9**

Figure I.9 – Structures of methylene blue (MB) **8** and pamaquine **9**.

PQ is active against BS parasites, including the gametocytes, and LS parasitic forms, including the hypnozoites, thus preventing relapses from *P. ovale* and *P. vivax*.[13,57] WHO recommends dosages between 0.25 and 0.5 mg/kg/day of primaquine for 14 days to achieve radical cure.[58] On the other hand, PQ causes methemoglobinemia, which induces hemolytic anemia, mainly in glucose 6-phosphate dehydrogenase (G6PD) deficient individuals.[57]

Although PQ has been used against malaria for several decades, its MoA in LS parasites was poorly known. Recently, a work published by Camarda, *et al* shows a possible MoA for PQ.[59] It is showed that PQ suffers oxidation via CYP2D6 (cytochrome P450 2D6) and cytochrome P450 reductase (CPR) generating the hydroxylated metabolite, 5-hydroxy-PQ (5-HPQ) **10**, which through spontaneous oxidation originate 5-quinoneimine (5-PQQI) **11** (**figure I.10**). On the other hand, 5-PQQI is reduced to 5-HPQ by CPR, creating an oxidation/reduction cycle. Along with 5-PQQI formation, H_2O_2 is generated. Due to the oxidation/reduction cycle, H_2O_2 accumulates on the liver and bone marrow (predominant metabolic transformation sites) and acts as anti-parasitic through damage of Fe- and FeS-containing proteins, or generation of superoxide and hydroxyl radicals. This mechanism does not involve direct parasite targets which can explain the lack of PQ resistance.[59] Additionally, PQ MoA to gametocytes and hypnozoites is also very unclear, but it is thought to be through interference with the electron transport chain.[13]

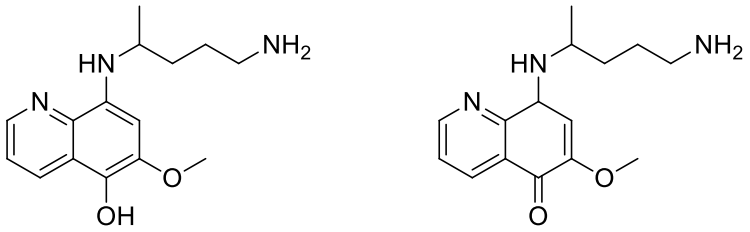

10 **11**

Figure I.10 – Structures of PQ metabolites, 5-hydroxy-PQ (5-HPQ) **10** and 5-quinoneimine (5-PQQI) **11**.

Tafenoquine (TQ) **12** (**figure I.11**), a derivative of PQ, was synthetized in 1979, and similarly to its original, TQ has activity against BS and LS parasites, including hypnozoites. In 2018 the use of TQ was indicated by the FDA for prevention and treatment of malaria relapses caused by *P. vivax*,[60,61] although compared to PQ anti-relapse activity, TQ has lower efficacy.[62] On the other hand, TQ showed to be 9 times more active against the BS than PQ.[63] Despite the fact compound **12** has a longer half-life time than PQ, their toxicities are identical. Thus, TQ is also not a drug designated for administration on patients with G6DP deficiency.[60,62] Additionally, similarly to PQ, TQ is activated by CYP2D6 to fulfill its MoA.[63]

NPC1161C **13** (**figure I.11**) consists in a racemic mixture of hypnozontocide 8-aminoquinolines with a core similar to the TQ core. NPC1161B, the (–) enantiomer, showed increased efficacy *in vitro* and *in vivo*, compared to compound **2** and NPC1161A, the (+) enantiomer. NPC1161B had an ED_{100} = 1 mg/kg in *P. berghei in vivo* prophylaxis mouse model, while PQ exhibited an ED_{100} = 20 mg/kg. The (+) enantiomer is much more toxic than the (–) enantiomer.[13,64] In 2014, the further development of this drug was depending on the possibility of this compound causing hemolytic anemia in individual with G6PD deficiency.[64] It was not found more recent literature relatively to this issue. Additionally, NPC1161B transmission-blocking activity was tested, and was discovered that when infected mosquitoes were treated with this compound, their salivary glands were free of sporozoites. Thus, making these mosquitoes non-infectious.[65]

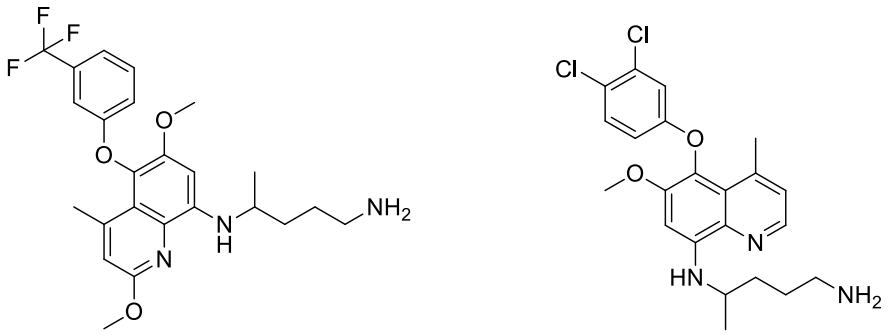

12 **13**

Figure I.11 – Structures of tafenoquine (TQ) **12** and NPC1161C **13**.

To oppose the fact most 8-aminoquinolines are unsuitable for G6PD deficient individuals, has been considered to take drugs from this compound class in combined therapies with drugs from other classes. This method aims to potentialize radical cure while softening the hemotoxicity, through reduction of 8-aminoquinolines dosage.[60]

I.1.4.4 Antifolates

Pyrimethamine (PYR) **14** and proguanil **15** (**figure I.12**) are dihydrofolate reductase (DHFR) inhibitors with activity to the erythrocytic stages, generally used in CQ-resistant strains and in combination with sulfadoxine **16** and atovaquone **17** (**figure I.13**), respectively.[13,66,67] Inhibition of this enzyme prevents the tetrahydrofolate production, which is needed for amino acid synthesis, thus killing the parasite.[68] However, there are resistant strains to both drug combinations.[66,69] In addition, both compounds **14** and **15** are active against hepatic schizonts, although they don't have hypnozontocidal activity. The PYR and proguanil activity against hepatic parasites is improved when these are used in combination with azithromycin **18** (**figure I.13**) and atovaquone **17**, respectively.[13]

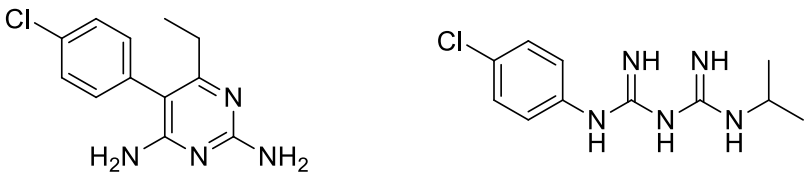

14 **15**

Figure I.12 – Structures of pyrimethamine (PYR) **14** and proguanil **15**.

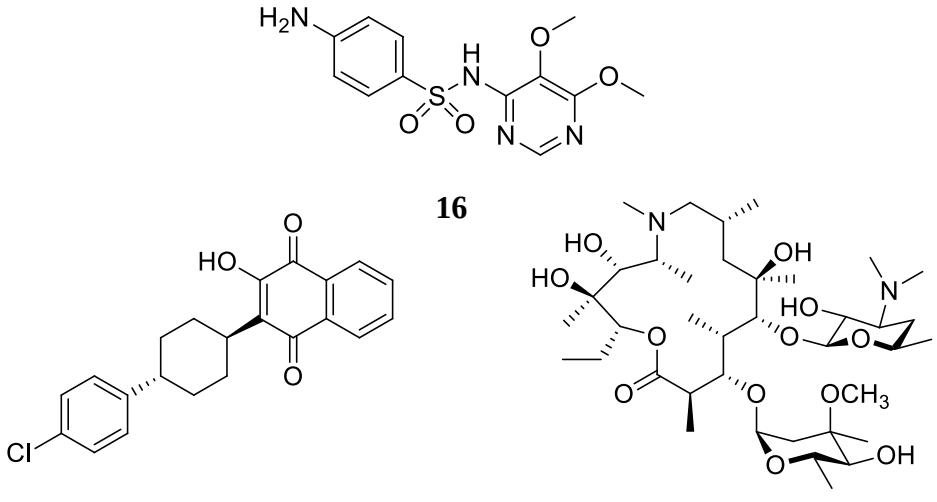

16

17 **18**

Figure I.13 – Structures of sulfadoxine **16**, atovaquone **17** and azithromycin **18**.

I.1.4.5 Pyrimidines

Pyrimidine-based compounds are another example of antimalarials. Usually these compounds target the BS. PYR **14** (**figure I.12**), an antifolate showed earlier, is also a pyrimidine-based drug. By studying several inhibitors of DHFR, the hybrid P218 **19** (**figure I.14**), which is an efficient and selective inhibitor of *P. falciparum* DHFR, was identified. This hybrid compound showed strong antimalarial activity to a resistant strain, with an EC_{50} = 56 nM *in vitro*.[23]

Several triazolopyrimidines have exhibited good antimalarial activity through inhibition of dihydroorotate dehydrogenase (DHODH). Further structure optimization led to the compound DSM265, **20** (**figure I.14**), which has good bioavailability, and great efficacy towards the *P. falciparum* DHODH (IC_{50} = 0.033 µM), comparing to the human DHODH. However its solubility did not reach desirable values.[23]

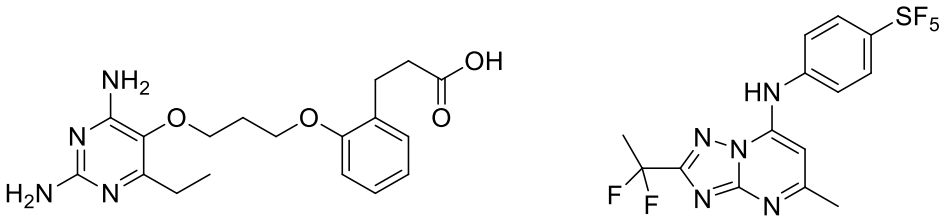

19 **20**

Figure I.14 – Structures of P218, **19** and DSM265, **20**.

Another target of pyrimidine-based compounds in the BS is the FP-2. Among these, 5-substituited-2-cyanopyrimidines exhibit the most promising results. The compounds **21** and **22** (**figure I.15**) showed IC_{50} values inferior to 0.5 nM against FP-2. Additionally, these compounds were also active against CQ-resistant strains of *P. falciparum*.[23]

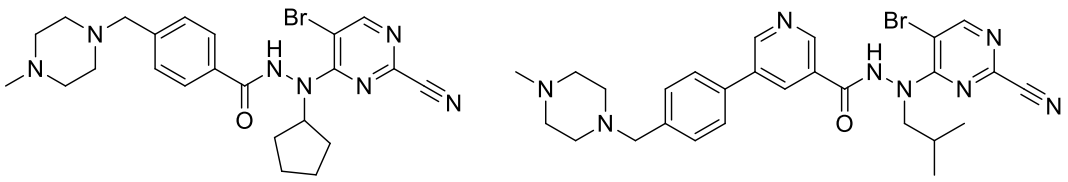

21 **22**

Figure I.15 – Structures of 2-cyano-5-bromopyrimidines **21** and **22**.

I.1.4.6 Endoperoxides

Endoperoxides are heterocycles containing peroxide residues (-O-O-). It is thought that the bioactivation of endoperoxides is caused by the Fe(II) of heme present in the parasite DV, leading to breakup of the peroxide bond. This event releases oxygen

centered radicals that, through rearrangement, form carbon centered radicals. Both these radical species may alkylate heme and other essential biomolecules for the parasite survival, such as DNA and proteins; inhibit parasitic enzymes, such as PfATP6; cause damage to the parasitic membrane; and disrupt the mitochondrial electron transport chain, leading to parasite death.[70] Nonetheless, endoperoxides generally only have antimalarial activity against BS parasites.[71]

Endoperoxides are toxic to both parasites and mammals. Whereas the parasite suffers toxicity at range of nanomolar concentrations, the mammals require micromolar concentrations. The selectivity of this compound class to the parasite is due to the high concentration of free Fe(II) present in the DV, compared to the low levels in mammal cells; and the increased uptake of these compounds by the parasite, thus ensuring the safety of antimalarial endoperoxides usage.[72,73]

Artemisinin (ART) **23** (**figure I.16**), isolated from the Chinese *Artemisia annua* in 1972, is a sesquiterpene lactone with a peroxide group. Its therapeutic use was first recorded around the 4th century.[73] Due to its short half-life time and high rate of recrudescence, nowadays ART is not used to treat malaria. Instead several derivatives (**figure I.16**) with longer half-lives have been developed, such as dihydroartemisinin (DHA) **24**, artemether **25**, arteether **26**, and artesunate **27**.[74] As mentioned before, artesunate is used in combined therapy with ADQ.[52] ART and derivatives are only active against the BS, both its asexual and sexual forms, at nanomolar concentrations.[70,73] ART bioactivation occurs inside the DV, the same way described for endoperoxides in general. The binding of Fe(II) to one of the endoperoxide oxygens of ART causes conformational changes leading to the cleavage of the peroxidic bond.[75]

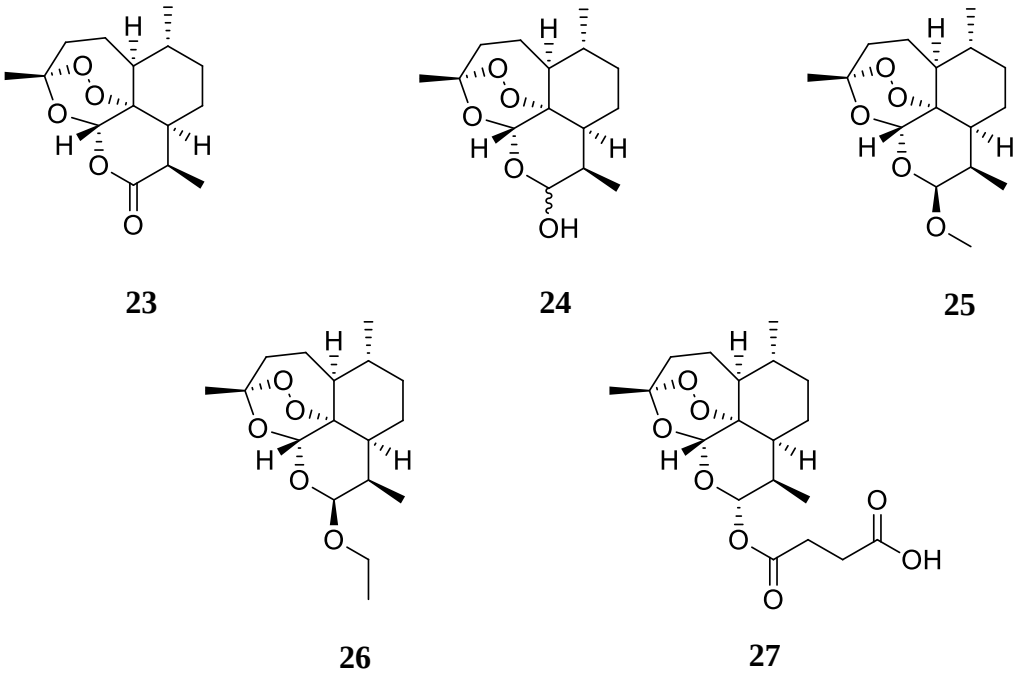

23 **24** **25**

26 **27**

Figure I.16 – Structures of artemisinin (ART) **23**, and its derivatives dihydroartemisinin (DHA) **24**, artemether **25**, arteether **26** and artesunate **27**.

Depending on which oxygen the Fe(II) binds, ART can lead to either a primary or secondary carbon centred radical (**Scheme I.1**). In both cases is firstly formed an oxygen centred radical, which rearranges into a carbon centred radical. When Fe(II) binds to oxygen 1, consequently occurs an electron transference which leads to scission of the bond between C3 and C4, producing a primary carbon centred radical. On the other hand, when Fe(II) binds to oxygen 2, one of the C4 protons undergoes a migration to oxygen 1 and gives rise to a secondary carbon centred radical. [70]

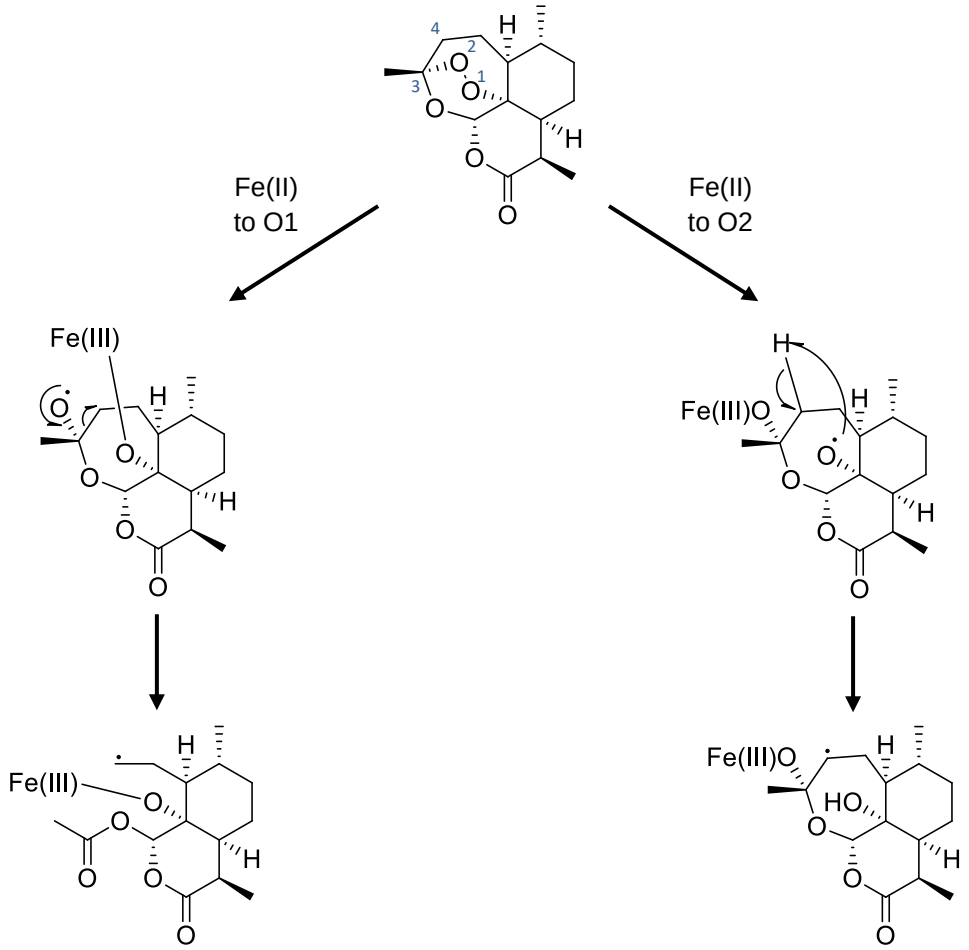

Scheme I.1 – ART activation mechanism by Fe(II)

Despite the heme iron is thought to be responsible for the bioactivation, there is evidence showing that intracellular iron is needed for the bioactivation of ART. In 2007, a group of scientists demonstrated that when ART was in the presence of desferrioxamine (an iron chelator selective for non-heme iron), its antimalarial efficacy was neutralized.[76] Nevertheless, a recent study confirmed the activation of endoperoxides by heme Fe(II)[77], thus some authors suggest that ARTs are activated by heme iron, while the free iron may increase this compounds activity.[78]

ART radicals react with proteins containing accessible nucleophiles, neutral membrane lipids and heme. ART radicals alkylate several housekeeping proteins, causing the protein ubiquitination levels to rise, as a sign of protein damage. It is thought that ART radicals cause accumulative damage to multiple important functional

pathways. When this damage is beyond repair the parasite dies.[75] It was discovered that ART radicals accumulate in neutral lipid membranes, inducing oxidative damage to these. The organelles thought to suffer early damage due to ART radicals are the endoplasmic reticulum (ER), the mitochondrion and the DV. Despite many of ART radicals interactions being known, there is no consensus in a specific target.[70,75]

In order to avoid the rise of resistant strains to ART and its derivatives, in 2006 WHO recommended the use of Artemisinin Combination Therapy (ACT) as first-line treatment.[35] Resistance to ART and its derivatives has emerged prior to 2001 in Southeast Asia, before the widespread of ACT. Nowadays 5 countries are threatened with resistance to artemisinins. In 2013 it was discovered that mutations on the protein Kelch 13 were correlated to artemisinins resistance.[75,79,80]

After the recognition of the endoperoxide linkage as the pharmacophore of ARTs, the interest in molecules containing this functionality rose. Also, the need to improve artemisinins activity profile and the emergence of resistance to these compounds led to the development of trioxanes, trioxolanes and tetraoxanes, particularly 1,2,4-trioxanes **28**, 1,2,4-trioxolanes **29** and 1,2,4,5-tetraoxanes **30** (**figure I.17**).[81,82]

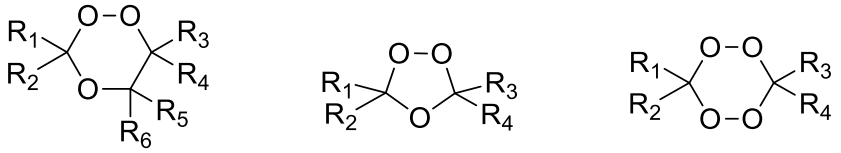

28 **29** **30**

Figure I.17 – General structures of 1,2,4-trioxanes, **28**, 1,2,4-trioxolanes **29** and 1,2,4,5-tetraoxanes, **30**.

These molecules are generally associated to low cytotoxicity and maximum tolerated doses relatively high. When compared to their trioxane counterpart, tetraoxanes show higher antimalarial activities, however some cases exhibited not so good blood stability and pharmacokinetic profiles.[82] Additionally, 1,2,4,5-tetraoxanes with adamantyl substituents tend to have an improved structure stability and antimalarial activity.[83] The bioactivation and MoA of tetraoxanes, trioxolanes and trioxanes occurs as described for ART. Nevertheless, it has been suggested that several tetraoxanes do not form carbon centered radicals, being the oxygen centered radicals accountable for the damage caused to the parasite.[84]

In 2010, O'Neill and co-workers found a tetraoxane, RKA182 **31** (**figure I.18**), with IC_{50} = 0.87 nM. This compound also exhibited exceptional stability and ADME properties, along with low toxicity, outstanding the activity profile of the previous synthetic and semisynthetic antimalarial endoperoxides.[85] Another 1,2,4,5-tetraoxane with great antimalarial activity is TDD E209, **32** (**figure I.18**). This compound exhibited efficacy to multidrug-resistant parasite strains and cure rates above 65% after a single oral dose of 30mg/kg in *in vivo* experiments.[86]

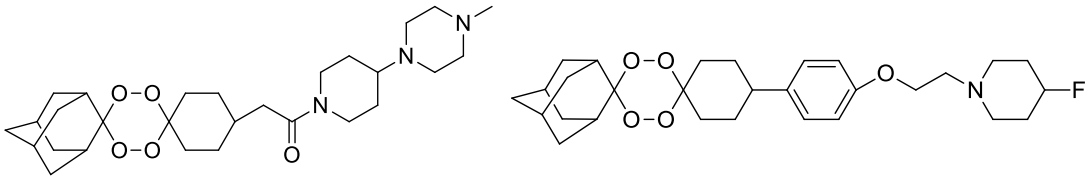

31 **32**

Figure I.18 – 1,2,4,5-tetraoxanes, RKA182 **31** and TDD E209 **32**.

I.1.4.7 Tetraoxane hybrids

After combination therapies, hybrid drugs are the next step to overcome drug resistance.[83] These drugs consist in two or more fused functional moieties with different pharmacophores in one single molecule, which each functionality acts through a different MoA, lessening the probability of resistance emerging from the parasite.[82] Hybrid compounds can trigger therapeutic responses similar to synergic drug actions, through the interaction of the several functionalities at different biological targets.[83] Tetraoxanes are used in hybrid drugs with various moieties. Some examples will be aborded below.

In 2016, two steroidal tetraoxane hybrids showed remarkable inhibitory activity to the LS *in vitro*. The steroidal tetraoxane hybrids **33a** and **33b** (**figure I.19**) had IC_{50} = 0.33 µM and IC_{50} < 1µM, respectively, and compound **33a** exhibited gametocidal activity. In *in vivo* assays compound **33a** revealed to reduce the parasite levels in hepatocytic cells by 91%, at 100 mg/kg.[53] The authors affirmed to exist a probability of the tetraoxane moiety having LS activity on its own, without further explanation to the endoperoxide bioactivation.[53]

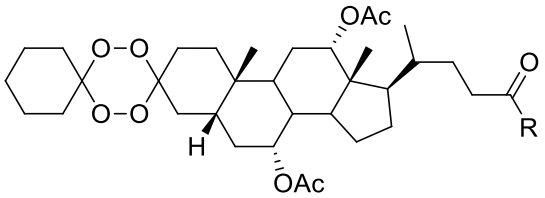

33a, R = $NH(CH_2)_2CH_3$
33b, R = OCH_3

Figure I.19 – Structures of steroidal tetraoxane hybrids **33a** and **33b**.

A series of tetraoxane-primaquine hybrids **34** (**figure I.20**) as dual-stage antimalarials, with IC_{50} in the range of 21 to 45 nM to BS, showed activity to either gametocytes or sporozoites. These hybrids also inhibited oocyst formation. Compound **34a** was the most potent, surpassing ART activity and showing complete oocyst inhibition in the mosquito midgut at a dose of 25 µmol/kg. Moreover compounds **34a**, **34c** and **34d** exhibited high potency against LS parasites, with IC_{50} values between 330 and 604 nM.[87]

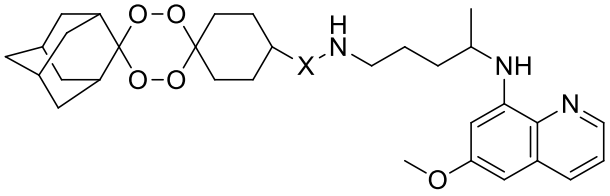

34a, X = CO
34b, X = CH_2
34c, X = CH_2CO
34d, X = ------

Figure I.20 – Structures of tetraoxane-primaquine hybrids **34a-d** as dual stage antimalarials.

Oliveira and co-workers found a series of several tetraoxane-pyrimidine nitrile hybrids as dual-stage antimalarials, which general structure, **35** is represented in **figure I.21**.

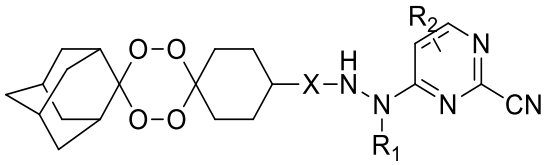

35a, R_1 = $CH_2CH(CH_3)_2$, R_2 = 5-Cl, X = CO
35b, R_1 = $CH_2CH(CH_3)_2$, R_2 = 5-Br, X = CO

Figure I.21 – Structures of tetraoxane-pyrimidine nitrile hybrids **35a** and **35b**.

All the hybrids **35**, at 10 μM concentration, inhibited the *P. berghei* hepatic stage infection almost completely. Nonetheless, the hybrids **35a** and **35b** were the most interesting. At a concentration of 2 μM, the hybrid **35a** showed the highest efficacy to the LS, inhibiting over 75% of infection. Moreover, both hybrids **35a** and **35b** exhibited the lowest IC_{50} values for FP-2 inhibition, 3.4±0.6 and 16.4±4.2 nM, respectively. The compound **35b** also exhibited great activity against a chloroquine resistant strain (CQ-R W2), showing IC_{50} = 9.8 nM.[25]

The pyrimidine nitrile moiety is a FP-2 inhibitor, acting as a Michael acceptor. Although this enzyme is not expressed on the hepatic stage, the pyrimidine nitrile moiety exhibited anti-LS activity, suggesting the presence of potential target(s) containing an active cysteine on this stage. The activity towards the hepatic stage could be associated to the tetraoxane moiety, as suggested in the work of Terzic, *et al.*.[53] However, the pyrimidine nitrile anti-LS activity was verified through observation of inhibitory activity to the hepatic stage by the pyrimidine nitrile **36** (**figure I.22**), which inhibited over 91% of the hepatic infection and lacks the tetraoxane moiety.[25]

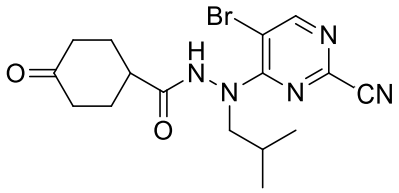

36

Figure I.22 – Structure of pyrimidine nitrile **36**.

I.1.4.8 Other molecules

The structural variety among compounds active against the pre-erythrocytic stages is quite large. There are molecules active against LS parasites in many compound classes, and these molecules can be synthetic or from natural resources.[13,88]

Several alkaloids have shown activity against LS parasites. This activity has been seen in several alkaloids with wide structural variety.[13] Compounds **37** (**figure I.23**), **38a**, **38b** and **38c** (**figure I.24**) exhibited IC_{50} = 9.2, 3.1, 4.5 and 3.3 µM against LS parasites, respectively[89,90], however compound **38a**, tazopsine, showed some toxicity. On the other hand, compound **38c**, NPC-tazopsine, had activity similar to **38a**, with the benefit of presenting considerably less toxicity.[90] Furthermore, compound **38a** demonstrated total inhibition, at 7.1 µM concentration.[91] Compound **39** (**figure I.25**), showed great inhibitory activity, inhibiting LS parasitic growth by 98.3%.[92]

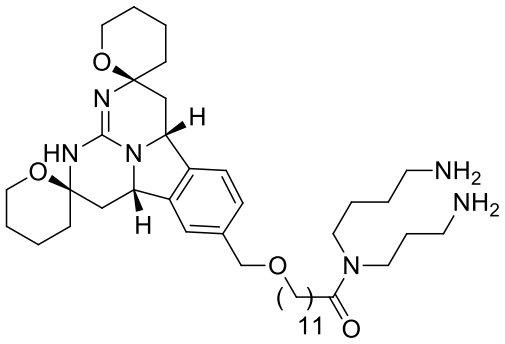

37

Figure I.23 – Structure of compound **37**.

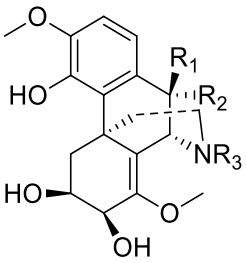

38a, R_1 = OH, R_2 = R_3 = H
38b, R_1 = R_2 = R_3 = H
38c, R_1 = OH, R_2 = H, R_3 = cyclopentyl

Figure I.24 – Structures of tazopsine **38a**, sinococuline **38b** and NPC-tazopsine **38c**.

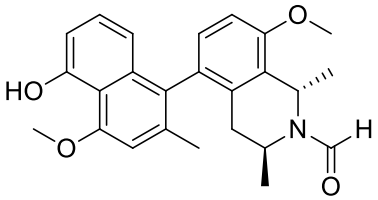

39

Figure I.25 – Structure of dioncophylline C derivative, *N*-formyl-8-O-methyldioncophylline C, **39**.

Several antihistaminics and antibiotics also have activity against LS parasites. In the end of the last century, some compounds with antimalarial prophylactic activity were found among antihistaminics. The molecules with better efficacy were cyproheptadine **40** and ketotifen **41** (**figure I.26**), which inhibited the establishment of infection in rodents, at 5 mg/kg orally for 3 days.[93]

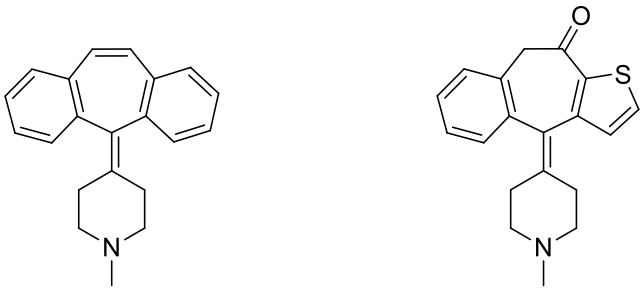

40 **41**

Figure I.26 – Structures of cyproheptadine **40** and ketotifen **41**.

The antibiotic azithromycin **18** (**figure I.13**), referred above, besides being used in combination therapies with PYR to improve its prophylactic activity, also has activity against LS parasites on its own. This antibiotic showed to be 100% effective at 160 mg/kg, and 80% effective at 40 mg/kg, through parenteral administration.[94] Another antibiotic active against hepatic parasites is rifampicin **42** (**figure I.27**), which acts through targeting the apicoplast. This organelle contains important metabolic pathways to the LS. Rifampicin has an IC_{50} = 22.2 µM against the hepatic forms of *P. yoelii*.[95] Nigericin **43** (**figureI.28**) is another antibiotic with antimalarial activity. This compound

is active against the LS and BS, exhibiting IC_{50} < 1 pM and complete inhibition on both stages. Nigericin carries its ionophoric activity by targeting K^+ channels.[96]

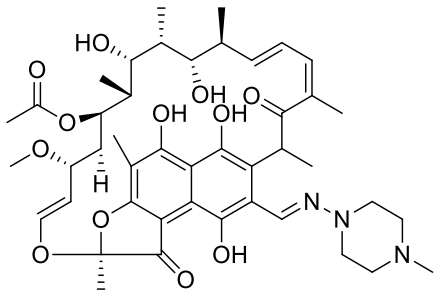

42

Figure I. 27 – Structure of rifampicin **42**.

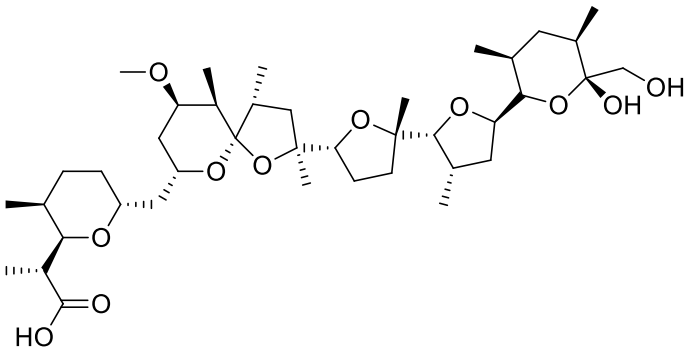

43

Figure I.28 – Structure of nigericin **43**.

Additionally, several inhibitors of the mitochondrial electron chain are other examples of compounds active to the LS. By inhibiting the parasite *bc₁* complex, these molecules destroy the mitochondrial membrane potential, interrupting the energy storage and leading to parasite death.[13,97] Atovaquone, **17** (**figure I.13**), referred above to be used in combination therapies with proguanil, is an efficient inhibitor of the *Plasmodium spp. bc₁* complex, exhibiting an IC_{50} = 3.95 nM to *P. falciparum* LS.[13] Licochalcone A **44** (**figure I.29**) is also an inhibitor of the parasitic *bc₁* complex. This compound was predicted to have high inhibitory activity to LS via virtual screening and exhibited an IC_{50} value of 0.927 nM *in vitro*.[13,96]

Furthermore, 4(1H)-pyridones **45** and 4(1H)-quinolones **46** (**figure I.30**) are chemical scaffolds of *bc₁* complex inhibitors with antimalarial LS activity.[13] The 4(1H)-quinolone, decoquinate **47** (**figure I.31**) showed to be highly potent against hepatic parasites, with an IC_{50} = 177 pM.[98]

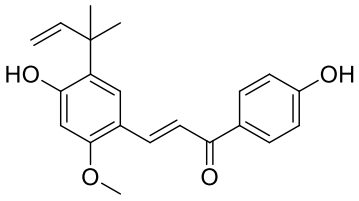

44

Figure I.29 – Structures of licochalcone A **44**.

45 **46**

Figure I.30 – General structures of 4(1H)-pyridones **45** and 4(1H)-quinolones **46**.

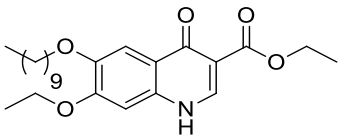

47

Figure I.31 – Structure of decoquinate **47**.

I.2 Chemical probes and click chemistry

Quoting C. Arrowsmith (2015): "A chemical probe is simply a reagent – a selective small-molecule modulator of a protein's function that allows the user to ask mechanistic and phenotypic questions about its molecular target in biochemical, cell-based or animal studies".[99] The use of chemical probes is useful to complement genetic approaches, characterize protein activity, understand MoA of molecules, follow the enzymatic functional regulation and validate drug targets.[99–101] Chemical probes can provide this information through fluorescence, intrinsic or chemically labelled.[101]

Chemical probes advantages include fast and reversible inhibition of a protein or a protein domain in living systems, can be used in most cell types, and reveal temporal characteristics of target inhibition. To achieve meaningful biological data, it is required to use, also a negative control, which consists in an inactive close derivative of the compound.[99]

Click chemistry is used as a mean to bioorthogonal reactions[99], to couple the chemical probes to fluorescent tags *in situ*.[102] This chemistry consists in a group of simple, fast, regio- and stereospecific reactions. They must be easy to purify, and the

product formation must have high yields. The pioneer and most widely used click reaction is the azide-alkyne Huisgen cycloaddition, which consists in a cooper-catalyzed 1,3-dipolar cycloaddition between an azide and an alkyne to give a 1,2,3-triazole. The specific term for this reaction is cooper(I)-catalyzed azide-alkyne cycloaddition (CuAAC)[102,103] (**Scheme I.2**).

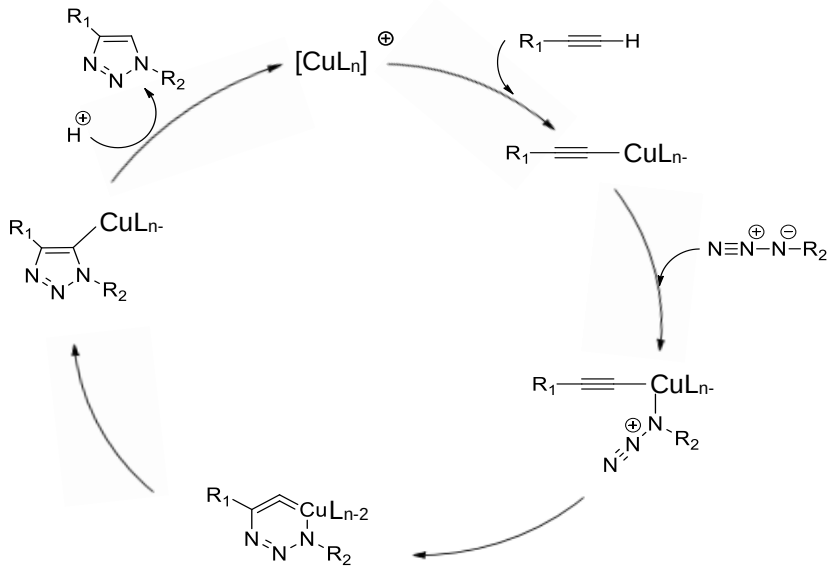

Scheme I.2 – CuAAC catalytic cycle. (adapted from[104])

I.3 Goals of the project

The large LS target diversity can be reached by a great variety of structures. Despite some LS targets being known, several targets of compounds with activity to the LS are yet to be discovered or confirmed.[13,88] Based on a previous series of tetraoxane-pyrimidine nitrile hybrids (**figure I.21**), developed in our lab by Oliveira and co-workers, the initial goal of this project was to synthetize and evaluate the biological activity of a novel tetraoxane-pyrimidine-2-(*E*)-ethyl 2-cyanoacrilate hybrid compound **48** (**figure I.32**). This hybrid compound should be activated in the DV by Fe(II) to enforce its anti-BS activity, through the release of a toxic radical (tetraoxane moiety) and the FP-2 inhibition (the pyrimidine moiety). Moreover, the pyrimidine moiety, should also present inhibitory activity to the LS, granting dual-stage activity. After its LS inhibitory activity being confirmed, to expose its MoA and identify the LS potential active cysteine containing target(s), a precursor chemical probe **49** (**figure I.33**) with an alkyne functionality[105], will be used in bioorthogonal reactions with fluorescent tags inside living *P. berghei*-infected hepatocytes. This would lead to a deeper understanding of *Plasmodium* spp. liver stage biology and help us come close to increase the fully validated LS drug target numbers.

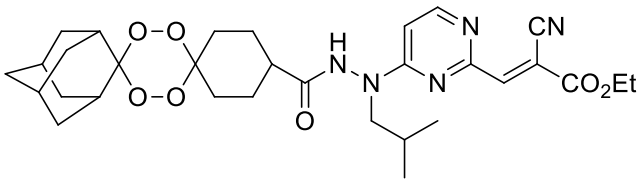

48

Figure I.32 – Structure of the novel tetraoxane-pyrimidine hybrid **48**.

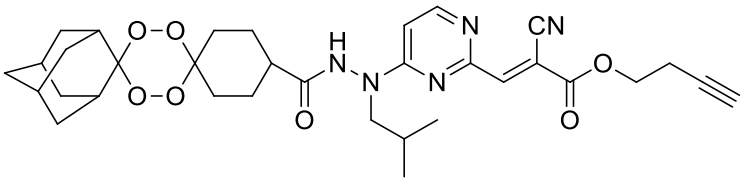

49

Figure I.33 – Structure of the chemical probe **49**.

Chapter II

II. Results and Discussion

The synthetic approach used to prepare the tetraoxane-pyrimidine-2-(*E*)-ethyl 2-cyanoacrilate hybrid was a convergent approach. Tetraoxane and pyrimidine-2-(*E*)-ethyl 2-cyanoacrilate intermediates were to be synthetized independently and coupled in a final step. The retrosynthetic pathway for the hybrid **48** synthesis is present in **Scheme II.1**.

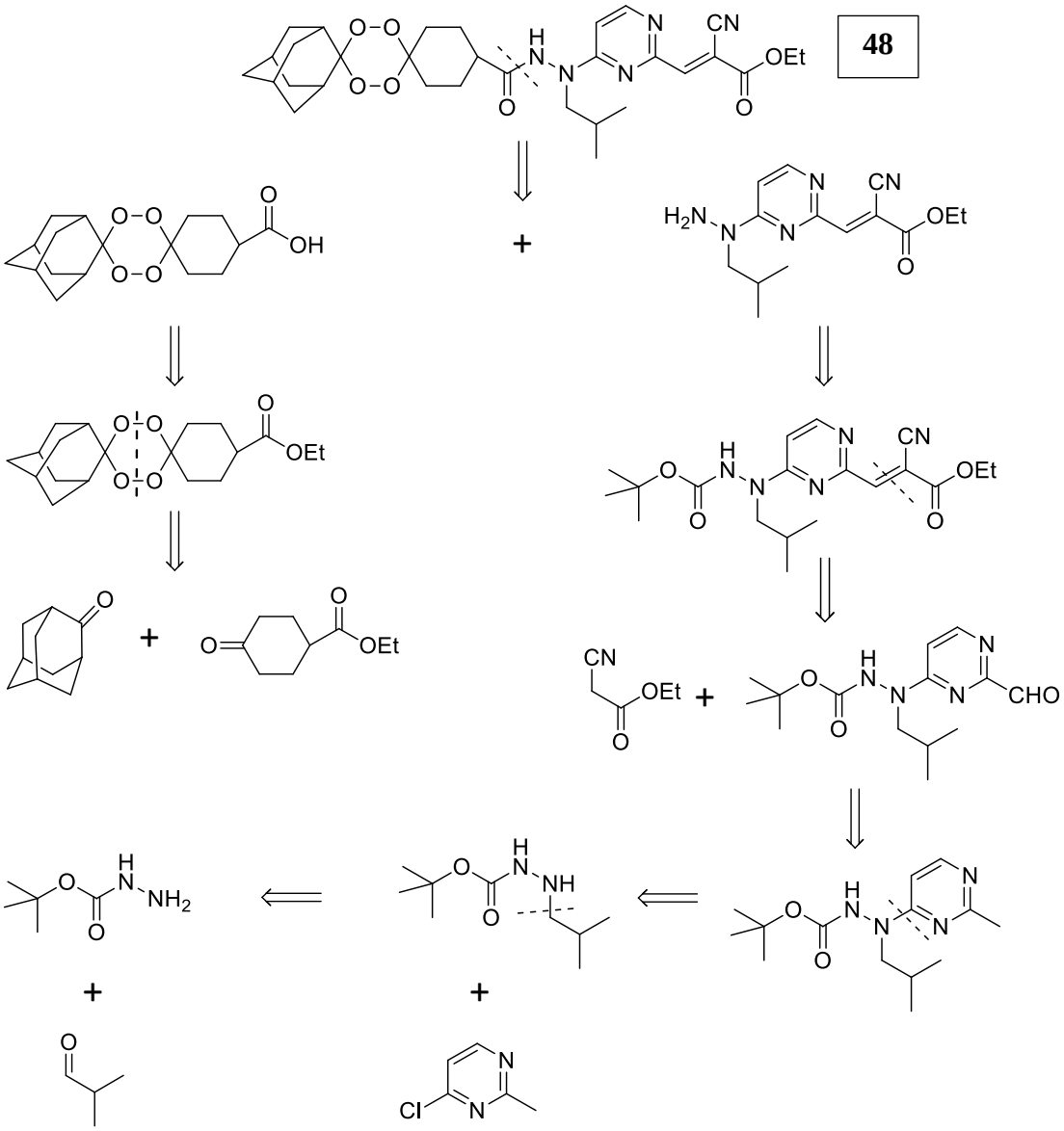

Scheme II.1 – Retrosynthetic pathway for the synthesis of hybrid **48**.

II.1 Pyrimidine-2-(*E*)-ethyl 2-cyanoacrilate

In order to synthetize the pyrimidine-2-(*E*)-ethyl 2-cyanoacrilate unit, the first step was to synthetize the intermediate hydrazine **52** through reductive amination of *tert*-butyl carbazate **50** with isobutyraldehyde, both commercially available reagents (**Scheme II.2**).

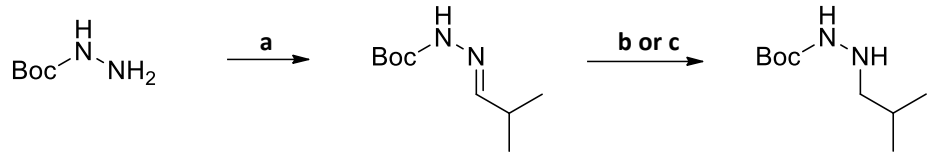

50 **51** **52**

Scheme II.2 – Synthesis of intermediate hydrazine **52**. *Reagents and conditions: (a) isobutyraldehyde, dry DCM, mol sieves 3Å, rt, 2 h, N_2 atm.;(b) H_2, Pd/C (10% by weight), dry MeOH, rt, ov; (c) $NaBH_3CN$, AcOH (75%), rt, 3 h.*

After the synthesis of the intermediate imine (**51**), the reduction was performed through two different approaches. The first was a catalytic hydrogenation using Pd/C (10% weight). This reaction gave a relatively low yield (39%) (**Annex 1 – Table VI.1**) and presented the safety disadvantage of using H_2.[25] In a second approach, the reduction was performed through the use of sodium cyanoborohydride, and showed to be more practical, safe, fast and presenting a better yield (79%) (**Table VI.1**). The product was confirmed by ^{1}H-NMR. The difference between the two intermediates, **51** and **52**, in the ^{1}H-NMR spectra (**Annex 2** – **Figure VI.1** and **Annex 3 – Figure VI.2**, respectively) could be observed by the appearance of a second broad signal at 3.90 ppm integrating to one proton, representing the hydrogen of the reduced nitrogen atom; and the replacement of the duplet at 7.02 ppm from the imine proton with a duplet at 2.62 ppm integrating for two protons that corresponds to the methylene group. The amination and both reduction approaches were performed according to the work described by Coterón and co-workers.[27]

II.1.1 Via 4-chloro-2-methylpyrimidine

The next step was to accomplish a nucleophilic aromatic substitution of hydrazine **52** in the 4-chloro-2-methylpyrimidine position 4 to synthetize compound **53**. To accomplish this synthesis, several modifications in the experimental procedure were performed in order to improve the reaction yield (**Scheme II.3**), the yields are shown in **Table VI.1**. In a first approach[27], the reaction was performed in *i*PrOH using DIPEA (**a**), which gave a yield of 13%. The second attempt (**b**) was very similar, with the use of the solvent EtOH.[72] Although the yield of the second approach was higher (42%), another reaction with a different base (K_2CO_3) and solvent (DMF) was performed (**c**) but did not lead to a yield improvement (21%).[106] So, a Buchwald amination to couple the hydrazine to pyrimidine position 4 (**d**) was performed and was successful with a

yield of 92% (**Table VI.1**) in a short amount of time. Approach (**d**) was performed according to the work described by García-Domínguez and co-workers.[107] The Buchwald amination catalytic cycle is represented in **Scheme II.4**.

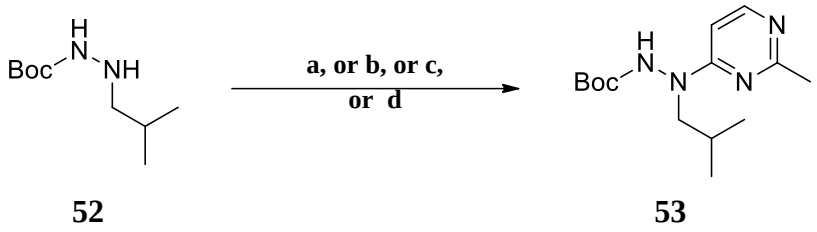

52 **53**

Scheme II.3 – Synthesis of intermediate **53**. *Reagents and conditions: (a) 2-methyl-4-chloropyrimidine, DIPEA, iPrOH, reflux, 22 h; (b) 2-methyl-4-chloropyrimidine, DIPEA, dry EtOH, reflux, 24 h; (c) 2-methyl-4-chloropyrimidine, K_2CO_3, dry DMF, reflux, 2 h; (d) Sealed tube, 2-methyl-4-chloropyrimidine, $Pd(OAc)_2$, XPhos, K_2CO_3, t-BuOH/degassed H_2O (2:1), 110ºC, 1.5 h.*

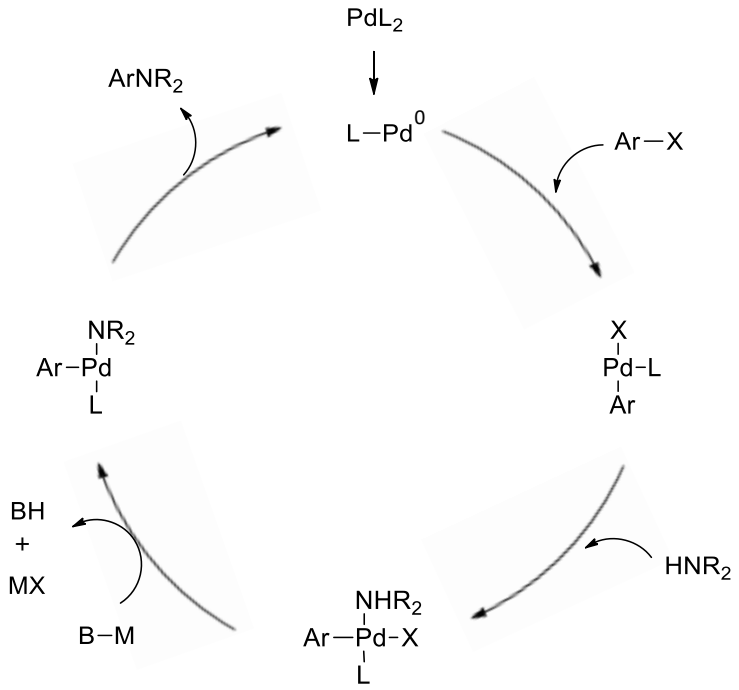

Scheme II.4 – General Buchwald amination catalytic cycle.

To achieve the intended pyrimidine-2-(*E*)-ethyl 2-cyanoacrilate intermediate **57** (**Scheme II.5**), an aldol condensation between pyrimidine-2-aldehyde **56** and ethyl cyanoacetate seemed to be the most viable path. This synthetic step, as well as the synthetic steps to achieve the intermediate **56** from pyrimidine-2-methyl **53**, consisted in modifications of the functional group present in pyrimidine position 2 and are represented in **Scheme II.5**.

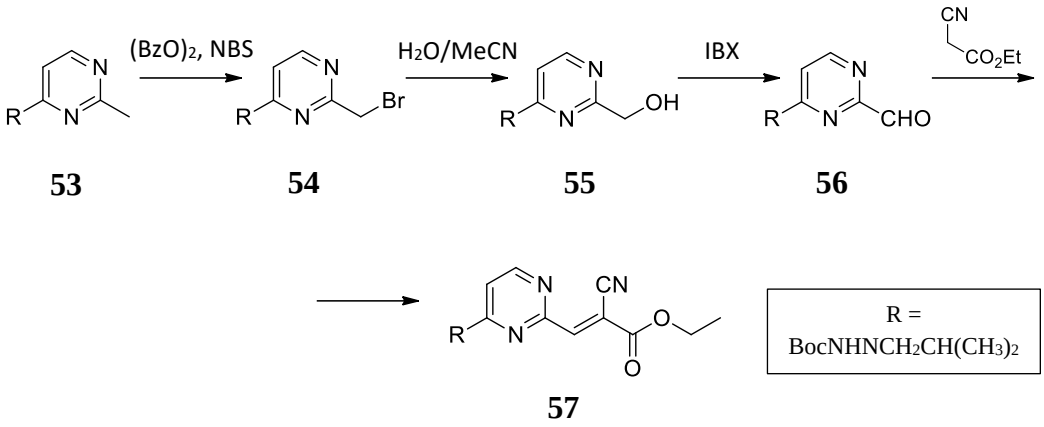

Scheme II.5 – Synthetic steps from pyrimidine-2-methyl, **53**, to pyrimidine-2-(*E*)-ethyl 2-cyanoacrylate, **57**.

The first reaction was a radical bromination, where the Br radical replaces one of the hydrogens of the methyl group in position 2 of the pyrimidine. It is known that radical halogenation, specially bromination, in primary carbons is quite difficult to occur.[108] Despite that, a patent published in 2011[109] showed a bromination in the methyl group of a 5-bromo-2-methylpyrimidine with *N*-bromosuccinimide (NBS) and benzoyl peroxide in tetrachloromethane, giving the product 5-bromo-2-bromomethylpyrimidine with a yield of 48%. Thus, was attempted to perform the radical bromination in the same conditions on the commercially available reagent 4-chloro-2-methylpyrimidine (**Scheme II.6**), with low yield (6%). The presence of the two protons (**H_8**) from the methylene group were confirmed through ^{1}H-NMR spectrum (singlet at 4.56 ppm) (**Figure II.1**). A second attempt was made with extended reactional time and double of NBS equivalents, although the yield afforded did not improve (6%) (**Table VI.1**).

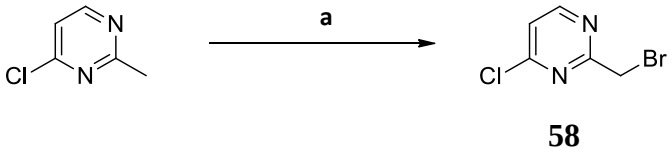

Scheme II.6 – Synthesis of 4-chloro-2-bromomethylpyrimidine **58**. *Reagents and conditions: (a) 4-chloro-2-methylpyrimidine, NBS, $(BzO)_2$, CCl_4, reflux, 72 h.*

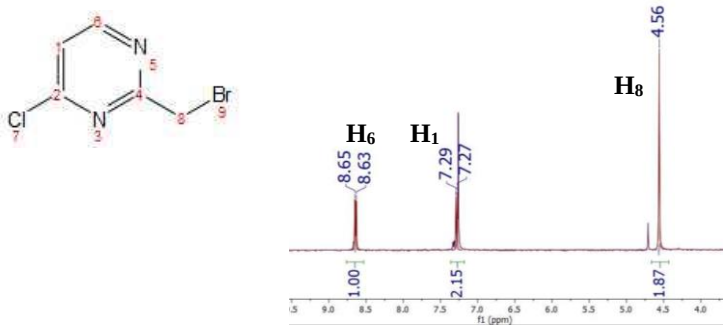

Figure II.1 – Compound **58** ^{1}H-NMR spectrum, in $CDCl_3$.

Due to the low yield obtained in the bromination of the methyl group in pyrimidine position 2, another approach was attempted to obtain the intermediate pyrimidine-2-aldehyde **56**.

II.1.2 Via 2,4-dichloropyrimidine

This approach consisted in achieving the aldehyde intermediate, **56**, from the commercially available reagent 2,4-dichloropyrimidine instead of 4-chloro-2-methylpyrimidine. The first synthetic step was to couple the hydrazine to the 2,4-dichloropyrimidne to obtain compound **59**. The same reaction from **Scheme II.3** (**b**) was used to accomplish this coupling (**Scheme II.7**). As described in the literature, this substitution occurs preferentially in position 4.[27]

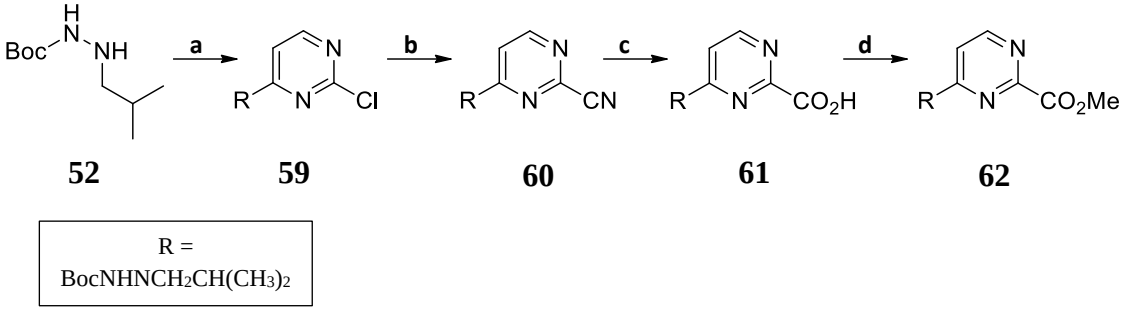

Scheme II.7 – Synthesis of intermediate **62**. *Reagents and conditions: (a) 2,4-dichloropyrimidine, DIPEA, dry EtOH, reflux, 24 h; (b) DABCO, KCN, DMSO/H_2O (9:1), reflux, 24 h; (c) KOH, H_2O_2 (50%), dry EtOH, dry MeOH, reflux, 2 h; (d) $SOCl_2$, dry MeOH, reflux, 4 h.*

Compound **60** was obtained through a nucleophilic substitution with pyrimidine intermediate **59** and KCN in the presence of DABCO. To obtain a good yield the reactional time was extended comparatively to the original work (3 h).[27] In order to follow the formation of the compound **60** during the synthesis, the dyeing reagent silver nitrate-ammonia-fluorescein, specific for halide ions detection, was used.[110] The appearance of the peak at 116.17 ppm in ^{13}C-APT NMR spectrum (**Annex 4 – Figure VI.3**), which corresponds to the nitrile carbon, proved the product formation. Additionally, the IR spectrum allowed to observe the appearance of the CN band at 2360.87 cm^{-1} (**Annex 5 – Figure VI.4**).

The only variation between the nucleophilic substitution performed in this thesis and in the original work[27], was the absence of a halogen atom on the pyrimidine position 5. The reaction with the 5-unsubstituted pyrimidine (**59**) in this thesis needed roughly eight-fold more time to bear a yield close to the yield obtained in the original work (92%) (**Table VI.1**). This evidence suggests that the presence of a halogen atom in position 5 may facilitate the nitrile nucleophilic attack on the pyrimidine position 2.

The next synthetic step was the nitrile hydrolysis to form the pyrimidine-2-carboxilic acid **61**. The reaction starts with the hydrogen peroxide deprotonation which generates the anion OOH^-. This leads to a slow reaction where the hydroperoxide anion

performs a nucleophilic attack on the nitrile carbon to form a peroxyimidic acid intermediate. This is followed by a rapid reaction of the peroxyimidic acid with hydrogen peroxide to form a carboxamide intermediate, as shown in **Scheme II.8**. This last intermediate, carboxamide, is then hydrolyzed to the carboxylic acid.[111] The compound was characterized by ^{1}H-NMR spectrum, and the IR spectrum (**Annex 6 – Figure VI.5**) showed a strong band at 2924.09 cm^{-1} corresponding to the aromatic carboxylic acid O-H bond, and a strong band at 1556.55 cm^{-1} corresponding to the bond C=O of the same functional unit.[112]

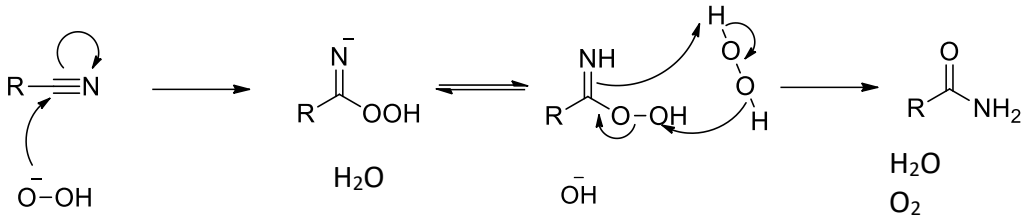

Scheme II.8 – Mechanism of nitrile hydrolysis (adapted from[111, 113]).

The synthesis of compound **62** required an esterification of compound **61**. This reaction was prepared according to the work described by Zhang and co-workers.[114] Nevertheless, this reaction did not lead to formation of the desired product. The intermediate compound **62** would serve as vehicle to synthetize the pyrimidine-2-aldehyde, through reduction.

Another approach thought to accomplish the pyrimidine-2-aldehyde was to synthetize compound **63** (pyrimidine with a Weinreb amide in position 2) (**Figure II.2**) through the pyrimidine-2-carboxylic acid **61**. The compound **63** would then suffer a reduction with $LiAlH_4$ to afford the pyrimidine-2-aldehyde. However, this reaction was tried in the past in our laboratory, but it resulted in an undesired non-aromatic product. It is also reported on the literature that the use of $LiAlH_4$ reduces the pyrimidine ring[115], thus this approach was not attempted.

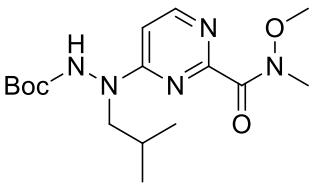

63

Figure II.2 – Structure of pyrimidine-2-Weinreb amide **63**.

II.2 Pyrimidine-2-(*E*)-ethyl acrylate

As the bromination at the subchapter **II.1.1** did not afford a reasonable yield to follow the next reaction, and the desired product from the esterification at **II.1.2** was not obtained in order to synthetize the pyrimidine-2-aldehyde, a new approach was adopted. This consisted in coupling an (*E*)-ethyl acrylate moiety to the pyrimidine position 2 through Suzuki-Miyaura cross-coupling (**Scheme II.9**) to obtain another compound with a Michael acceptor group, compound **64** (**Figure II.3**).

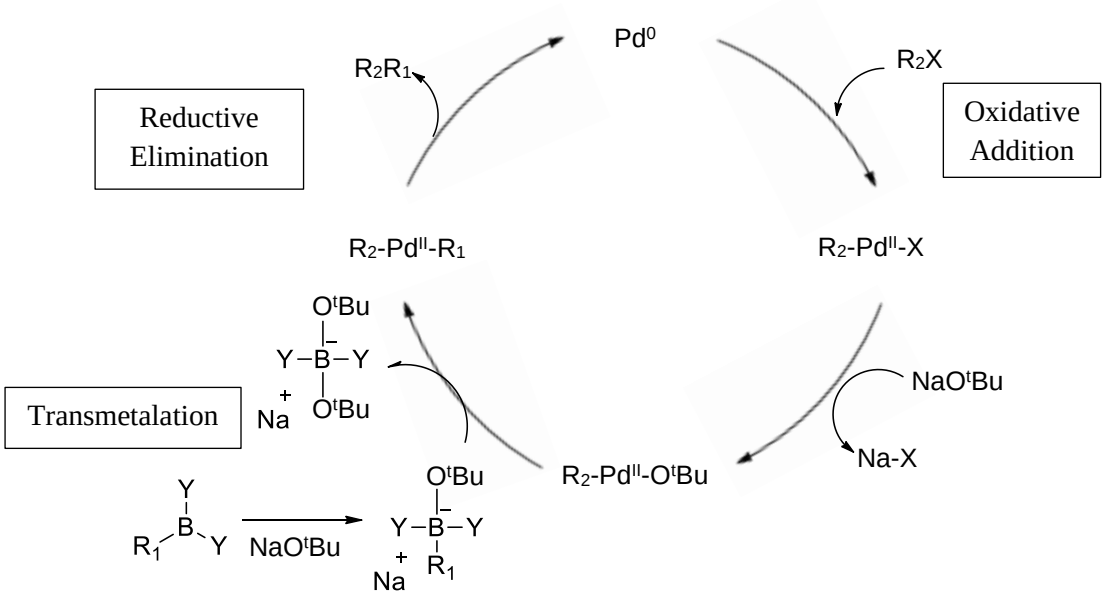

Scheme II.9 – General Suzuki-Miyaura reaction catalytic cycle.

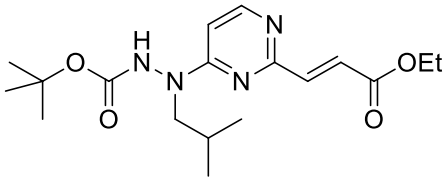

64

Figure II.3 – Structure of the novel pyrimidine-2-(*E*)-ethyl acrylate **64**.

II.2.1 Via 2-chloropyrimidine

Two similar methodologies were made to accomplish the product pyrimidin-2-(*E*)-ethyl acrylate **64**. The first approach (**Scheme II.10 a**) was performed according to the work of Asano and co-workers[116], where is showed a Suzuki-Miyaura coupling specifically in pyrimidine position 2 using the catalyst $Pd(OAc)_2$ and the ligand SPhos. This ligand generally exhibits great yields in Suzuki-Miyaura reactions between

heteroaryl halides and vinylboronic acids.[117] Furthermore, the use of 4 eq. of LiOH (base) and dioxane/H_2O (4:1) (solvent) were showed in the original work to be the conditions which improved further the yield.[116] The first attempt of this reaction gave an extremely low yield (2%) (**Table VI.1**), and after several attempts, the yield did not improve. Thus a second approach (**Scheme II.10 b**) was performed with the catalyst tetrakis(triphenylphosphine)palladium(0) ($Pd(PPh_3)_4$), according to the work of Yates and co-workers.[118] Nonetheless, although this catalyst has been reported to be efficient in coupling other aryl chlorides[119], the reaction yield was even lower (1%). The product was confirmed through the presence of the alkene protons in the ^{1}H-NMR spectrum (**Annex 7 – Figure VI.6**), and the presence of the vinyl ester C=O bond (1714.72 cm^{-1}) on the IR spectrum (**Annex 8 – Figure VI.7**).

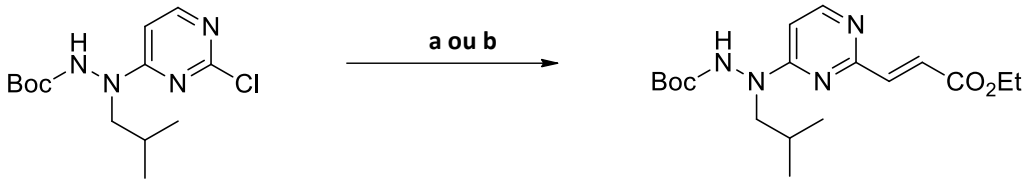

59 **64**

Scheme II.10 – Synthesis of final compound **64**. *Reagents and conditions: (a) [(E)-2-(ethoxycarbonyl)vinyl]boronic acid pinacol ester, LiOH, $Pd(OAc)_2$, SPhos, dioxane/H_2O (4:1), reflux, 1 h; (b)[(E)-2-(ethoxycarbonyl)vinyl]boronic acid pinacol ester, Na_2CO_3, $Pd(PPh_3)_4$, dioxane/H_2O (4:1), reflux, 20 h.*

II.2.2 Via 2-chloro-5-bromopyrimidine

Due to the low yield obtained in the Suzuki reaction with pyrimidine-5-H, and since this coupling, in the work of Yates and co-workers, was performed on a pyrimidine 5-Br substituted[118], the Suzuki coupling in this thesis was also attempted in a pyrimidine 5-Br substituted, affording compound **65** (**Scheme II.11**). Thus, the first step consisted in coupling the hydrazine to the commercially available 2,4-dichloro-5-bromopyrimidine to give compound **66**, using the same procedure described for the synthesis of compounds **53** and **59**. Intermediate **66** formation was identified by ^{1}H-NMR (**Annex 9 – Figure VI.8**) Afterward, was used the method described by Yates and co-workers[118] to attempt a Suzuki coupling on intermediate **66** (**Scheme II.11**).

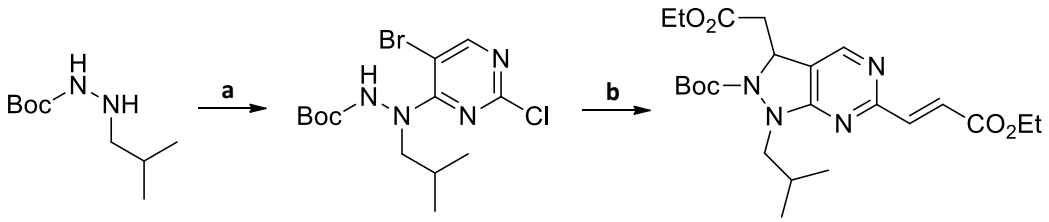

54 **66** **65**

Scheme II.11 – Synthesis of the final compound **65**. *Reagents and conditions: (a) 2,4-dichloro-5-bromopyrimidine, DIPEA, iPrOH, reflux, ov; (b)[(E)-2-(ethoxycarbonyl)vinyl]boronic acid pinacol ester, Na_2CO_3, $Pd(PPh_3)_4$, dioxane/H_2O (4:1), reflux, ov.*

According to the work developed by Yates and co-workers[118], it was expected that the Suzuki coupling occurred only on pyrimidine position 2 of compound **66**. Product formation was verified through thin layer chromatography (TLC), however after mass spectrometry (MS) (**Annex 10 – Figure VI.9**) and ^{1}H-NMR spectrum (**Annex 11 – Figure VI.10** analysis, it was concluded that the expected product **67** (**Figure II.4**) was not formed, but instead this reaction lead to the formation of compound **65**.

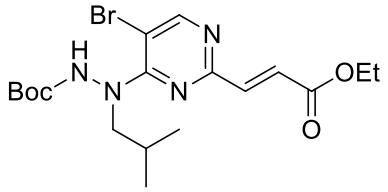

67

Figure II.4 – Structure of the expected product, **67**, from the Suzuki reaction between intermediate **66** and pinacol ester.

Comparation of the ^{1}H-NMR spectra of intermediate **66** and final compound **65** (**Figure VI.9** and **Figure VI.10**, respectively) showed the disappearance of the proton signal of the nitrogen (6.93 ppm on **Figure VI.8**) and the presence of two ethyl units from the acrylates (1.28; 1.33; 4.20; 4.27 ppm on **Figure VI.10**). This was confirmed with MS analysis, since the mass of two (*E*)-ethyl acrylate units were found in the MS spectrum, suggesting the coupling of this unit in both positions 2 and 5 of the pyrimidine ring.

Considering this, the ^{1}H-NMR spectrum also showed the absence of three expecting proton signals: the broad singlet from the nitrogen, and the two duplets resulting from the alkene of the extra acrylate unit. Instead, three double doublets shown up (2.63; 2.94; 5.61 ppm), which each one integrated to one proton, suggesting an intramolecular attack of the nitrogen to the acrylate double bond on pyrimidine position 5, creating a chiral center.

To understand the compound **65** structure, ^{13}C-NMR (**Annex 12 – Figure VI.11**), HMQC NMR (**Annex 13 – Figure VI.12**) and HMBC NMR (**Annex 14 – Figure VI.13**) were performed. The HMQC spectrum showed that the two signals (2.63 and 2.94 ppm) interacted with one single carbon atom (**Figure II.5**). Through HMBC spectrum analysis, was observed that these two protons interacted with the carbonyl carbon of the ester (169.7 ppm) (**Figure II.6**), suggesting that these two protons belong to the initial α-carbon of the alkene linked at pyrimidine position 5. The HMBC also showed a similar interaction between these two protons and the initial β-carbon of the same alkene (57.9 ppm).

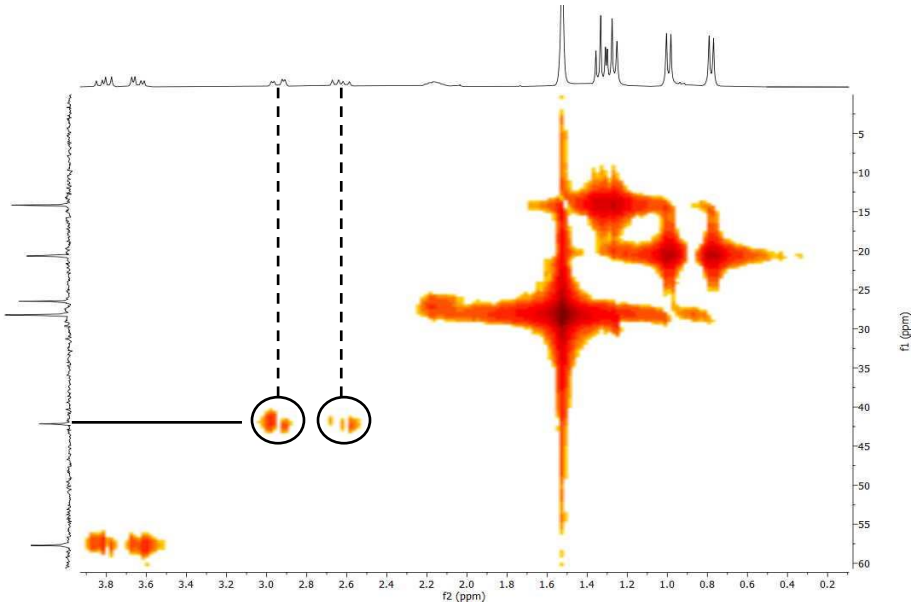

Figure II.5 – Compounds **65** HMQC NMR spectrum, in $CDCl_3$. Interaction between the protons (2.63 and 2.94 ppm) and initial α-carbon (42.2 ppm) highlighted.

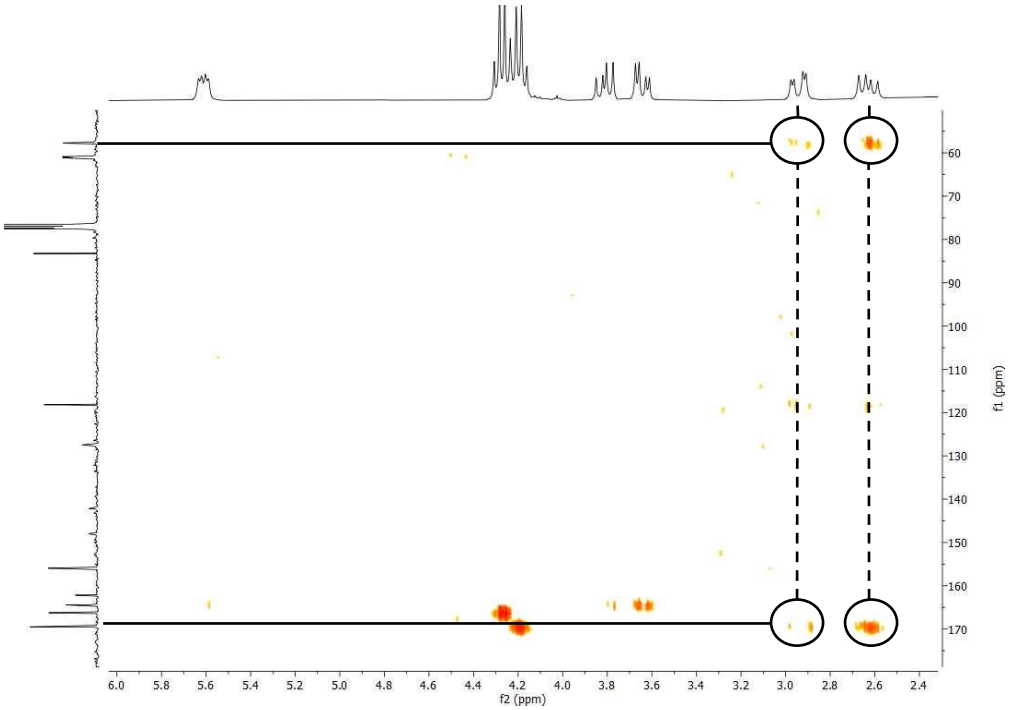

Figure II.6 – Compound **65** HMBC NMR spectrum, in $CDCl_3$. Interactions between the protons (2.63 and 2.94 ppm) and the carbonyl carbon of the ester (169.7 ppm) and the initial β-carbon (57.9 ppm) highlighted.

These interactions confirmed the formation of the five-membered ring through a Michael addition in the pyrimidine intermediate with (*E*)-ethyl acrylate units in position 2 and 5 (first structure on **Scheme II.12**). The Michael addition was possible due to the presence of base in the Suzuki coupling (Na_2CO_3), which abstracted the proton of the nitrogen. Then, the negatively charged nitrogen performed a nucleophilic attack on the β-carbon. Posteriorly, the enolate abstracted the proton from the reaction medium[108], **Scheme II.12**.

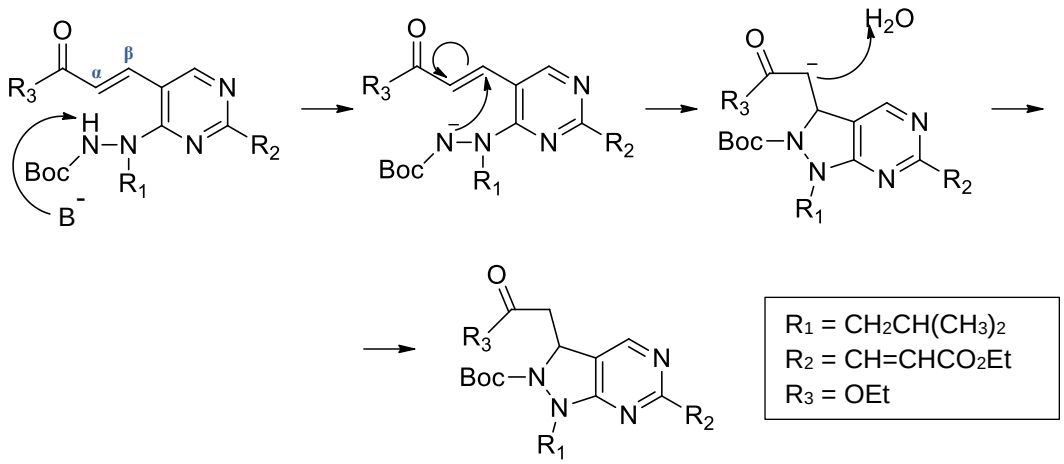

Scheme II.12 – Michael addition mechanism on pyrimidine intermediate with (*E*)-ethyl acrylate units in positions 2 and 5.

The three protons (2.63, 2.94 and 5.61 ppm) constitute an ABX pattern (**Figure II.7**), and all three signals exhibit coupling constants in common with each other. Furthermore, the protons from CH_2CH present in the isobutyl group (2.10 – 2.23, 3.65 and 3.81 ppm) also expressed an ABX pattern.

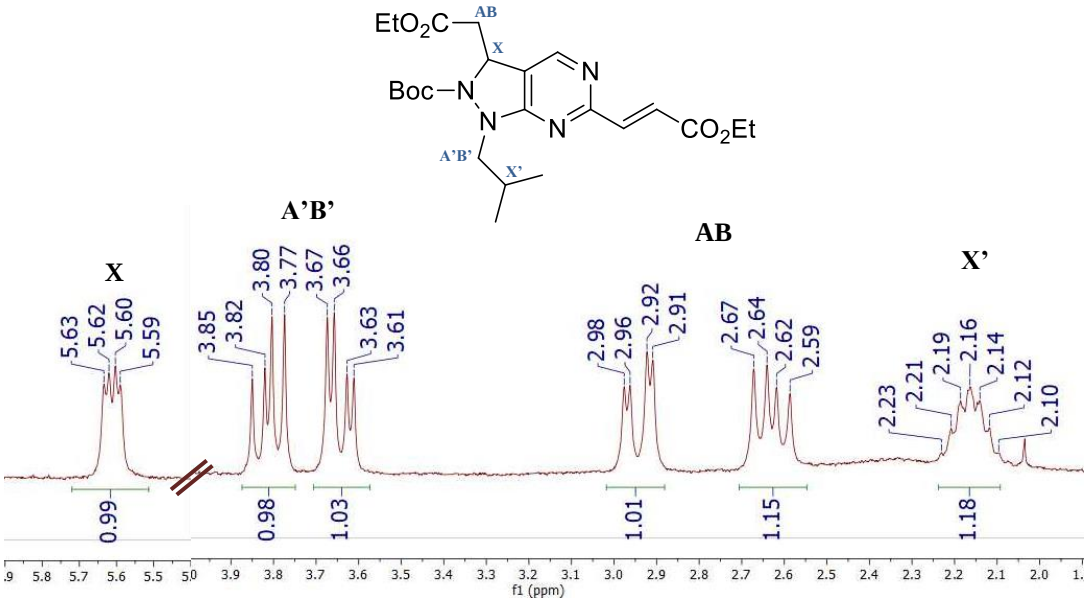

Figure II.7 – Two ABX patters present on compound **65** ^{1}H-NMR spectrum, in $CDCl_3$.

At first, this Suzuki coupling was made with 1.4 eq. of pinacol ester and 3 mol% $Pd(PPh_3)_4$, giving a yield of 8%. In order to increase the yield, was tried to double the equivalents of pinacol ester and increase the $Pd(PPh_3)_4$ to 5.5 mol%, which improved the yield to 13%. As this methodology had such a positive result, the same was attempted to obtain the final compound **64**, in the Suzuki coupling of intermediate **59** using $Pd(PPh_3)_4$ (**Scheme II.10 b**) to optimize this reaction, which increased its yield from 1% up to 6%.

II.3 *In Vitro* Biological Assays

II.3.1 Antimalarial Activity

Antimalarial activity of compounds **64** and **65** was evaluated against the BS (in RBC infected with synchronized ring-stage *P. falciparum*), and LS (in Huh-7 cells infected with *P. berghei*).

Blood Stage Activity

Compound **64** did not exhibit inhibitory activity to BS parasites up to the concentration of 200 nM. From this concentration up to 750 nM, there is a curve dose-response. At a concentration of 500 nM, compound **64** inhibited roughly 38% of infection, at 750 nM the inhibition percentage was about 50%. At the concentration of 1000 nM, compound **64** did not show a significant increase in inhibition (53%), relatively to the previous concentration. (**Figure II.8**). On the other hand, compound **65** showed little or no inhibitory activity up to a concentration of 1000 nM (about 5% inhibition).

Results from the BS assays allowed to observe the difference between both compounds activity, although both compounds **64** and **65** have the same functionality. The presence of the pyrazolidine ring and/or the adjacent ester, showed to greatly decrease compound inhibitory activity, causing compound **65** to lose roughly all its inhibitory activity. This suggests that the steric hindrance, or the rigidity given to the molecule due to the five membered ring and adjacent ester may interfere on the pyrimidine inhibitory efficacy to the BS. Compound **64** IC_{50} is estimated to be roughly 689 nM, whereas other BS inhibitors containing Michael acceptor groups, such as nitriles and vinyl sulfones, have showed IC_{50} values ranging from 3 nM to <0.5 nM.[21,27]

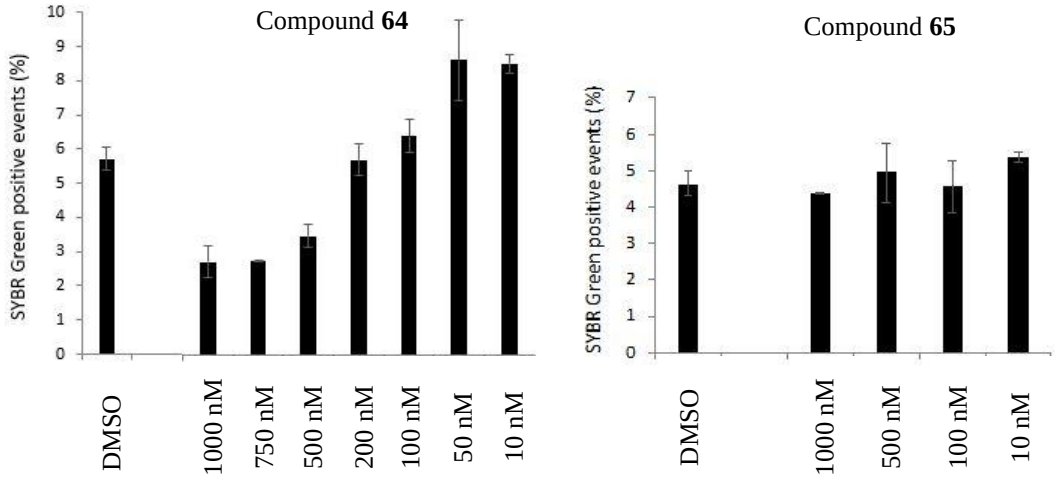

Figure II.8 – BS SYBR Green positive events (%) at the described concentrations of compounds **64** and **65**.

Liver Stage Activity

Compound **64** results were rather incoherent. In one of the two independent assays, this compound at 1 µM promoted the infection about 15%, while on the other assay at the same concentration it inhibited the infection by roughly 30% (**Figure II.9**). However, from the concentration of 2.5 µM onwards, the results were concise, and it is possible to see a relation between dose/response (**Figure II.9**). At this concentration, compound **64** promoted a mild growth of infection on both assays, and at 5 µM it exhibited a slight reduction of the infection (up to 5% inhibition). At the concentration of 10 µM the infection was inhibited for about 40%, and at the highest concentration, 15 µM, compound **64** inhibited roughly 75% of infection. The highest concentration exhibited to decrease cell confluency, implying the possibility of toxicity at higher concentration. Thus, the IC_{50} was not determined.

The LS assay for compound **65** exhibited a dose/response relation. At the concentrations of 1 and 5 µM inhibited the infection by almost 25%, whereas at 10 µM this compound led to an infection inhibition roughly above 50% and at a concentration of 15 µM this compound gave an inhibition of 75% (**Figure II.9**). Compound **65** exhibited an IC_{50} of 9.49 µM (**Table VI.2**).

Relatively to LS assays, both compounds exhibited similar activity, although compound **65** showed to be slightly more active. Nonetheless, compound **64** results were rather inconsistent on the lower concentrations, not allowing a precise evaluation. Compound **65** activity *in vitro* is identical to that of PQ, whose IC_{50} *in vitro* is 9.5 µM.[24] *In vivo*, PQ is more active against LS parasites due to its metabolization products. As such, this hypothesis cannot be ruled out for compound **65**, although there is no evidence to support it.

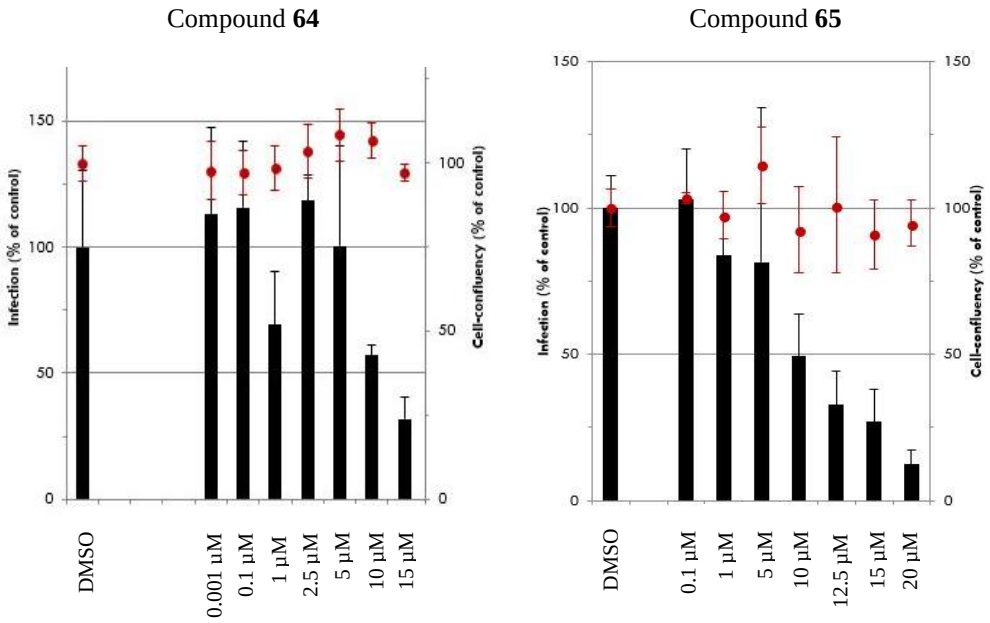

Figure II.9 – LS Infection (%) at the described concentrations of compounds **64** and **65**.

II.3.2 Anticancer Activity

Several compounds with antimalarial activity have also been reported to exhibit anticancer activity. CQ analogs and several tetraoxanes are some examples.[33,82,84] On the monolayer assay, both compounds **64** (35.56 µM) and **65** (28.96 µM) (**Annex 16 – Table VI.3**) exhibited an IC_{50} roughly seven and six-fold higher than fluorouracil (5-Fu) (5.48 µM). On the assay against CSC-like spheres, both compounds exhibited similar IC_{50} values, compound **64** (0.77 µM) and compound **65** (0.70 µM). Despite both compounds showed anticancer activity on the CSC-like spheres assay, they are considered to have low anticancer activity on the monolayer assay (compounds **64** and **65** IC_{50} = 35.56 and 28.96 µM, respectively), comparing to other compounds evaluated against HT-29 cells. Oxaliplatin **68**, IC_{50} = 0.88 µM, (**Figure II.10**) is an example of a compound with anticancer activity to HT-29 monolayer, much higher than compounds **64** and **65**.[120] The dose/response curves of anticancer assays for both compounds are present in **Figure II.11**.

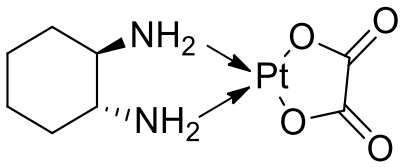

Figure II.10 – Structure of oxaliplatin **68**.

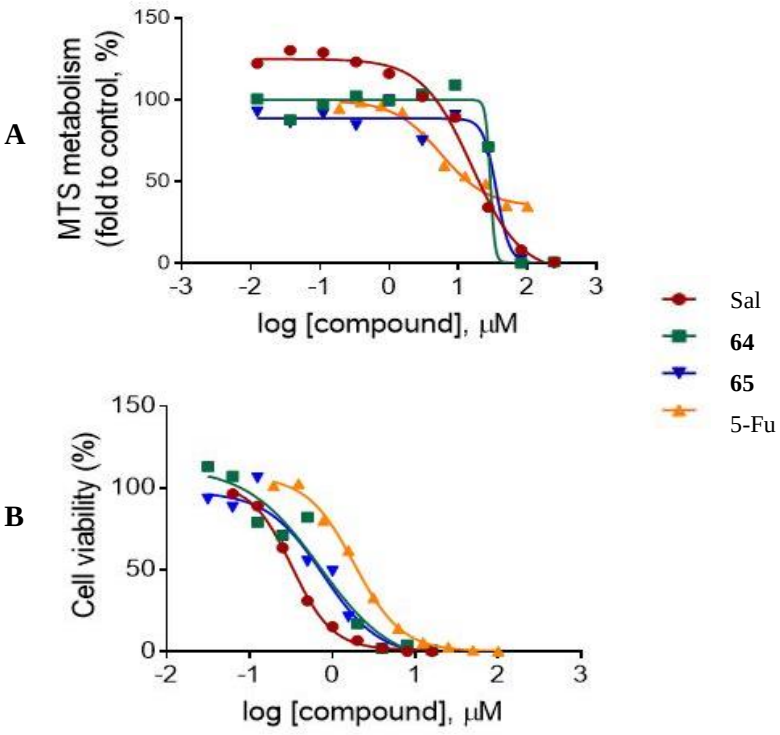

Figure II.11 – Dose/response curves om anticancer assays (**A**) Monolayer HT-29 MTS metabolism and (**B**) CSC-like spheres HT-29, cell viability (%) at the described concentration of compounds **64** and **65**, positive and negative control (Sal and 5-Fu, respectively).

Chapter III

III. Conclusion

In this thesis, two different pyrimidine-2-acrylate, compounds **64** and **65** were synthetized. The initial goal was to synthetize compound **48**, a tetraoxane-pyrimidine hybrid. The pyrimidine moiety was supposed to have an (*E*)-ethyl 2-cyanoacrylate unit coupled to position 2. However, the synthesis of the intermediaries to achieve this derivative was more complicated than expected, due to the low reactivity of pyrimidine position 2, not being possible to synthetize compound **48** and the respective probe, compound **49.** Thus, after repeated failed attempts, was chose to couple directly an (*E*)-ethyl acrylate unit to the same pyrimidine position by a Suzuki coupling instead. Unfortunately, both compounds **64** and **65** were also not coupled to the tetraoxane unit, due to lack of time.

During this thesis, several approaches were attempted to synthetize the intended compounds and some optimization reactions were performed:

a) The reduction of intermediate **51** into compound **52**, was shown to be more efficient and safer when resorting to sodium cyanoborohydride instead of Pd/C and H_2, decreasing the reaction time and improving the yield.

b) On the synthesis of compound **53**, the use of EtOH instead of *i*PrOH with DIPEA, provided a better yield. On the other hand, the use of the base K_2CO_3 and solvent DMF gave a mild yield. Additionally, the use of a catalytic reaction, Buchwald amination, improved the yield to 92%.

c) The synthesis of compound **64**, using Suzuki-Miyaura coupling, was attempted with $Pd(OAc)_2$ and gave an extremely low yield (2%). This yield was not improved with the use of $Pd(PPh_3)_4$, 3 mol% and 1.4 eq. of pinacol ester. Nonetheless, the percentage of catalyst and eq. of pinacol ester were increased (5.5 mol% and 2.8 eq., respectively), to bear a better yield (6%). The same increase of percentage of catalyst and eq. of reagent demonstrated the same effect on compound **65** synthesis.

d) The use of the 5-bromopyrimidine (compound **66**) in the Suzuki coupling improved the yield to 6%, comparatively to the 1% afforded in the Suzuki coupling in a pyrimidine unsubstituted in position 5 (compound **59**). However, the Suzuki coupling in compound **66** afforded the di-substituted intermediary, which through an intramolecular attack originated the final compound (**65**).

Oliveira and co-workers designed tetraoxane-pyrimidine nitrile hybrids with BS activity[25], whose target is the FP-2. These compounds contain a Michael acceptor group, functionality known to target the FP-2. In this thesis, compounds with a Michael acceptor group (compounds **64** and **65**) were also design. Compound **64** exhibited inhibitory activity against BS parasites, despite being low. Although compound **64** activity against FP-2 was not evaluated, through analogy it is possible to affirm that

compound **64** may target FP-2. On the other hand, compound **65**, more steric hindered by the pyrazolidine ring and the adjacent ester, virtually did not show inhibitory activity to the BS parasites. This may suggest, that the steric hinderance or the rigidity given to the molecule due to the five membered ring and adjacent ester may interfere on the pyrimidines inhibitory efficacy to the BS. Compound **64** inhibited about 50% of infection at a concentration of 750 nM. When compared to other BS inhibitors containing Michael acceptor groups activities (IC_{50} < 0.5 nM)[27] it is explicit to conclude that compound **64** activity is extremely low.

Although FP-2 is an enzyme not expressed in the LS, the pyrimidine nitrile unit of the hybrid compounds (**35**) designed by Oliveira and co-workers also exhibited inhibitory activity to this stage. Thus, was hypothesized the existence of one or more target(s) containing an active cysteine in the LS. In this thesis, compounds **64** and **65**, thought to act in the BS through FP-2 inhibition, has also their anti-LS activity evaluated. LS results from compound **64** did not allow a precise evaluation of its biological activity due to the inconsistent results at lower concentrations and to the possibility of toxicity at higher concentrations. For this reason, the IC_{50} of this compound could not be determined. Despite this, both compounds showed to be slightly active to LS, with compound **65** exhibiting to be slightly more active. Compound **65** exhibited an *in vitro* activity similar to PQ. Compound **65** IC_{50} value is 9.49 µM, roughly the same value determined for PQ *in vitro* assays.

Both compounds **64** and **65**, contain a Michael acceptor group and compound **64** exhibited activity against BS parasites, and the fact that these compounds exhibited mild inhibitory activity against the LS, reinforces the hypothesis given by Oliveira and co-workers.

Further work must be done as the introduction of the nitrile group in the acrylate moiety and the coupling of the tetraoxane unit, in order to obtain the hybrid compound **48** (synthetized from compound **64**) and another derivative (synthetized from compound **65**). The synthesis of a chemical probe, which englobes the introduction of a triple bond suitable for click chemistry and posterior reaction with fluorescent tags inside living *P. berghei*-infected hepatocytes, to study the MoA and therapeutic target must be also done. Due to the presence of the tetraoxane unit, activation assays with Fe(II) can also be performed, which allow to visualize and quantify the pyrimidine moiety released. Furthermore, compound **64** anti-BS inhibitory activity should be tested for the FP-2.

Chapter IV

IV. Experimental Procedure

IV.1 Chemistry

All chemicals were of reagent grade and were purchased from Alfa Aesar, Sigma-Aldrich, Merck, Apollo Scientific, Honeywell or Fluorochem.

All solvents were of analytical grade and were obtained from commercial suppliers. Dichloromethane, methanol and ethanol were dried from calcium hydride. Dioxane was dried from sodium metal. Anhydrous dimethylformamide was purchased from Sigma Aldrich. All the solvents used in purification were distilled under reduced pressure.

TLC was performed on pre-coated silica gel 60 F_{254} aluminium plates (Merck) and visualized using a CAMAG UV camera at UV wavelength, iodine, ninhydrin dip, and silver nitrate-ammonia-fluorescein dip. Flash column chromatography was performed with silica gel 60, 0.400-0.063 mm (Merck) eluted with several solvent mixtures and using an air aquarium pump to apply pressure. Preparative thin-layer chromatography was performed with silica gel 60 GF_{254} (Merck) eluted with several solvent mixtures.

NMR spectra (1D and 2D) were obtained on a Bruker 300 UltraShield, using deuterated chloroform as solvent. Chemical shifts, δ, are expressed in ppm, and coupling constants, J, are expressed in Hz. Multiplicities are given as: s (singlet), bs (broad singlet), d (doublet), dd (double doublet), t (triplet), q (quartet) and m (multiplet).

Infrared (IR) spectra were performed on an IRAffinity-1 Shimadzu FTIR spectrophotometer. All the spectra were performed on a NaCl cell. Only the most significant absorption bands are reported. Electrospray ionization mass spectrometry (ESI-MS) analyses were determined using a Micromass Quattro Micro API spectrometer. Melting points were determined using a Kofler Bock Monoscop M and are uncorrected.

IV.1.1 Synthesis of tert-butyl 2-isobutylhydrazinecarboxylate (52)

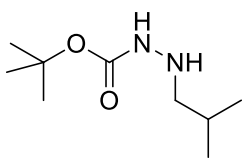

A solution of *tert*-butyl carbazate **50** (198.3 mg, 1.50 mmol), isobutyraldehyde (106.7 mg, 1.50 mmol) and molecular sieves 3Å in dry dichloromethane (3 mL) was stirred for 2 h at room temperature, under nitrogen atmosphere. After confirmation that product **51** formation occurred through TLC, the reaction mixture was filtered, and the

filtrate was concentrated under reduced pressure. (**A**) The crude and palladium on carbon (10% by weight) were taken up in dry methanol (3 mL) and flushed with nitrogen for 5 minutes. The atmosphere was then filled with hydrogen and the mixture was stirred overnight at room temperature. A flow of nitrogen was used to remove any remaining hydrogen gas from the reaction mixture before suspension was filtered through celite to remove the catalyst. The filtrate was concentrated under reduced pressure. Purification by flash column chromatography (10% ethyl acetate in dichloromethane) afforded the pure compound. Clear oil (39% yield). (**B**) The crude and sodium cyanoborohydride (141.4 mg, 2.25 mmol) were taken up in acetic acid 75% (2.85 mL). The mixture was stirred at room temperature for 3 h and followed by TLC. After that, the pH was neutralized with NaOH 5M and 1M. The solution was extracted with dichloromethane (3 × 20 mL) and washed with a saturated solution of sodium bicarbonate (3 × 20 mL). The combined organic extracts were dried over anhydrous sodium sulphate, filtered and concentrated under reduced pressure. Purification by flash column chromatography (10% ethyl acetate in dichloromethane) afforded the pure compound. Clear oil (79% yield).

^{1}H NMR (300.18 MHz, $CDCl_3$): δ (ppm): 6.31 (bs, 1H, NH), 3.90 (bs, 1H, NH), 2.62 (d, J = 6.9 Hz, 2H, CH_2), 1.76 – 1.63 (m, 1H, CH), 1.43 (s, 9H, Boc), 0.89 (d, J = 6.7 Hz, 6H, CH_3).

IV.1.2 Synthesis of tert-butyl 2-isobutyl-2-(2-methylpyrimidin-4-yl)hydrazinecarboxylate (53)

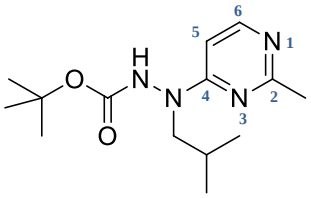

(**A**) To a solution of compound **52** (100.0 mg, 0.53 mmol) in isopropanol (1.56 mL), was added 2-methyl-4-chloropyrimidine (92.2 mg, 0.72 mmol) and *N*,*N*-diisopropylethylamine (120.9 mg, 0.94 mmol). The reaction proceeded under reflux for 22 h. The solution was concentrated under reduced pressure and the crude was diluted in dichloromethane (20 mL) and washed with a saturated solution of ammonium chloride (3 × 20 mL), water (3 × 20 mL) and brine (3 × 20 mL). The combined organic extracts were dried over anhydrous sodium sulphate, filtered and concentrated under reduced pressure. The residue was purified by flash column chromatography (40% ethyl acetate in hexane). White solid (13% yield). (**B**) To a solution of compound **52** (50.0 mg, 0.27 mmol) in dry ethanol (2 mL), was added 2-methyl-4-chloropyrimidine (41.7 mg, 0.32 mmol) and *N*,*N*-diisopropylethylamine (86.7 mg, 0.68 mmol). The reaction proceeded under refluxed for 24 h. The solution was concentrated under reduced pressure and the crude was diluted in dichloromethane (20 mL) and washed with a saturated solution of ammonium chloride (3 × 20 mL), water (3 × 20 mL) and brine (3 × 20 mL). The combined organic extracts were dried over anhydrous sodium sulphate, filtered and concentrated under reduced pressure. Purification by flash column chromatography (40% ethyl acetate in hexane) afforded the pure compound. White solid (42% yield).

(**C**) To a solution of compound **52** (50.0 mg, 0.27 mmol) in dry dimethylformamide (DMF) (2.7 mL), was added 2-methyl-4-chloropyrimidine (34.1 mg, 0.27 mmol) and potassium carbonate (44.8 mg, 0.32 mmol). The solution was refluxed for 2 h. The reaction mixture was extracted with ethyl acetate (3 × 20 mL) and washed with water (3 × 20 mL) and brine (3 × 20 mL). The combined organic extracts were dried over anhydrous sodium sulphate, filtered and concentrated under reduced pressure. The crude material was purified by flash column chromatography (40% ethyl acetate in hexane). White solid (21% yield). (**D**) A solution of, palladium(II) acetate (5 mol%) and XPhos (5 mol%) in *tert*-butanol/water 2:1 v/v (0.82 mL) was added to a sealed tube. The mixture was heated to 80 ºC for 1 minute and potassium carbonate (57.1 mg, 0.41 mmol), 2-methyl-4-chloropyrimidine (28.9 mg, 0.22 mmol) and compound **52** (38.0 mg, 0.20 mmol) was added. The solution was heated to 110 ºC for 1.5 h. The residue was purified by preparative TLC (30% hexane in ethyl acetate). All reactions were followed by TLC. White solid (92% yield).

^{1}H NMR (300.18 MHz, $CDCl_3$) δ (ppm): 8.17 (d, J = 6.1 Hz,1H, C_6H_{pyri}), 6.59 (bs, 1H, NH), 6.43 (d, J = 5.9 Hz, 1H, C_5H_{pyri}), 3.58 (bs, 2H, CH_2), 2.51 (s, 3H, $ArCH_3$), 2.11 – 1.96 (m, 1H, CH), 1.49 (s, 9H, Boc), 0.94 (d, J = 6.7 Hz, 6H, CH_3).

IV.1.3 Synthesis of 2-(bromomethyl)-4-chloropyrimidine (58)

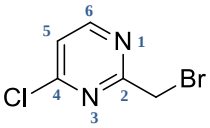

To a solution of 2-methyl-4-chloropyrimidine (50.0 mg, 0.39 mmol) in carbon tetrachloride (3.11 mL), was added *N*-bromosuccinimide (138.4 mg, 0.78 mmol) and benzoyl peroxide (1 mol%). The reaction mixture was filtered and concentrated under reduced pressure, after 72 h under reflux and followed by TLC. Purification by preparative TLC (30% ethyl acetate in hexane) afforded the pure compound. Yellow solid (6% yield).

^{1}H NMR (300.18 MHz, $CDCl_3$) δ (ppm): 8.64 (d, J = 5.4 Hz, 1H, C_6H_{pyri}), 7.28 (d, J = 5.3 Hz, 1H, C_5H_{pyri}), 4.56 (s, 2H, CH_2).

IV.1.4 Synthesis of tert-butyl 2-(2-chloropyrimidin-4-yl)-2-isobutylhydrazinecarboxylate (59)

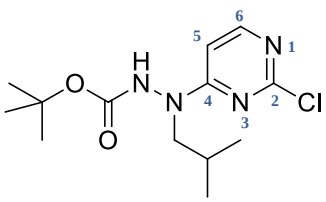

Prepared according to the procedure IV.1.2 (**B**), using 2,4-dichloropyrimidine as starting material. White solid 62% yield). Product formation was followed through TLC.

Melting Point (MP): 139ºC.

^{1}H NMR (300.18 MHz, $CDCl_3$) δ (ppm): 8.11 (d, J = 6.0 Hz, 1H, C_6H_{pyri}), 6.60 (bs, 1H, NH), 6.55 (d, J = 5.8 Hz, 1H, C_5H_{pyri}), 3.58 (bs, 2H, CH_2), 2.12 – 1.98 (m, 1H, CH), 1.48 (s, 9H, Boc), 0.96 (d, J = 6.7 Hz, 6H, CH_3).

IV.1.5 Synthesis of tert-butyl 2-(2-cyanopyrimidin-4-yl)-2-isobutylhydrazinecarboxylate (60)

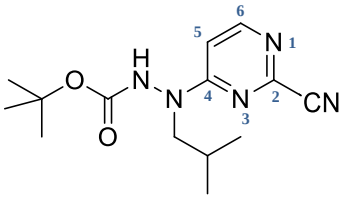

To a solution of compound **59** (273.9 mg, 0.91 mmol) in dimethyl sulfoxide/water 9:1 v/v (8.58 mL), was added DABCO (102.2 mg, 0.91 mmol) and potassium cyanide (88.9 mg, 1.37 mmol). The solution was refluxed for 24 h and followed by TLC. The reaction was carefully quenched with cold water (30 mL) and the reaction mixture was extracted with ethyl acetate (3 × 20 mL) and washed with a saturated solution of sodium bicarbonate (3 × 20 mL). The combined organic extracts were dried over anhydrous sodium sulphate, filtered and concentrated under reduced pressure. The residue was purified by flash column chromatography using gradient from 50% hexane in ethyl acetate to 30%. All the laboratory material in contact with potassium cyanide was decontaminated with bleach. Orange syrup (77% yield).

^{1}H NMR (300.18 MHz, $CDCl_3$) δ (ppm): 8.27 (d, J = 6.2 Hz, 1H, C_6H_{pyri}), 6.78 (d, J = 6.1 Hz, 1H, C_5H_{pyri}), 6.76 (bs, 1H, NH), 3.50 (bs, 2H, CH2), 2.12 – 1.98 (m, 1H, CH), 1.47 (s, 9H, Boc), 0.95 (d, J = 6.7 Hz, 6H, CH_3);

^{13}C NMR (75.48 MHz, $CDCl_3$) δ (ppm): 164.2 (C_{4pyri}), 156.4 (C_{6pyri}), 156.3 (CO), 144.2 (C_{2pyri}), 116.2 (CN), 105.8 (C_{5pyri}), 82.8 (C_{qBoc}), 60.9 (CH_2), 28.3 (CH_{3Boc}), 26.6 (CH), 20.9 (CH_3)

IV.1.6 Synthesis of 4-(2-(tert-butoxycarbonyl)-1-isobutyl hydrazinyl)pyrimidine-2-carboxylic acid (61)

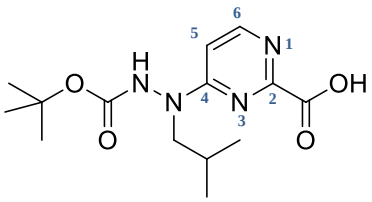

To a solution of compound **60** (112.2 mg, 0.39 mmol) and potassium hydroxide pellets (319.4 mg, 5.69 mmol) in dry methanol (0.19 mL) and dry ethanol (1.64 mL) was added hydrogen peroxide 50% (0.19 mL) dropwise. The reaction was refluxed for 2 h and followed by TLC. To set the pH of the solution to 2.0, HCl 0.2M (75 mL) and 0.013M (150 mL) was added. The actual pH value was measured potentiometrically. The compound was extracted with dichloromethane (3 × 20 mL), dried with sodium sulfate, filtered and concentrated under reduced pressure. Yellow oil (50% yield).

^{1}H NMR (300.18 MHz, $CDCl_3$) δ (ppm): 8.40 (bs, 1H, C_6H_{pyri}), 6.97 (bs, 1H, NH), 6.83 (bs, 1H, C_5H_{pyri}), 3.63 (bs, 2H, CH_2), 2.18 – 1.99 (m, 1H, CH), 1.49 (s, 9H, Boc), 0.98 (d, J = 6.6 Hz, 6H, CH_3).

IV.1.7 Synthesis of methyl (*E*)-tert-butyl 2-(2-(3-ethoxy-3-oxoprop-1-en-1-yl)pyrimidin-4-yl)-2-isobutylhydrazinecarboxylate (64)

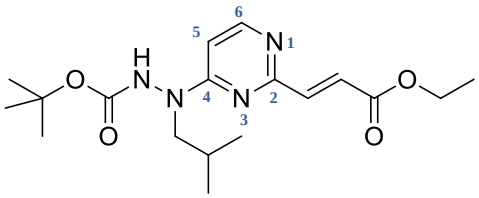

(**A**) To a solution of compound **59** (50.0 mg, 0.17 mmol) in dioxane/water 4:1 (1.66 mL) in a atmosphere filled with nitrogen, was added [(*E*)-2-(ethoxycarbonyl)vinyl]boronic acid pinacol ester (45.1 mg, 0.20 mmol), palladium(II) acetate (1 mol%), SPhos (2 mol%) and lithium hydroxide 2M (0.33 mL). The reaction was refluxed for 1 h. The reaction was quenched with water (20 mL), extracted with ethyl acetate (3 × 20 mL) and washed with brine (3 × 20 mL) and dried with sodium sulfate. The crude was filtered and concentrated under reduced pressure. Purification by flash column chromatography using gradient from 100% hexane to 40% ethyl acetate in hexane afforded the pure compound. Clear oil (2% yield). (**B**) To a solution of compound **59** (100 mg, 0.33 mmol) in dioxane/water 4:1 (1.91 mL) in an atmosphere filled with nitrogen, was added [(*E*)-2-(ethoxycarbonyl)vinyl]boronic acid pinacol ester (197.0 mg, 0.87 mmol) and sodium carbonate (83.73 mg, 0.79 mmol). The atmosphere was purged with nitrogen for 5 minutes and then $Pd(PPh_3)_4$ (5.5 mol%) was added. The reaction mixture, after 20 h under reflux, was diluted in water (30 mL) and extracted with ethyl acetate (3 × 20 mL). The combined organic extracts were washed with water (3 × 20 mL), dried with sodium sulfate, filtered and concentrated under reduced pressure. Purification by preparative TLC (40% ethyl acetate in dichloromethane) afforded pure compound. Clear oil (6% yield). All these approaches were followed by TLC.

^{1}H NMR (300.18 MHz, $CDCl_3$) δ (ppm): 8.31 (d, J = 6.0 Hz, 1H, C_6H_{pyri}), 7.53 (d, J = 15.7 Hz, 1H, C<u>H</u>CHCO$_2$Et), 7.05 (d, J = 15.6 Hz, 1H, CHC<u>H</u>CO$_2$Et), 6.64 (bs, 1H, NH), 6.56 (d, J = 6.0 Hz, 1H, C_5H_{pyri}), 4.27 (q, J = 7.1 Hz, 2H, CO$_2$C<u>H</u>$_2$CH$_3$), 3.62 (bs, 2H, NC<u>H</u>$_2$CH(CH$_3$)$_2$), 2.14 – 2.00 (m, 1H, NCH$_2$C<u>H</u>(CH$_3$)$_2$), 1.49 (s, 9H, Boc), 1.33 (t, J = 7.1 Hz, 3H, CO$_2$CH$_2$C<u>H</u>$_3$), 0.97 (d, J = 6.7 Hz, 6H, NCH$_2$CH(C<u>H</u>$_3$)$_2$);

^{13}C NMR (75.48 MHz, $CDCl_3$) δ (ppm): 166.7 (<u>C</u>=O$_{vinyl}$), 163.9 (C_{4pyri}), 161.9 (C_{2pyri}), 156.4 (C_{6pyri}), 154.8 (<u>C</u>=O$_{Boc}$), 144.6 (<u>C</u>H=CHCO$_2$), 126.1 (CH=<u>C</u>HCO$_2$), 102.7 (C_{5pyri}), 82.3 (C_{qBoc}), 60.9 (CH_{2ester}), 57.2 ($CH_{2isobutyl}$), 28.3 (CH_{3Boc}), 26.9 ($CH_{isobutyl}$), 20.4 (2 x $CH_{3isobutyl}$), 14.9 (CH_{3ester}).

MS (ESI) m/z: $C_{18}H_{28}N_4O_4$ **exp.:** 365.1 [M+H] **calc.:** 364.2

IV.1.8 Synthesis of tert-butyl 2-(5-bromo-2-chloropyrimidin-4-yl)-2-isobutylhydrazinecarboxylate (66)

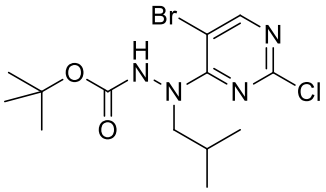

To a solution of compound **52** (87.5 mg, 0.46 mmol) in isopropanol (2.83 mL), was added 5-bromo-2,4-dichloropyrimidine (105.99 mg, 0.47 mmol) and *N*,*N*-diisopropylethylamine (78.68 mg, 0.61 mmol). The reaction was refluxed overnight and followed by TLC. The reaction mixture was extracted with dichloromethane and washed with ammonium chloride (3 × 20 mL), water (3 × 20 mL) and brine (3 × 20 mL). The mixture was dried with sodium sulphate, filtrated and concentrated under reduced pressure. The crude material was purified by flash column chromatography (40% ethyl acetate in hexane). White solid (70% yield).

Melting Point (MP): 105 ºC.

^{1}H NMR (300.18 MHz, $CDCl_3$) δ (ppm): 8.26 (s, 1H, ArH) 6.93 (s, 1H, NH) 3.65 (bs, 2H, CH_2), 2.12 – 1.98 (m, 1H, CH), 1.46 (s, 9H, Boc), 0.95 (d, J = 6.7 Hz, 6H, CH_3).

IV.1.9 Synthesis of methyl (*E*)-tert-butyl 3-(2-ethoxy-2-oxoethyl)-6-(3-ethoxy-3-oxoprop-1-en-1-yl)-1-isobutyl-1H-pyrazolo [3,4-d]pyrimidin-2(3H)-carboxylate (65)

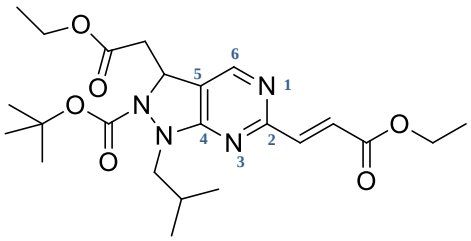

To a solution of compound **66** (116.2 mg, 0.31 mmol) in dioxane/water 4:1 (2.66 mL) in an atmosphere filled with nitrogen, was added [(*E*)-2-(ethoxycarbonyl)vinyl]boronic acid pinacol ester (184.6 mg, 0.82 mmol) and sodium carbonate (113.0 mg, 1.07 mmol). The atmosphere was purged with nitrogen for 5 minutes and $Pd(PPh_3)_4$ (5.5 mol%) was added. The reaction mixture was refluxed for 18 h, during which it was followed by TLC. The mixture was diluted in water (30 mL) and extracted with ethyl acetate (3 × 20 mL). The combined organic extracts were washed with water (3 × 20 mL), dried with sodium sulfate, filtered and concentrated under reduced pressure. Purification by preparative TLC (20% ethyl acetate in hexane) afforded the pure compound. Yellow oil (13% yield).

^{1}H NMR (300.18 MHz, $CDCl_3$) δ (ppm): 8.21 (s, 1H, C_6H_{pyri}), 7.56 (d, J = 15.7 Hz, 1H, C<u>H</u>=CHCO$_2$), 7.11 (d, J = 15.7 Hz, 1H, CH=C<u>H</u>CO$_2$), 5.61 (dd, J = 9.3, 3.9 Hz, 1H, CH_{pyra}), 4.27 (q, J = 7.2 Hz, 2H, $CH_{2vinylester}$), 4.20 (q, J = 7.1 Hz, 2H, CH_{2ester}), 3.81 (dd, J = 13.9, 8.9 Hz, 1H, $CH_{2isobutyl}$), 3.65 (dd, J = 13.8, 4.9 Hz, 1H, $CH_{2isobutyl}$), 2.94 (dd, J = 16.2, 4.3 Hz, 1H, C<u>H</u>$_2$CO$_2$), 2.63 (dd, J = 16.1, 9.4, 1H, C<u>H</u>$_2$CO$_2$), 2.23 – 2.10 (m, 1H,

$CH_{isobutyl}$), 1.52 (s, 9H, Boc), 1.33 (t, J = 7.1 Hz, 3H, $CH_{3vinylester}$), 1.28 (t, J = 7.1 Hz, 3H, CH_{3ester}), 0.99 (d, J = 6.7 Hz, 3H, $CH_{3isobutyl}$), 0.78 (d, J = 6.5 Hz, 3H, $CH_{3isobutyl}$);

^{13}C NMR (75.48 MHz, $CDCl_3$) δ (ppm): 169.7 ($CH_2\underline{C}O_2$), 166.4 (CO_{2vinyl}), 164.6 (C_{4pyri}), 162.3 (C_{2pyri}), 156.1 (CO_{2Boc}), 148.1 (C_{6pyri}), 142.2 ($\underline{C}H=CHCO_2$), 127.6 ($CH=\underline{C}HCO_2$), 118.3 (C_{5pyri}), 83.4 (C_{qBoc}), 61.3 ($CH_{2vinylester}$), 61.0 (CH_{2ester}), 57.9 ($CH_{2isobutyl}$), 57.9 (CH_{pyra}), 42.3 (CH_2CO_2), 28.4 (CH_{3Boc}), 26.6 ($CH_{isobutyl}$), 20.8 (2 × $CH_{3isobutyl}$), 14.3 ($CH_{3vinylester}$), 14.3 (CH_{3ester}).

MS (ESI) m/z: $C_{23}H_{34}N_4O_6$ **exp.**: 463.3 [M+H] **calc.**: 462.3.

IV.2 *In Vitro* Assays

IV.2.1 *In Vitro* Assay Against Blood Stage

Test compounds inhibitory activity to BS was determined through flow cytometric measurement. The compounds (diluted in DMSO) were further diluted in MCM (Malaria Complete Medium) to multiple concentrations and 100 µL of each dilution was added to a 96-well plate, prior to the addition of the same volume of a culture of RBC infected with synchronized ring-stage *P. falciparum* (1% parasitemia) diluted in MCM. MCM is constituted by RPMI 1640 supplemented with 25 mM 4-(2-hydroxyethyl)-1-piperazine ethanesulfonic acid (HEPES), 204 mM L-glutamine, 50 µg/mL gentamicin, 0.5% (w/v) Albumax, 11mM glucose, 1.47 mM hypoxanthine and 37.3 mM $NaHCO_3$. After incubation for 48 h at 37ºC, 5% CO_2 and 5% O_2, 50 µL/well of a solution of SYBR Green I reagent diluted in phosphate-buffered saline (PBS) (1:10000) was added to a new 96-well plate. The plate containing the culture and the test compounds was resuspended, and 5 µL of this solution was added the SYBR Green plate and incubated at rt, in the dark, for 20 min. An additional 150 µL of PBS was added to each well. The cells were lysed using 20 mM of NaOH and TritonX-100 at 0.063%. Parasitemia was determined from dot plot (forward scatter vs. side scatter) acquired on a Sysmec Cube 6 – Robbyflow cytometer using FlowJo Software.[121]

IV.2.2 *In Vitro* Assay Against Liver Stage

To determine the compounds inhibitory activity to the LS, was measured the luminescence intensity in Huh-7 cells infected with *P. berghei* line expressing firefly luciferase, as previously described.[122] Huh-7 cells, from a human hepatoma cell line, were seeded at $1x10^4$ cells/well of a 96-well plate in 100 µL of cRPMI. cRPMI is a culture medium constituted by 1640 RPMI medium supplemented with 10% v/v fetal calf serum (FCS), 1% v/v penicillin/streptomycin, 1% v/v glutamine, 1% v/v nonessential amino acids and 10 mM HEPES, pH 7, and incubated at 37ºC with 5% CO_2, ov. The test compounds were diluted in cRPMI+F+G (cRPMI + 1:1000 getamicin

+ 1:3000 fungizone). The culture medium was replaced with the compound dilutions and incubated for 1 h at the same conditions. Then, *P. berghei* sporozoites expressing luciferase, freshly obtained through disruption of salivary glands of infected female *Anopheles stephensi* mosquitoes, were added to the cells at a proportion of 1:1, and the plate was centrifuged for 5 minutes at 1800 xg, rt and incubated for 46 h at the same conditions. Afterwards, 80 µL of a solution of thaw alamar-blue/cell-titer blue reagent aliquots diluted in cRPMI (1:20) was added to each well and incubated at the same conditions previously described for 1:30 h. After the cells were washed with PBS, such was aspirated and 70 µL of lysis buffer was added to each well. The plate was put in the shaker at 600 rpm for 15 minutes at rt, then centrifuged for 5 minutes at 1800 xg and 30 µL of the supernatant was pipetted to a 96-well plate. 50 µL/well of luciferin solution diluted in FLAB (1:50) was added and the luminescence intensity in each well was measured in order to determine the compounds inhibitory activity to LS. To determine the IC_{50} values, was used GraphPad prims and employed a nonlinear regression analysis to fit the normalized results of the dose-response curves.

IV.2.3 *In Vitro* Assay Against Cancer (Monolayer)

Briefly, stem cells from the cell line HT-29 human colorectal adenocarcinoma were plated in 96-well plates (100 cell/well) in undifferentiated medium in ultra-low attachment conditions for sphere formation, and treated with a previously reported CSC-targeting agent (salinomycin (Sal); 1 µM - positive control), test compounds (concentrations ranging from 0.01 to 100 µM) and 5-Fu; 1 µM - negative control). Following seven days of incubation, cell viability was assessed based on measurement of MTS, using the CellTiter-Glo^{TM} Luminescent Cell Viability Assay (Promega). All data analysis and IC_{50} value calculations were performed using GraphPad Prim version 6.01.

IV.2.4 *In Vitro* Assay Against Cancer (CSC-like spheres)

The anti-CSC effect of those compounds was further validated by assessing their impact on tumorsphere formation. To measure tumorsphere formation, colon cancer cells were plated as single cells in 24-well ultra-low attachment plates (500 cell/well), and cultured in 1 mL serum-free DMEM/F12 supplemented with 2% B27 supplement, 1% N_2 supplement, 1% non-essential amino acids, 1% sodium pyruvate, 1% penicillin-streptavidin, 4 µg/mL heparin, 40 ng/mL recombinant human EGF and 20 ng/mL recombinant human bFGF. Tumorsphere numbers were counted and spheres area were determined using image analysis software after spheroids images acquisition through brighfield microscopy. Test compounds concentrations were ranging from 0.03 to 20 µM). Salinomycin (anti-CSC agent) and 5-Fu (traditional chemotherapeutic) were used as a positive and negative controls, respectively.

Chapter V

V. Bibliography

1. Sinka, M. E. *et al.* A global map of dominant malaria vectors. *Parasit. Vectors* **5,** 69 (2012).

2. WHO Media Centre. Malaria Fact sheet Nº94. https://web.archive.org/web/20140925071732/http://www.who.int/mediacentre/factsheets/fs094/en/ (accessed Aug 9, 2019).

3. White, N. J. *et al.* Malaria. *Lancet* **6736,** (2013).

4. Kantele, A. & Jokiranta, T. S. Review of Cases With the Emerging Fifth Human Malaria Parasite , Plasmodium knowlesi. *Clin. Infect. Dis.* **52,** 1356–1362 (2011).

5. *World Health Organization, World Malaria Report 2019*. (2019).

6. Feachem, R., Phillips, A., Targett, G. and Snow, R. Call to action : priorities for malaria elimination. *Lancet* **376,** 1517–1521 (2010).

7. White, N. J. *et al.* Averting a malaria disaster. *Lancet* **353,** 1965–1967 (1999).

8. Coslédan, F., Fraisse, F., Pellet, A., Guillou, F., et al. Selection of a trioxaquine as an antimalarial drug candidate. *PNAS* **105,** 17579–17584 (2008).

9. Wyler, D. J. Malaria - Resurgence, Resistance, and Research. *NEJM* **308,** 934–940 (1983).

10. Alonso, P. L. *et al.* A Research Agenda to Underpin Malaria Eradication. *PLOS Med.* **8,** (2011).

11. Centers for Disease Control and Prevention, Malaria's Impact Worldwide. https://www.cdc.gov/malaria/malaria_worldwide/impact.html (accessed Aug 10, 2019).

12. Greenwood, B. M. *et al.* Malaria : progress , perils , and prospects for eradication. *J. Clin. Invest.* **118,** 1266–1276 (2008).

13. Rodrigues, T., Prudêncio, M., Moreira, R., Mota, M. M. & Lopes, F. Targeting the Liver Stage of Malaria Parasites: A Yet Unmet Goal. *J. Med. Chem.* **55,** 995–1012 (2011).

14. JHSPHOPEN courseware. Topic: Malaria. http://ocw.jhsph.edu/index.cfm/go/imageLib:il.viewImageDetails/resourceID/438DCC50%2DFFE9%2D0B64%2D8515BF619797AA48/browseTopic/Malaria/topicID/16/ (accessed Aug 25, 2019).

15. Tham, W., Healer, J. & Cowman, A. F. Erythrocyte and reticulocyte binding-like proteins of Plasmodium falciparum. *Trends Parasitol.* **28,** 23–30 (2012).

16. Moore, L. R. *et al.* Hemoglobin degradation in malaria-infected erythrocytes determined from live cell magnetophoresis. *FASEB J.* **19,** 1–19 (2006).

17. Delves, M. *et al.* The Activities of Current Antimalarial Drugs on the Life Cycle Stages of Plasmodium : A Comparative Study with Human and Rodent Parasites. *PLOS Med.* **9,** (2012).

18. Aravind, L., Iyer, L. M., Wellems, T. E. & Miller, L. H. Plasmodium Biology : Genomic Gleanings. *Cell Press* **115,** 771–785 (2003).

19. *World Health Organization, World Malaria Report 2018*. (2018).

20. Tangpukdee, N., Duangdee, C., Wilairatana, P. & Krudsood, S. Malaria Diagnosis : A Brief Review. *Korean J. Parasitol.* **47,** 93–102 (2009).

21. Ettari, R., Bova, F., Zappala, M., Grasso, S. & Micale, N. Falcipain-2 Inhibitors. *Med. Res. Rev.* **30,** 136–167 (2010).

22. Rosenthal, P. J. Falcipain cysteine proteases of malaria parasites : An update. *BBA - Proteins Proteomics* **1868,** (2020).

23. Singh, K. & Kaur, T. Pyrimidine based antimalarials: Design strategies and antiplasmodial effects. *Med. Chem. Commun.* **7,** 1–35 (2016).

24. Ribeiro, C. J. A. *et al.* Novel squaramides with in vitro liver stage antiplasmodial activity. *Bioorganic Med. Chem.* **24,** 1786–1792 (2016).

25. Oliveira, R. *et al.* Tetraoxane − Pyrimidine Nitrile Hybrids as Dual Stage Antimalarials. *J. Med. Chem.* **57,** 4916–4923 (2014).

26. Veronika, E. *et al.* Tuning and predicting biological affinity: aryl nitriles as cysteine protease inhibitors. *Org. Biomol. Chem.* **10,** 5764–5768 (2012).

27. Coterón, J. *et al.* Falcipain Inhibitors : Optimization Studies of the 2-Pyrimidinecarbonitrile Lead Series. *J. Med. Chem.* **53,** 6129–6152 (2010).

28. Smith, D. L., Klein, E. Y., Mckenzie, F. E. & Laxminarayan, R. Prospective strategies to delay the evolution of anti-malarial drug resistance : weighing the uncertainty. *Malar. J.* **9,** 1–10 (2010).

29. Antony, H. & Parija, S. Antimalarial drug resistance: An overview. *Trop. Parasitol.* **6,** 30–41 (2016).

30. Tarun, A. S. *et al.* A combined transcriptome and proteome survey of malaria parasite liver stages. *PNAS* **105,** 305–310 (2008).

31. Derbyshire, E. R., Mota, M. M. & Clardy, J. The Next Opportunity in Anti-Malaria Drug Discovery : The Liver Stage. *PLOS Pathog.* **7,** (2011).

32. Kori, L. D., Valecha, N. & Anvikar, A. R. Insights into the early liver stage biology of Plasmodium. *J. Vector Borne Dis.* **55,** 9–13 (2018).

33. Al-Bari, A. Chloroquine analogues in drug discovery: new directions of uses, mechanisms of actions and toxic manifestations from malaria to multifarious diseases. *J. Antimicrob. Chemother.* **70,** 1608–1621 (2015).

34. Sullivan, D. J. Cinchona Alkaloids : Quinine and Quinidine. in *Treatment and Prevention of Malaria: Antimalarial Drug Chemistry, Action and Use* 45–68

(2012). doi:10.1007/978-3-0346-0480-2

35. *WHO Guidelines for thetreatment of malaria*. 32 (2006).

36. A., C. A lesson learnt: the rise and fall of Lariam and Halfan. *J. R. Soc. Med.* **100,** 17–174 (2007).

37. Drugbank. Halofantrine. https://www.drugbank.ca/drugs/DB01218 (accessed Set 01, 2019).

38. Drugbank. Mefloquine. https://www.drugbank.ca/drugs/DB00358 (accessed Set 01, 2019).

39. Foley, M. & Tilley, L. Quinoline Antimalarials : Mechanisms of Action and Resistance. *Int. J. Parasitol.* **27,** 231–240 (1997).

40. Nevin, R. L. A serious nightmare : psychiatric and neurologic adverse reactions to mefloquine are serious adverse reactions. *Pharmacol. Res. Perspect.* **5,** 2016–2018 (2017).

41. Padberg, S. Anti-infective Agents. in *Drugs During Pregnancy and Lactation* 115–176 (Elsevier B.V., 2015). doi:10.1016/B978-0-12-408078-2.00007-X

42. Lawrenson, A. S., Cooper, D. L., Neill, P. M. O. & Berry, N. G. Study of the antimalarial activity of 4-aminoquinoline compounds against chloroquine-sensitive and chloroquine-resistant parasite strains. *J. Mol. Model.* **24,** (2018).

43. Combrinck, J. M. *et al.* Insights into the Role of Heme in the Mechanism of Action of Antimalarials. *ACS Chem. Biol.* **8,** 133–137 (2013).

44. Vanderesse, R., Colombeau, L., Frochot, C. & Acherar, S. Inactivation of Malaria Parasites in Blood : PDT vs Inhibition of Hemozoin Formation. in *Current Topics in Malaria* 205–233 (2016). doi:10.5772/65053

45. Murphy, K. V. Design and Synthesis of Novel Chloroquine-based Antimalarials. (2015).

46. Burgess, S. J. *et al.* A Chloroquine-like Molecule Designed to Reverse Resistance in Plasmodium falciparum. *J. Med. Chem.* **49,** 5623–5625 (2006).

47. Teixeira, C., Gomes, J. R. B. & Gomes, P. Falcipains , Plasmodium falciparum Cysteine Proteases as Key Drug Targets Against Malaria. *Curr. Med. Chem.* **18,** 1555–1572 (2011).

48. Martin, R. E. & Kirk, K. The Malaria Parasite ' s Chloroquine Resistance Transporter is a Member of the Drug / Metabolite Transporter Superfamily. *Mol. Biol. Evol.* **21,** 1938–1949 (2004).

49. Chinappi, M., Via, A., Marcatili, P. & Tramontano, A. On the Mechanism of Chloroquine Resistance in Plasmodium falciparum. *PLoS One* **5,** (2010).

50. Juge, N. *et al.* Plasmodium falciparum chloroquine resistance transporter is a H + -coupled polyspecific nutrient and drug exporter. *PNAS* **112,** 1–6 (2015).

51. NCIT . Concept Report. Amodiaquine (Code C65231). Terms & Properties.

https://ncit.nci.nih.gov/ncitbrowser/ConceptReport.jsp?dictionary=NCI_Thesaurus&ns=NCI_Thesaurus&code=C65231 (accessed Aug 25,2019).

52. Nair, A. *et al.* Biowaiver Monographs for Immediate Release Solid Oral Dosage Forms : Amodiaquine Hydrochloride. *J. Pharm. Sci.* 1–12 (2012). doi:10.1002/jps

53. Terzic, N. *et al.* Reinvestigating Old Pharmacophores: Are 4 - Aminoquinolines and Tetraoxanes Potential Two-Stage Antimalarials? *J. Med. Chem.* **59,** 264–281 (2016).

54. Lu, G. *et al.* Efficacy and safety of methylene blue in the treatment of malaria : a systematic review. *BMC Med.* **16,** 1–16 (2018).

55. Mccarthy, S. Neuropsychiatric Illness , and Risk-Benefit Analysis in the Australian Defence Force. *J. Parasitol. Res.* **2015,** 1–23 (2015).

56. Schlitzer, M. Malaria Chemotherapeutics Part I : History of Antimalarial Drug Development , Currently Used Therapeutics , and Drugs in Clinical Development. *ChemMedChem* **2,** 944–986 (2007).

57. Nothdurft, H. D. & Kain, K. C. *CHAPTER 6 Malaria Prevention*. *The Travel and Tropical Medicine Manual (Fifth Edition)* (Elsevier Inc., 2017). doi:10.1016/B978-0-323-37506-1.00006-4

58. Milligan, R., Daher, A. & Pm, G. Primaquine at alternative dosing schedules for preventing relapse in people with Plasmodium vivax malaria. *Cochrane Libr.* (2019). doi:10.1002/14651858.CD012656.pub2.www.cochranelibrary.com

59. Camarda, G. *et al.* Antimalarial activity of primaquine operates via a two-step biochemical relay. *Nat. Commun.* **10,** 1–9 (2019).

60. Baird, J. K. 8-Aminoquinoline Therapy for Latent Malaria. *Clin. Microbiol. Rev.* **32,** 1–68 (2019).

61. Krintafel (tafenoquine succinate tablets) FDA Advisory Committee Briefing Document. 1–129 (2018).

62. Llanos-Cuentas, A., Lacerda, G., Hien, T., Vélez, D. & Namaik-Iarp, C. Tafenoquine versus Primaquine to Prevent Relapse of Plasmodium vivax Malaria. *N. Engl. J. Med.* **380,** 229–241 (2019).

63. Hounkpatin, A. B., Kreidenweiss, A. & Held, J. Clinical utility of tafenoquine in the prevention of relapse of Plasmodium vivax malaria : a review on the mode of action and emerging trial data. *Infect. Drug Resist.* **12,** 553–570 (2019).

64. Campo, B., Vandal, O., Wesche, D. L. & Burrows, J. N. Killing the hypnozoite – drug discovery approaches to prevent relapse in Plasmodium vivax. *Pathog. Glob. Health* **109,** 107–122 (2015).

65. Hamerly, T. *et al.* NPC1161B, an 8-Aminoquinoline Analog, Is Metabolized in the Mosquito and Inhibits Plasmodium falciparum Oocyst Maturation. *Front. Pharmacol.* **10,** 1–11 (2019).

66. Abdul-ghani, R., Farag, H. F. & Allam, A. F. Sulfadoxine-pyrimethamine resistance in Plasmodium falciparum : A zoomed image at the molecular level within a geographic context. *Acta Trop.* **125,** 163–190 (2013).

67. *Atovaquone and Proguanil Hydrochloride. https://www.drugs.com/monograph/atovaquone-and-proguanil-hydrochloride.html (acessed Set 25, 2019).*

68. Boggild, A. K., Parise, M. E., Lewis, L. S. & Kain, K. C. Atovaquone-Proguanil : Report From The CDC Expert Meeting On Malaria Chemoprophylaxis (II). **76,** 208–223 (2007).

69. Staines, H. M. *et al.* Clinical implications of Plasmodium resistance to atovaquone / proguanil : a systematic review and meta-analysis. *J. Antimicrob. Chemother.* **73,** 581–595 (2018).

70. Neill, P. M. O., Barton, V. E. & Ward, S. A. The Molecular Mechanism of Action of Artemisinin—The Debate Continues. *Molecules* **15,** 1705–1721 (2010).

71. Rudrapal, M. & Chetia, D. Endoperoxide antimalarials : development , structural diversity and pharmacodynamic aspects with reference to 1 , 2 , 4-trioxane-based structural scaffold. *Drug Des. Devel. Ther.* **10,** 3575–3590 (2016).

72. Ribeiro, J. Synthesis and evaluation of chemical probes to study the biology of liver stage malaria parasites. (ULisboa, Faculty of Pharmacy, 2017).

73. Meshnick, S. R. & Taylor, T. E. Artemisinin and the Antimalarial Endoperoxides : from Herbal Remedy to Targeted Chemotherapy. *Microbiol. Rev.* **60,** 301–315 (1996).

74. Ridder, S. De, Kooy, F. Van Der & Verpoorte, R. Artemisia annua as a self-reliant treatment for malaria in developing countries. *J. Ethnopharmacol.* **120,** 302–314 (2008).

75. Tilley, L., Straimer, J., Gnädig, N. F., Ralph, S. A. & Fidock, D. A. Artemisinin action and resistance in Plasmodium falciparum Leann. *Trends Parasitol.* **32,** 682–696 (2016).

76. Stocks, P. A. *et al.* Evidence for a Common Non-Heme Chelatable-Iron-Dependent Activation Mechanism for Semisynthetic and Synthetic Endoperoxide Antimalarial Drugs. *Angew. Chemie Int. Ed.* **46,** 6278–6283 (2007).

77. Giannangelo, C. *et al.* Ozonide antimalarials alkylate heme in the malaria parasite Plasmodium falciparum. *ACS Infect. Dis.* (2019). doi:10.1021/acsinfecdis.9b00257

78. Kannan, D. *et al.* Pre-clinical study of iron oxide nanoparticles forti fi ed artesunate for ef fi cient targeting of malarial parasite. *EBioMedicine* **45,** 261–277 (2019).

79. WHO. Malaria. Q&A on artemisinin resistance. https://www.who.int/malaria/media/artemisinin_resistance_qa/en/ (accessed Out 27, 2019).

80. Suresh, N. & Haldar, K. Mechanisms of artemisinin resistance in Plasmodium falciparum malaria. *Curr. Opin. Pharmacol.* **42,** 46–54 (2018).

81. Narula, A. K., Azad, C. S. & Nainwal, L. M. New dimensions in the field of antimalarial research against malaria resurgence. *Eur. J. Med. Chem.* **181,** 1–78 (2019).

82. Fisher, L. C. & Blackie, M. A. L. Tetraoxanes as Antimalarials : Harnessing the Endoperoxide. 123–135 (2014).

83. Press, D. Endoperoxide antimalarials : development , structural diversity and pharmacodynamic aspects with reference to 1 , 2 , 4-trioxane-based structural scaffold. 3575–3590 (2016).

84. Opsenica, I. *et al.* Tetraoxane Antimalarials and Their Reaction with Fe (II). *J. Med. Chem.* **49,** 3790–3799 (2006).

85. Neill, P. M. O. *et al.* Identification of a 1,2,4,5-Tetraoxane Antimalarial Drug-Development Candidate (RKA182) with Superior Properties to the Semisynthetic Artemisinins. *Anal. Chem.* **49,** 5693–5697 (2010).

86. Straimer, J. *et al.* A tetraoxane-based antimalarial drug candidate that overcomes PfK13-C580Y dependent artemisinin resistance. *Nat. Commun.* **8,** 1–10 (2017).

87. Miranda, D. *et al.* Novel Endoperoxide-Based Transmission-Blocking Antimalarials with Liver- and Blood-Schizontocidal Activities. *J. Med. Chem.* **5,** 108–112 (2014).

88. Derbyshire, E. R., Prudêncio, M., Mota, M. M. & Clardy, J. Liver-stage malaria parasites vulnerable to diverse chemical scaffolds. *PNAS* **109,** 8511–8516 (2012).

89. Lazaro, J. E. H. *et al.* Antimalarial Activity of Crambescidin 800 and Synthetic Analogues against Liver and Blood Stage of Plasmodium sp. *J. Antibiot. (Tokyo).* **59,** 583–590 (2006).

90. Carraz, M. *et al.* A Plant-Derived Morphinan as a Novel Lead Compound Active against Malaria Liver Stages. *PLOS Med.* **3,** 2392–2402 (2006).

91. Carraz, M., Jossang, A., Rasoanaivo, P., Mazier, D. & Frappier, F. Isolation and antimalarial activity of new morphinan alkaloids on Plasmodium yoelii liver stage. *Bioorganic Med. Chem.* **16,** 6186–6192 (2008).

92. François, G. *et al.* In vitro inhibition of liver forms of the rodent malaria parasite Plasmodium bergheiby naphthylisoquinoline alkaloids - structure-activity relationships of dioncophyllines A and C and ancistrocladine. *Parasitol. Res.* **83,** 673–679 (1997).

93. Singh, N. & Puri, S. K. Causal prophylactic activity of antihistaminic agents against Plasmodium yoelii nigeriensis infection in Swiss mice. *Acta Trop.* **69,** 255–260 (1998).

94. Andersen, S. L. *et al.* Efficacy of Azithromycin as a Causal Prophylactic Agent against Murine Malaria. *Antimicrob. Agents Chemother.* **38,** 1862–1863 (1994).

95. Goodman, C. D., Su, V. & Mcfadden, G. I. The effects of anti-bacterials on the malaria parasite Plasmodium falciparum. *Mol. Biochem. Parasitol.* **152,** 181–191 (2007).

96. Mahmoudi, N. *et al.* New Active Drugs against Liver Stages of Plasmodium Predicted by Molecular Topology. *Antimicrob. Agents Chemother.* **52,** 1215–1220 (2008).

97. Crofts, A. R. The Cytochrome BC1 Complex: Function in the Context of Structure. *Annu. Rev. Physiol.* **66,** 689–733 (2004).

98. Nam, T. *et al.* A Chemical Genomic Analysis of Decoquinate, a Plasmodium falciparum Cytochrome b Inhibitor. *ACS Chem. Biol.* **6,** 1214–1222 (2011).

99. Arrowsmith, C. H. *et al.* The promise and peril of chemical probes. *Nat. Chem. Biol.* **11,** 536–541 (2015).

100. Fonovic, M. & Bogyo, M. Activity Based Probes as a Tool for Functional Proteomic Analysis of Proteases. *Expert Rev. Proteomics* **5,** 721–730 (2010).

101. Cañeque, T., Müller, S. & Rodriguez, R. Visualizing biologically active small molecules in cells using click chemistry. *Nat. Rev. Chem.* **2,** 202–215 (2018).

102. Horisawa, K. Specific and quantitative labeling of biomolecules using click chemistry. *Front. Physiol.* **5,** 1–7 (2014).

103. Hein, C. D., Liu, X. & Wang, D. Click Chemistry, A Powerful Tool for Pharmaceutical Sciences. *Pharm. Res.* **25,** 2216–2230 (2008).

104. Singh, M. S., Chowdhury, S. & Koley, S. Advances of azide-alkyne cycloaddition-click chemistry over the recent decade. *Tetrahedron* (2016). doi:10.1016/j.tet.2016.07.044

105. D'Ascenzio, M. *et al.* An Activity-Based Probe Targeting Non-Catalytic , Highly Conserved Amino Acid Residues within Bromodomains. *Angew. Chemie Int. Ed.* **58,** 1007–1012 (2019).

106. Miltz, W. *et al.* Design and synthesis of potent and orally active GPR4 antagonists with modulatory effects on nociception , inflammation , and angiogenesis. *Bioorg. Med. Chem.* **25,** 4512–4525 (2017).

107. García-Domínguez, P., Dell, C., Alvarez, R., Altucci, L. & Lera, Á. R. De. Synthetic approaches to DNMT inhibitor SGI-1027 and effects on the U937 leukemia cell line. *Bioorg. Med. Chem. Lett.* **23,** 1631–1635 (2013).

108. Vollhardt, P. & Schore, N. *Organic Chemistry Structure and Function 6th Edition*. (2010).

109. Bao, R., Lai, C. & Qian, C. Treatment of cancers having k-ras mutations. (2011).

110. Seiler, H. & Kaffenbergér, T. Anorganische Dünnschicht-Chromatographie. *Helv. Chim. Acta* **XLIV,** 1282–1283 (1961).

111. Prihod, R. *et al.* Layered double hydroxides as catalysts for aromatic nitrile hydrolysis. *Microporous Mesoporou Mater.* **56,** 241–255 (2002).

112. Pavia, D., Lampman, G. & Kriz, G. *Introduction to Spectroscopy*. (2001).

113. Sawaki, Y. & Ogata, Y. Mechanism of the reaction of nitrile with alkaline hydrogen peroxide. Reactivity of peroxycarboximidic acid and application to superoxide ion reaction. *Bull. Chem. Soc. Jpn.* **54,** 793–799 (1981).

114. Zhang, G. *et al.* 5-Amino-1H-1,2,4-triazole-3-carbohydrazide and its applications in the synthesis of energetic salts: a new strategy for constructing the nitrogen-rich cation based on the energetic moiety combination. *R. Soc. Chem.* **47,** 13391–13401 (2018).

115. Kraft, K., Moreira, R. & Capela, R. *Synthesis of and its optimisation of a potential malaria liver stage inhibitor*. (2016).

116. Asano, S., Kamioka, S. & Isobe, Y. Suzuki e Miyaura cross-coupling reaction of aryl and heteroaryl pinacol boronates for the synthesis of 2-substituted pyrimidines. *Tetrahedron* **68,** 272–279 (2012).

117. Barder, T. E., Walker, S. D., Martinelli, J. R. & Buchwald, S. L. Catalysts for Suzuki - Miyaura Coupling Processes : Scope and Studies of the Effect of Ligand Structure. *J. Am. Chem. Soc.* **127,** 4685–4696 (2005).

118. Yates, C., Shaver, S. & Hoekstra, W. Metalloenzyme inhibitor compounds. (2017).

119. Thiemann, T., Tanaka, Y. & Kaabi, M. Suzuki–Miyaura reaction of chloroarenes using Pd (PPh3)4 as catalyst. *J. Chem. Res.* 34–38 (2010).

120. Richard, S. M., Lucrecia, V. & Marignac, M. Sensitization to oxaliplatin in HCT116 and HT29 cell lines by metformin and ribavirin and differences in response to mitochondrial glutaminase inhibition. *J. Cancer Res. Ther.* **11,** 336–340 (2015).

121. Francisco, D. R. Optimization of a flow cytometric assay to measure antimalarial drug effects. (2017).

122. Ploemen, I., Prudêncio, M., Douradinha, B., Ramesar, J. & Fonager, J. Visualisation and Quantitative Analysis of the Rodent Malaria Liver Stage by Real Time Imaging. *PLoS One* **4,** 1–12 (2009).

Chapter VI

VI. Annexes

Annex 1 – Table VI.1 – Synthetic methods and respective yields.

Compound	Method	Yield (%)
52	**A**	39
	B	79
53	**A**	13
	B	42
	C	21
	D	92
58		6
59		62
60		77
61		50
64	**A**	2
	B	6
66		70
65		13

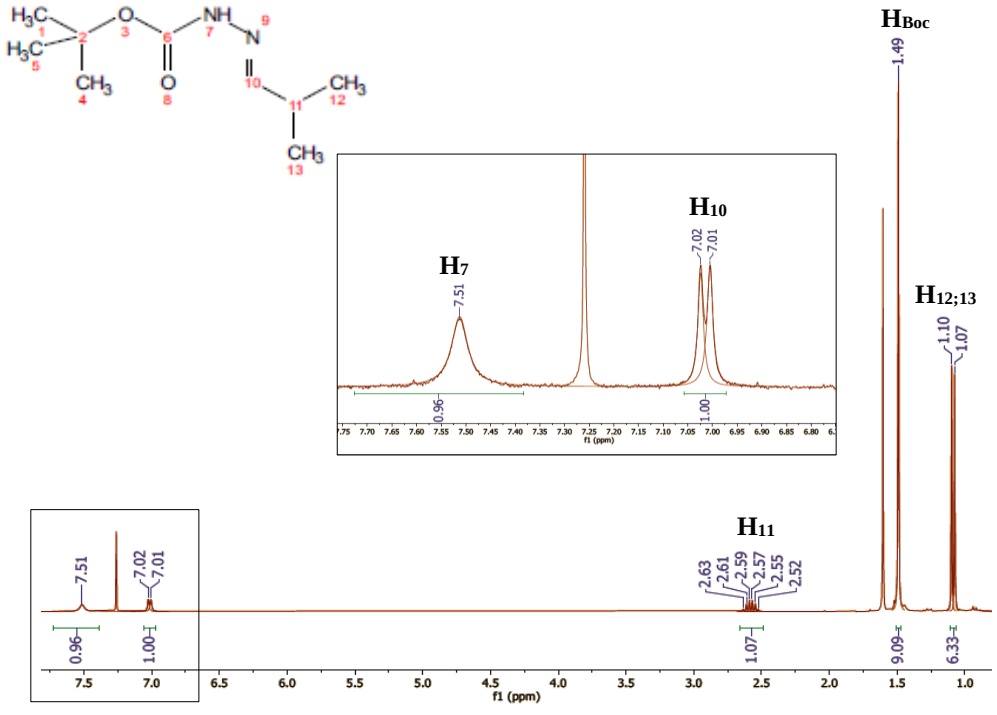

Annex 2 – Figure VI.1 – Compound **51** ^{1}H-NMR spectrum, in $CDCl_3$.

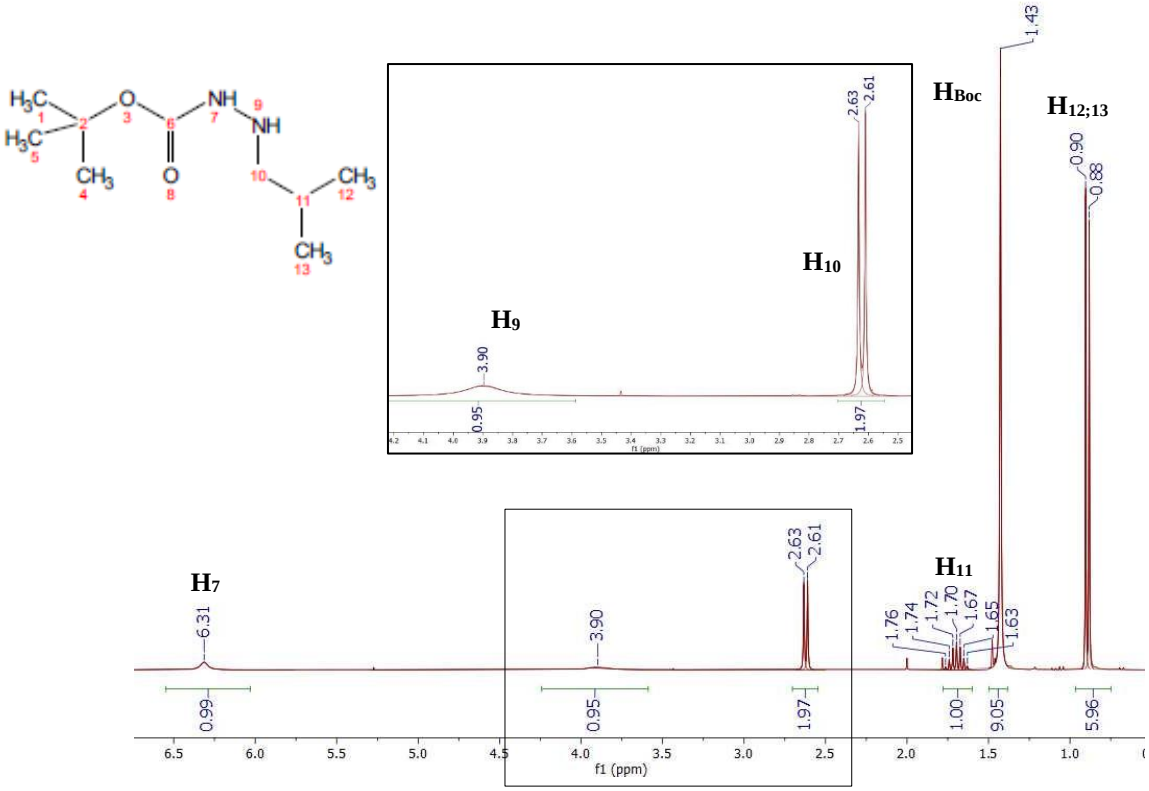

Annex 3 – Figure VI.2 – Compound **52** ^{1}H-NMR spectrum, in $CDCl_3$.

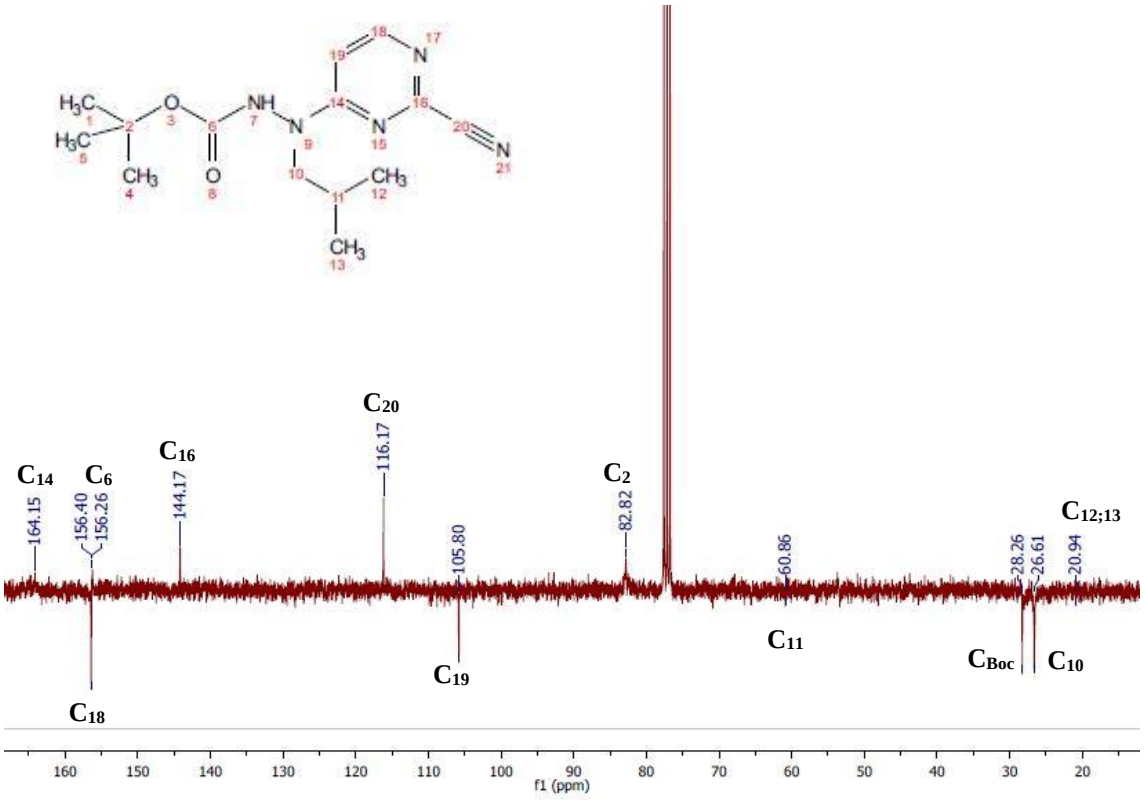

Annex 4 – Figure VI.3 – Compound **60** ^{13}C-APT NMR spectrum, in $CDCl_3$.

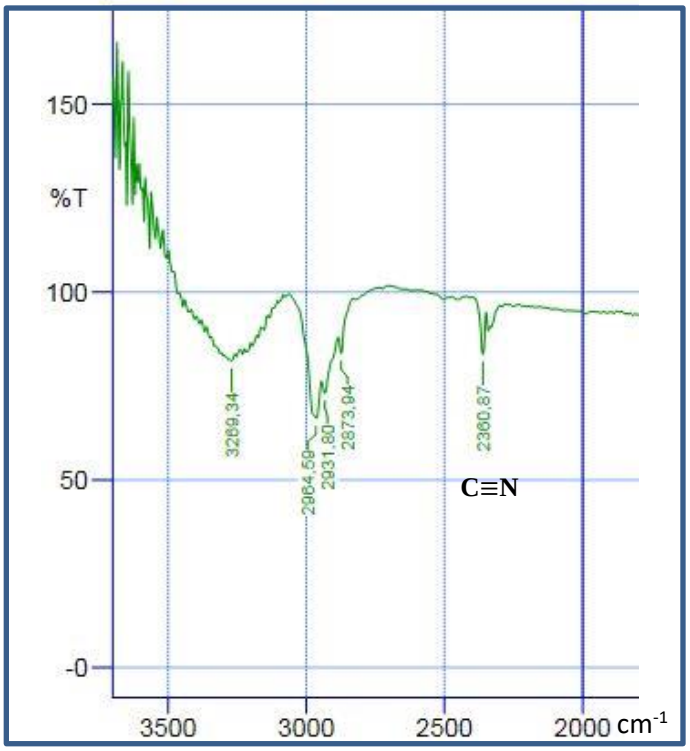

Annex 5 – Figure VI.4 – Compound **60** IR spectrum, in NaCl cells.

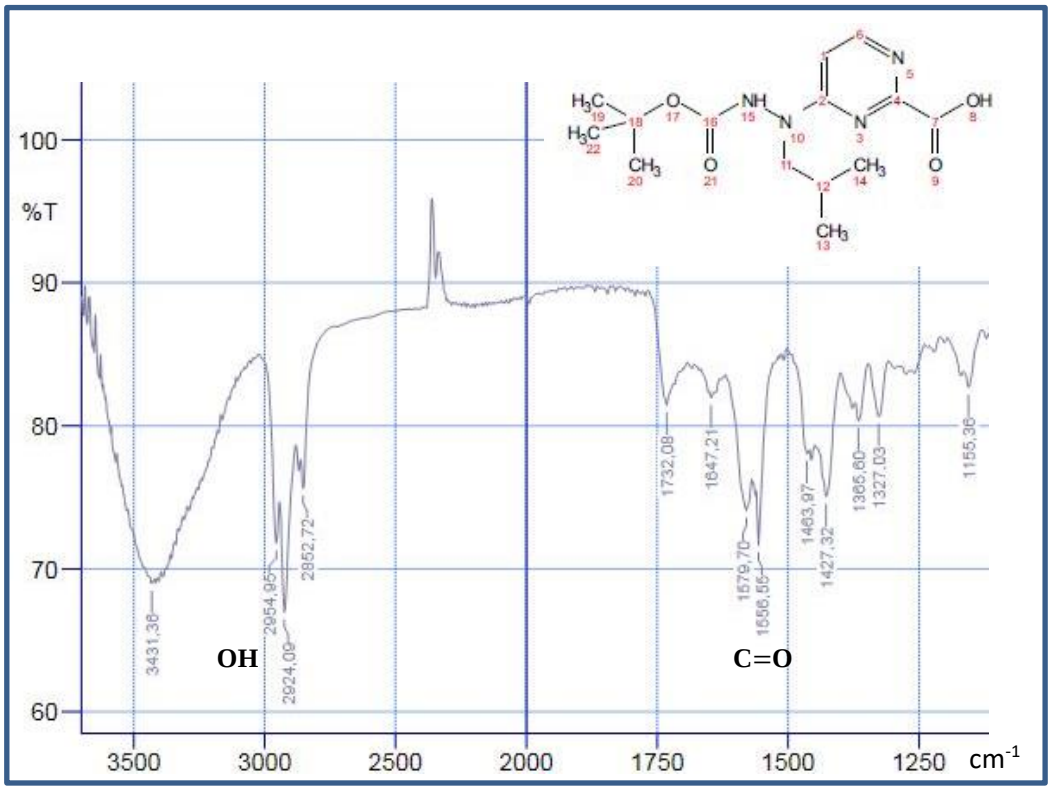

Annex 6 – Figure VI.5 – Compound **61** IR spectrum, in NaCl cells.

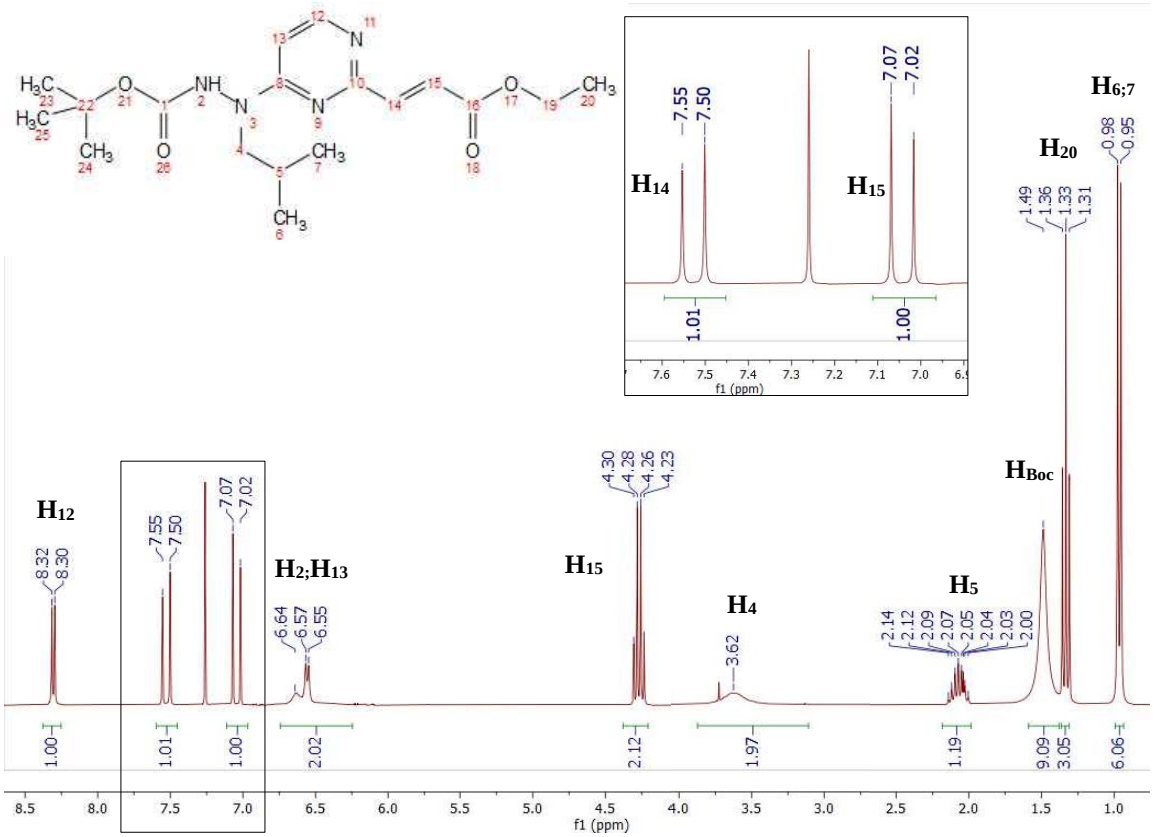

Annex 7 – Figure VI.6 – Compound **64** ^{1}H-NMR, in $CDCl_3$.

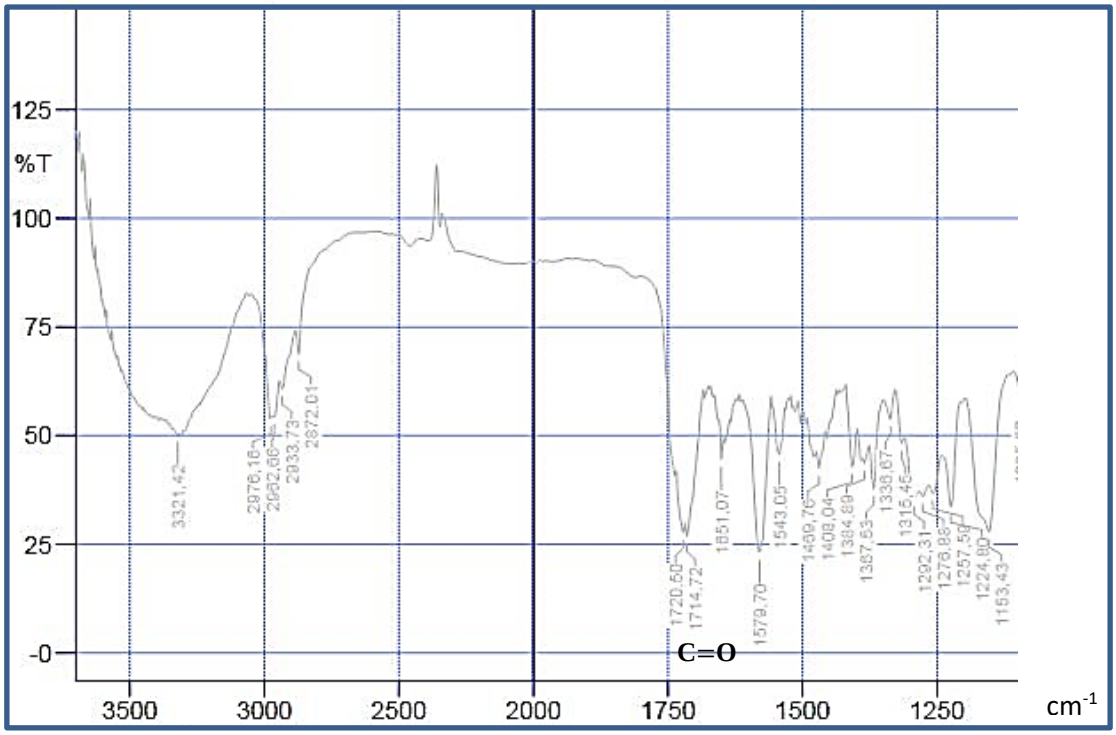

Annex 8 – Figure VI.7 – Compound **64** IR spectrum, in NaCl cells.

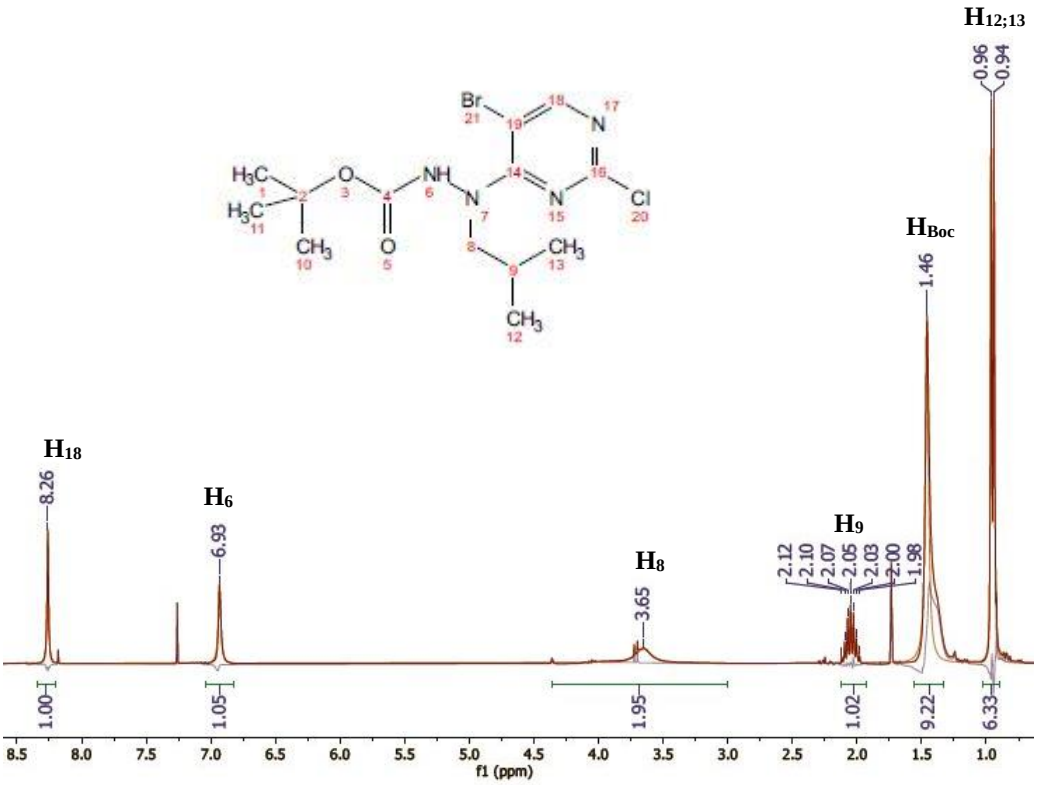

Annex 9 – Figure VI.8 – Compound **66** ^{1}H-NMR, in $CDCl_3$.

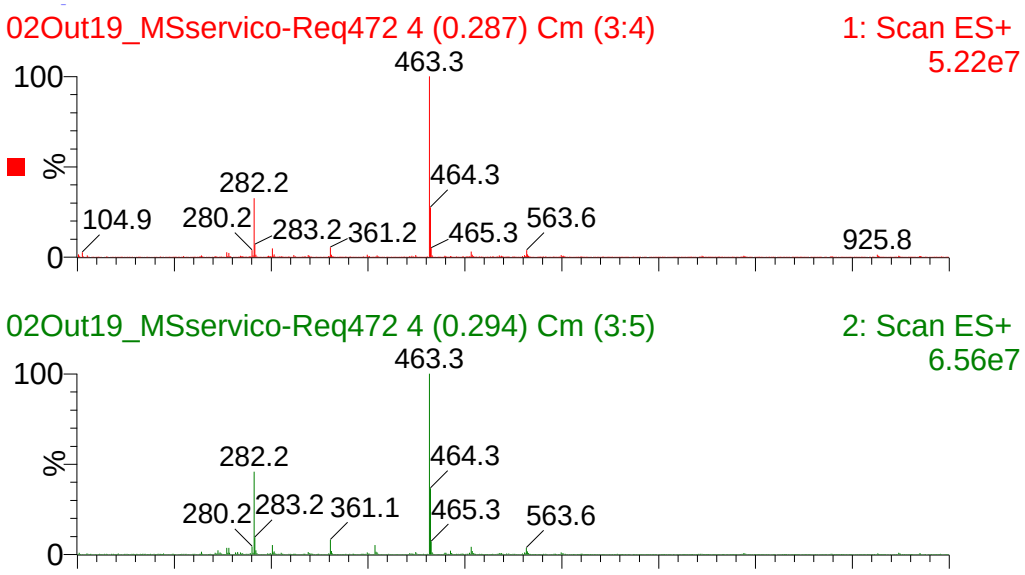

Annex 10 – Figure VI.9 – Compound **65** ESI-MS spectrum, in ACN.

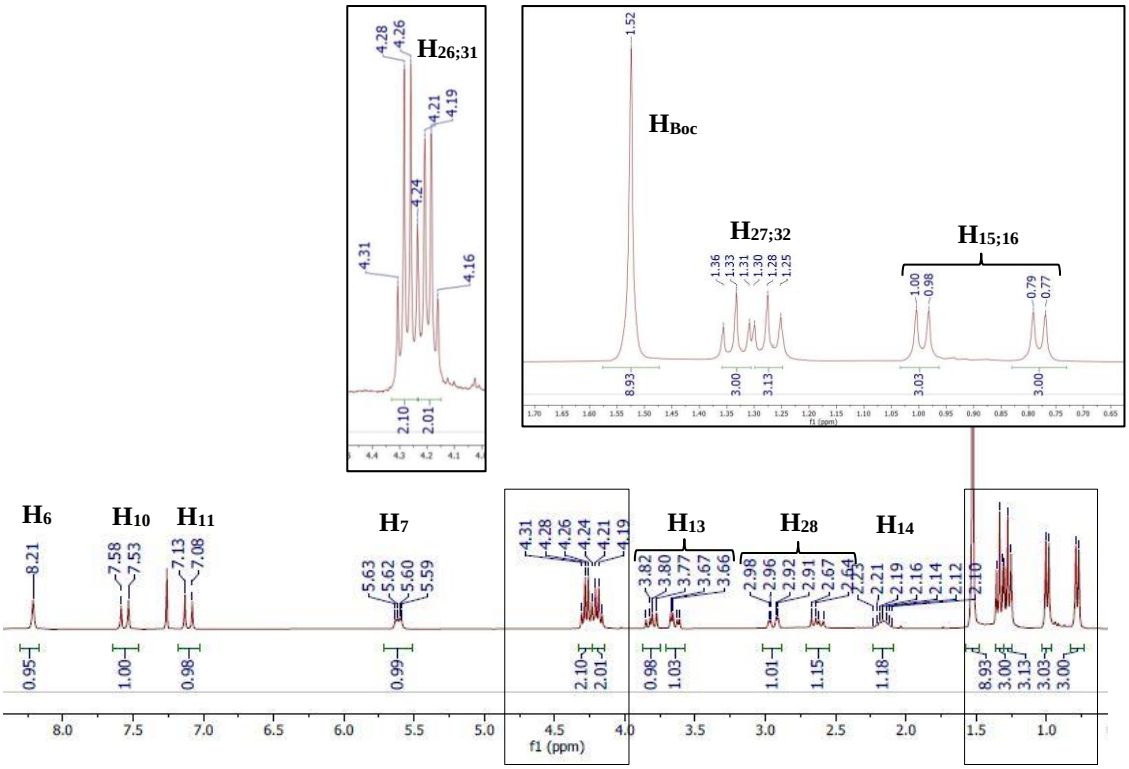

Annex 11 – Figure VI.10 – Compound **65** ^{1}H-NMR, in $CDCl_3$.

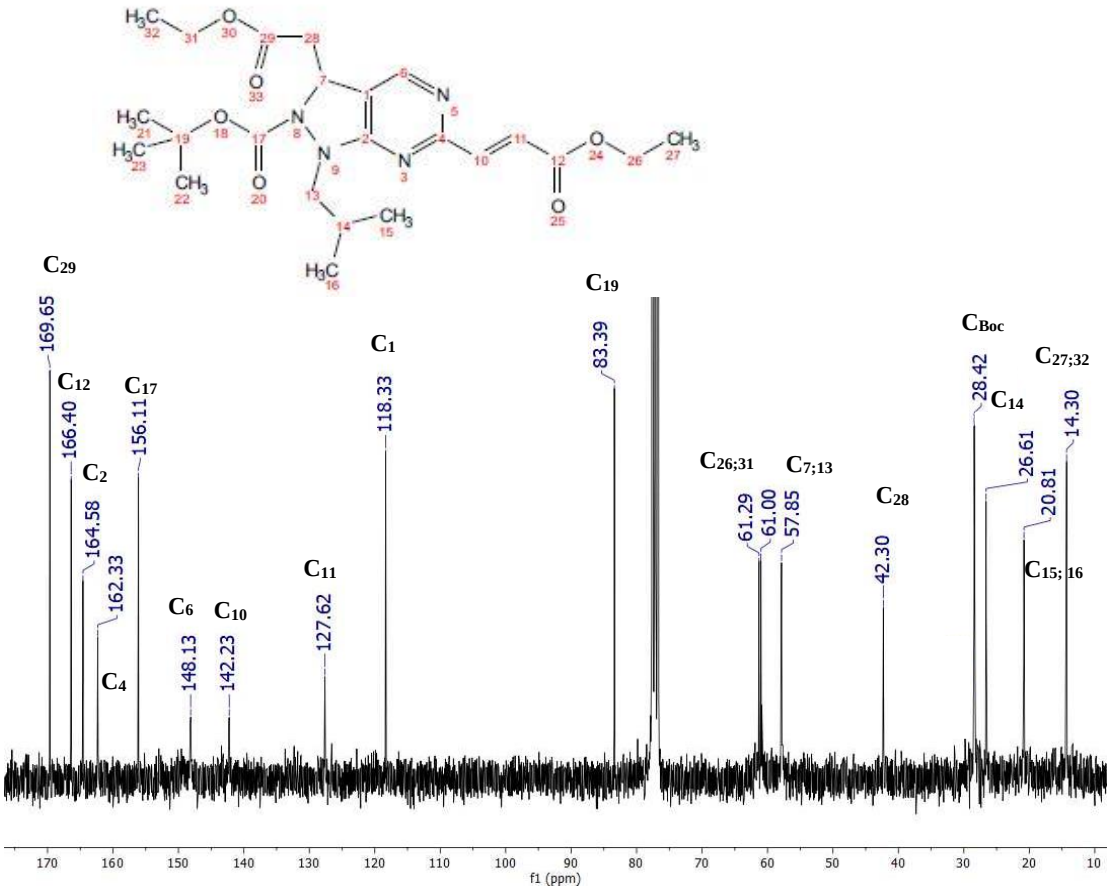

Annex 12 – Figure VI.11 – Compound **65** ^{13}C-NMR spectrum, in $CDCl_3$.

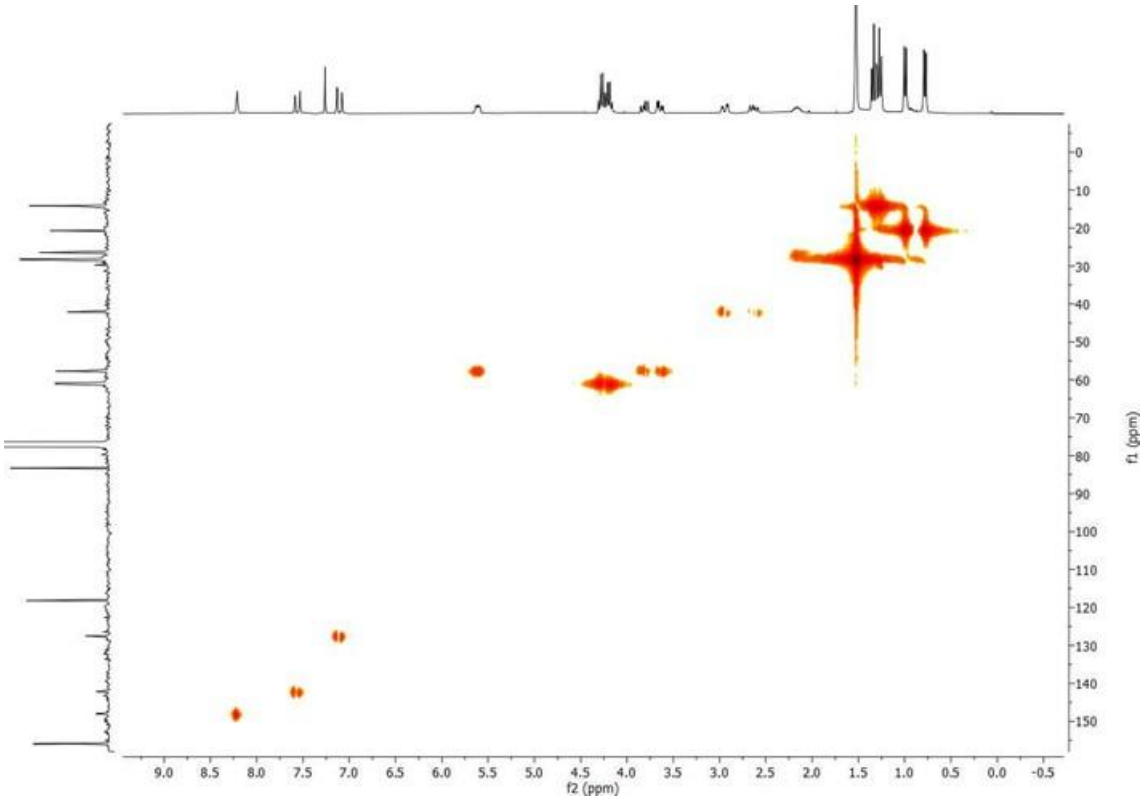

Annex 13 – Figure VI.12 – Compound **65** HMQC NMR spectrum, in $CDCl_3$.

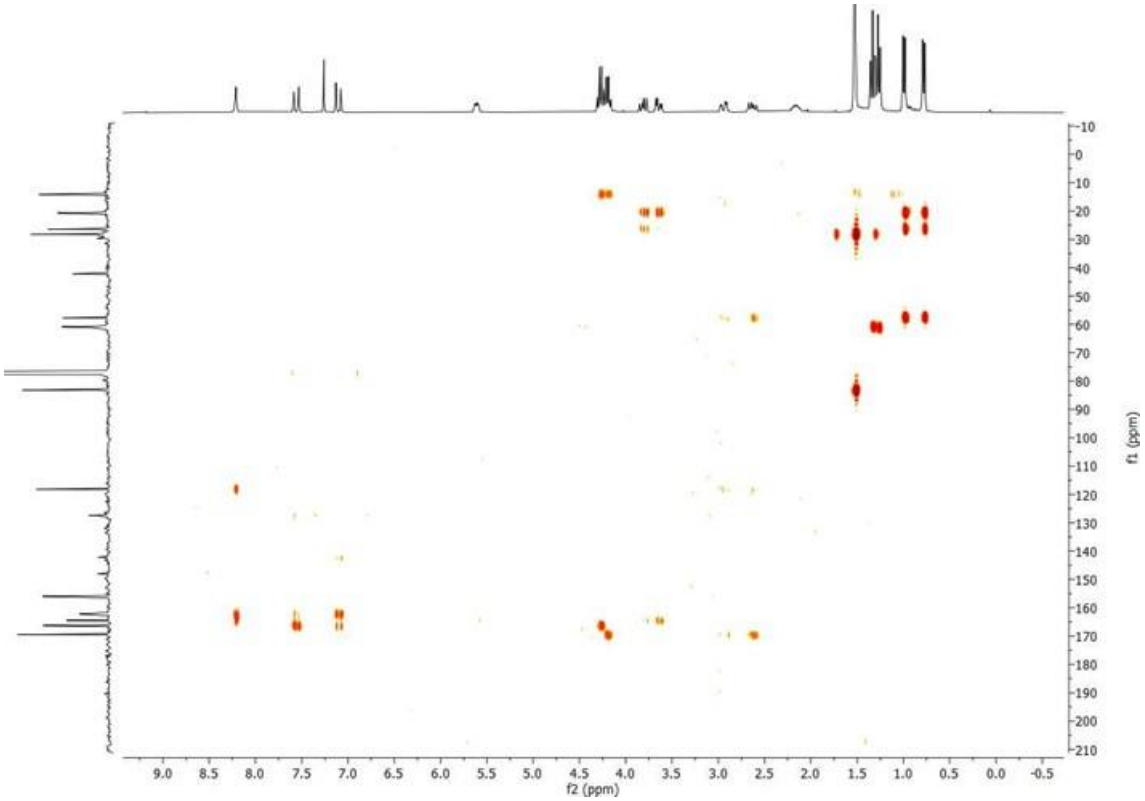

Annex 14 – Figure VI.13 – Compound **65** HMBC NMR spectrum, in $CDCl_3$.

Annex 15 – Table VI.2 – Antimalarial LS IC_{50} values of compounds **64**, **65** and controls

Compound	Liver Stage IC_{50} (μM)
64	N.D.[a]
65	9.49
Control	(PQ) 9.50 [24]

N.D. – Not determined

Annex 16 – Table VI.3 – Anticancer IC_{50} values of compounds **64**, **65** and controls.

Compound	Monolayer (μM)	CSC-like spheres (μM)
64	35.56	0.77
65	28.96	0.70
Positive Control (Sal)	15.42	0.32
Negative Control (5-Fu)	5.48	1.83